RCR Russian Chemical Reviews

https://doi.org/10.59761/RCR5272

Accepted Manuscript

Grafted and Pore-Filled Ion-Exchange Membranes: Synthesis, Properties and Applications

Submitted: 5 October 2026

Published: 20 November 2026

Cite this article as: A.D.Manin, I.A.Stenina, Y.Wang, T.Xu, A.B.Yaroslavtsev. Grafted and Pore-Filled Ion-Exchange Membranes: Synthesis, Properties and Applications. *Russ. Chem. Rev.*, RCR5272; https://doi.org/10.59761/RCR5272

A.D. Manin, I.A. Stenina, Y. Wang, T. Xu & A.B. Yaroslavtsev

This is a PDF file of a peer-reviewed manuscript that has been accepted for publication in Russian Chemical Reviews. The text and figures will undergo editing, formatting and proof reading before the article is published in its final form. The file will be replaced with the Version of Record.

Accepted Manuscript
This manuscript will be edited, formatted, and proof read. This text will be replaced with Version of Record.

Grafted and Pore-Filled Ion-Exchange Membranes: Synthesis, Properties and Applications

A.D.Manin[1,2], I.A.Stenina[1], Y.Wang[3], T.Xu[3], A.B.Yaroslavtsev[1]

[1]Kurnakov Institute of General and Inorganic Chemistry, Russian Academy of Sciences, 31 Leninsky Prospekt, Moscow 119071, Russian Federation

[2]Faculty of Chemistry, National Research University Higher School of Economics, 7 Vavilova Street, Moscow 117312, Russian Federation

[3]Department of Applied Chemistry, Anhui Provincial Engineering Laboratory of Functional Membrane Science and Technology, School of Chemistry and Materials Science, University of Science and Technology of China, Hefei, Anhui 230026, People's Republic of China

Accepted manuscript

This manuscript will be edited, formatted and proofread, some fields will be replaced with Version of Record.

Abstract

Growing demand for membranes in modern technologies is driving their continuous development, particularly for membranes that combine high conductivity with high selectivity. However, no commercially available membrane currently offers high conductivity, high selectivity, and low cost at the same time. Graft-modified, pore-filled membranes with an optimized pore and channel structure can overcome this limitation. Moreover, the choice of base film allows the production of relatively thin membranes with high mechanical strength. In addition, the wide range of available base and graft polymers makes it possible to tailor these membranes to the demands of modern industry. This review covers the preparation methods and key properties of pore-filled and grafted membranes. Considerable attention is given to their current and potential applications in water treatment and electrochemical energy generation and storage, including electrodialysis, reverse electrodialysis, hydrogen energy, redox flow batteries, and lithium-ion batteries.

Keywords: ion exchange membranes, grafted membranes, pore-filled membranes, ion conductivity, selectivity, electrodialysis, hydrogen energy, energy storage

Table of contents

1. Introduction 3

2. Grafted membranes 4

2.1. Synthesis of grafted membranes 4

2.2. Properties of grafted membranes 9

3. Pore-filled membranes 12

3.1. Synthesis of pore-filled membranes 12

3.2. Properties of pore-filled membranes 14

4. Practical applications 16

4.1. Electrodialysis 17

4.2. Reverse electrodialysis 25

4.3. Hydrogen energy 33

4.4. Energy storage devices 48

5. Conclusion 60

6. List of abbreviations and symbols 62

7. References 64

Accepted manuscript
This manuscript will be edited, formatted, and proof read. The file will be replaced with Version of Record

1. Introduction

Ion-exchange membranes are used in many areas of modern life, including water purification, electrochemical synthesis, sensor technology, etc.[1–7] In recent years, their use in hydrogen energy and energy storage[8–14], as well as in the recovery of valuable components from industrial wastewater[15–18], has attracted considerable attention. Since the requirements for membranes differ significantly depending on the specific technology, universal and scalable methods for synthesizing ion-exchange materials with tunable physicochemical and transport properties are highly desirable.[3,19] High ionic conductivity and high selectivity are generally regarded as the most important properties of any ion-exchange material. However, these two properties are inherently in conflict: increasing the transport rates usually reduce selectivity, and vice versa. This trade-off is common to all membranes, including gas separation membranes, for which the Robeson plot was proposed in 1991 to describe the relationship between gas permeability and selectivity.[20] The plot has since been revised and updated to reflect new advances in the field.[21–24] The same issue applies to ion-exchange membranes. In electrodialysis, for example, the priorities are high selectivity for counterions (ions with a charge opposite to that of the functional groups) and low permeability of co-ions (ions with the same charge). Fuel cells, in contrast, require low permeability to uncharged species such as gases and alcohols. In recent years, this correlation has become one of the most discussed topics in the field.[25–27]

Some homogeneous ion-exchange membranes, such as the well-known perfluorinated sulfonic acid membranes Nafion and Aquivion, offer both high conductivity and selectivity.[28–30] However, their high cost and environmental concerns restrict their use to applications that demand exceptional reliability under harsh conditions, primarily hydrogen-air fuel cells and electrolyzers for green hydrogen and chlorine production. In these devices, Nafion remains the material of choice for efficient energy conversion. Most other electrochemical processes, including electrodialysis, rely on much cheaper heterogeneous membranes, which are made by pressing ion-exchange resin granules (e.g., sulfonated polystyrene) with a binder such as polyethylene. These membranes contain large, typically micrometer-sized, secondary pores between the particles.[31,32] Unlike nanometer pores, these large pores allow non-selective transport of co-ions and small non-polar molecules[33,34], which is the main reason for the low selectivity of heterogeneous membranes.

Accepted manuscript
This manuscript will be edited, formatted, and proof read. The final version may differ from this version.

Developing cost-effective methods for synthesizing ion-exchange membranes that combine high ionic conductivity and selectivity without secondary porosity is therefore a highly attractive goal. A promising approach is to introduce an ionomer into a polymer base film. This allows the membrane volume to be filled completely, or almost completely, with ionomer, which prevents the formation of large pores. Depending on the morphology of the base film and the synthesis route, two main approaches can be distinguished: radiation-induced graft polymerization and pore filling. This review examines these approaches in detail and provides an overview of the properties and potential applications of the resulting membranes. This review covers the literature published mainly over the last decade (2015–2026); earlier studies are cited where they are needed to explain the fundamentals of membrane synthesis and structure. Among existing reviews on this topic, three recent publications are particularly relevant.[35–37] The present review differs in that it examines and compares both membrane types, which have similar properties, in depth. It also describes their structure and characteristics in greater detail and covers a broader range of practical applications than the most recent of these reviews.

2. Grafted membranes

2.1. Synthesis of grafted membranes

A grafted polymer is represented by a main chain $(\text{-A-})_n$ with side branches of a different polymer $(\text{-B-})_m$ (Fig. 1).[38–41] Grafted membranes (GMs) are typically produced from polymer films that have been activated to generate radicals, which act as reaction centers for initiating the graft polymerization.[42–46] Because the enthalpy of radical formation is generally high and reactions between radicals have no activation barrier, the radical concentration in most conventional systems is low. Radicals recombine very rapidly, returning the system to thermodynamic equilibrium. Exceptions include nitrogen and chlorine oxides, whose bond dissociation energies are relatively low and comparable to the entropic term ($T\Delta S$). In addition, organic radicals with the unpaired electron localized on a tertiary carbon atom ($R_3C\bullet$) are effectively shielded by three substituents, which kinetically hinder recombination. This effect is even more pronounced in polymers. Unlike conventional chemical reactions, irradiation with high-energy particles detaches atoms instantaneously at the moment of collision, typically leaving the macromolecule unexcited. This process requires significantly more energy than chemical or thermally

Accepted manuscript
This manuscript will be edited for style and proof read. The final version may differ from this version of record.

activated bond cleavage and often displaces atoms to positions far from their original sites. If no atom is displaced, the excess energy rapidly dissipates along the chain and the broken bond reforms. If the atom moves to a different position, its return to the cleavage site may take a long time because diffusion in solids is slow. This is why radicals can persist in the polymer for extended periods, especially at low temperatures.[47] They can also be stabilized, for example, by reaction with air to form less reactive peroxy radicals (R-OO•), a method used in the fabrication of track-etched membranes.[48] This makes it possible to separate the activation and grafting steps by a substantial time interval, a procedure known as post-activation (post-irradiation) graft polymerization.[42,49] As a result, the production of grafted membranes becomes much simpler.

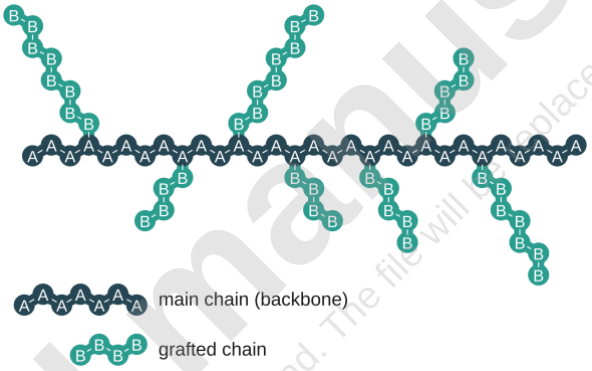


Figure 1. Schematic of a graft copolymer structure

Various approaches can be used to generate radicals in the base polymer film, but all of them require exposing the material to radiation of sufficient energy. Examples include plasma treatment[50], UV radiation[51,52], ionizing radiation, etc.[53–55] Low linear energy transfer ionizing radiation with, primarily γ-radiation with energies up to 10 MeV, is one of the main polymerization initiators.[56] γ-ray photons generally have energies above 0.1 MeV (e.g., 1.17–1.33 MeV for a ^{60}Co source). This is sufficient to generate radicals in polymers containing C-H bonds, enabling graft polymerization to be performed on most polymers, including polyethylene.[57,58] The interaction of radiation with the polymer matrix takes less than 1 ns. The degree of polymerization can be controlled by varying the absorbed radiation dose. Depending on the polymer, cross-linking or chain scission may also occur.[56] Because radioactive sources are not always readily accessible, activation with milder and more widely available ultraviolet (UV) radiation has drawn considerable research interest. UV radiation can be used to graft onto films containing tertiary carbon atoms (R_3C-H), including polypropylene or poly(methylpentene).[59]

Accepted manuscript
This manuscript will be edited, formatted and proofread. The file will be replaced with Version of Record

Chemical activation offers an alternative to radiation-induced radical generation. In this method, double bonds are created within the macromolecules of the base film, and graft polymerization is then initiated by adding a radical initiator such as benzoyl peroxide[60–62]. The choice of activation method depends on the chemical structure of the starting polymer. In most cases, films based on carbon-chain polymers are used.[40] Polytetrafluoroethylene (PTFE) is often regarded as a highly attractive base film. However, its exceptional chemical resistance requires special activation methods, because conventional radiation or chemical treatment is generally insufficient to initiate grafting. Attempts to graft onto PTFE films irradiated with higher-energy xenon heavy ions were also unsuccessful. These results point to a general limitation: although various track-etched membranes are available, fabricating them from PTFE remains challenging because of its poor activation efficiency. Since the energy of the heavy ions is far higher than the C-F bond energy, it seems unlikely that an energy of several MeV[48] would be insufficient to break the bond. A more likely explanation is that fluorine atoms, being larger and heavier than protons, cannot move far enough away from the cleavage site and therefore inevitably recombine with the chain radicals. Styrene has nevertheless been grafted onto PTFE at 80 °C by γ-irradiation, and adding magnesium powder to the reaction system was shown to enhance the process effectively.[47] Radiation grafting of N-vinylpyrrolidone has also been reported.[63]

Despite the difficulty of making grafted membranes based on PTFE films, such membranes have been successfully produced from other fluorinated carbon-chain polymers, which are attractive because of their high thermal and chemical stability.[64] The most commonly used base films are poly(ethylene-co-tetrafluoroethylene) (ETFE)[65,66] and poly(vinylidene fluoride) (PVDF)[67]. However, the phase-out of fluoropolymers is now being actively discussed worldwide because of their environmental risks and their accumulation as persistent organic pollutants (so-called “forever chemicals”). Potential alternatives for grafted membrane production include high-density polyethylene[68,69], low-density polyethylene[70–72], ultra-high-molecular-weight polyethylene[73], polypropylene[46], polymethylpentene[59], polyesters[74], and natural polymers such as cellulose[75,76].

Producing grafted membranes requires a second polymer, whose chains are grafted onto the macromolecules of the base film. The corresponding monomer can be introduced either directly during activation of the base film or in a subsequent step. In the simultaneous

Accepted manuscript
This manuscript will be edited, formatted, and proofread. The final version may differ from this version of record.

(direct) grafting, the base film is immersed in a monomer solution and irradiated under an inert atmosphere, so activation and graft polymerization occur in parallel.[47,76] The process can also be carried out with a gaseous monomer.[42,77] However, when irradiation and grafting proceed simultaneously, monomer homopolymerization can occur as a side reaction. Several studies have reported ways for suppressing it, for example by adding polymerization inhibitors.[78] The main drawbacks of this approach are poor scalability and high monomer consumption, both of which conflict with the principles of green chemistry. For these reasons, most researchers prefer sequential (post-irradiation) grafting.[79] This approach not only separates the two steps in time, but also uses the monomer more efficiently, for example when grafting is carried out in a surfactant-stabilized emulsion.[69,79]

The chemical structure of the grafted polymer, which is determined by the nature and ratio of the monomers in the reaction mixture, is one of the most important factors influencing the properties of grafted membrane. All monomers used in graft polymerization contain a reactive double bond. They can be divided into two groups: polar monomers with ion-exchange functional groups and non-polar monomers that require post-functionalization to introduce such groups.[40] Commonly used polar monomers include acrylates[80–82], monomers containing sulfonic acid groups[61,83,84], monomers containing phosphate groups[85], vinylimidazole[86], and vinylbenzyl trimethylammonium chloride[87–90]. However, polar monomers are used less often than non-polar ones, because they are difficult to introduce into a non-polar base film. New polymer chains form and grow at the radical sites of the base film macromolecules.[35,58] The process starts at the film surface and advances into the bulk by monomer diffusion. Non-polar monomers have a stronger affinity for non-polar films, which allows easier penetration and more efficient graft polymerization. Among non-polar monomers, the most widely used are styrene and its derivatives[39,40,59,67,91,92], vinylbenzyl chloride[93–96], pentafluorostyrene[19] and vinyl pyridine.[97] Grafting can also be carried out with a mixture of two or more monomers, including polar/polar[98], polar/non-polar[61,99], and non-polar/non-polar[100–102].

When non-polar monomers are grafted, the copolymer is functionalized in a subsequent step. Cation-exchange membranes are produced by sulfonation with sulfuric or chlorosulfonic acid, or by thiolation followed by oxidation of the thiol groups.[19,103–105] Cation-exchange membranes containing phosphonic acid groups can also be prepared, for example, with tris(trimethylsilyl)phosphite followed by hydrolysis of the ester groups.[19]

Accepted manuscript
This manuscript will be edited for style and proof read. The file will be replaced with Version of Record

Sulfonation of the grafted polymer is limited by reagent diffusion into the film and follows a solution-diffusion mechanism.[19] The grafted polymer is hydrophobic, whereas the sulfonating reagents are hydrophilic, so the reagents penetrate and dissolve much more readily in regions that have already been sulfonated. This makes the sulfonation reaction autocatalytic.[67] Because both grafting and functionalization proceed by diffusion of the reagents from the surface into the bulk of the film, the distribution of the grafted polymer and functional groups through the membrane thickness is non-uniform at low degrees of grafting* or functionalization, and the central part of the membrane may contain almost no functional groups (Fig. 2). Membranes with a low degree of grafting therefore typically exhibit lower ionic conductivity[58,106,107], which also affects their other properties. A recent study[67] showed that the distribution of sulfonic acid groups strongly influences not only the transport properties but also the efficiency of electrodialysis desalination.

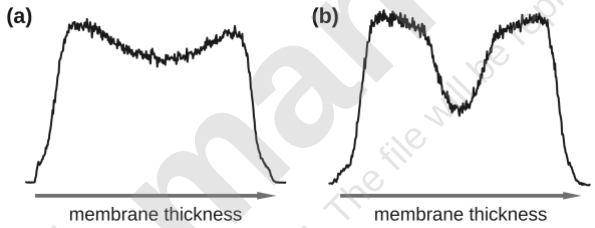


Figure 2. Distribution of functional groups across the thickness of a cation-exchange membrane containing grafted poly(styrene sulfonate) at a high (a) and low (b) degree of grafting/sulfonation[67]

The method for introducing positively charged functional groups to produce anion-exchange membranes also depends on the monomer type and the structure of the graft polymer. For example, styrene requires chloromethylation followed by amination.[108] Vinylbenzyl chloride already contains chloromethyl groups, so amination occurs in a single step by nucleophilic substitution, most commonly with trimethylamine.[35,71,94,109] Other aminating agents can also be used[95,110], including diamines, which can additionally act as cross-linkers[55,110]. When the monomers contain nitrogen atoms with unshared electron pairs, such as vinylimidazole[111] or vinylpyridine[112], are used, anion-exchange groups can be introduced into the graft polymer by quaternization with alkyl halides.

Thus, by varying the base film, the activation method, the grafting conditions, and the grafted monomers, the properties of the resulting membranes can be tuned over a wide

* The grafting degree (GD) is the relative increase in the mass of the base film after grafting, expressed as a percentage of its initial mass.

Accepted manuscript
This manuscript will be edited, formatted, and proofread. The file will be replaced with Version of Record.

range. Specific examples of base films, grafted polymers, and activation methods used to prepare grafted membranes are summarized in Sections 4.1–4.4.

2.2. Properties of grafted membranes

In ion-exchange polymer membranes, functional groups assemble into clusters, which minimizes their interaction with the non-polar polymer matrix. In a humid atmosphere or in contact with aqueous solutions, functional groups hydrate and form a pore-channel network containing sorbed water and the counterions released by dissociation of the functional groups (Fig. 3). Fixed ions line the pore walls, giving them a charge.[113–115] Because of Coulomb interactions, oppositely charged counterions are localized near the pore walls within the Debye layer, which is about 1 nm thick. The central part of each pore contains the so-called electroneutral solution, which is almost pure water (Fig. 3).[116] When the membrane is in contact with an aqueous salt solution, the electroneutral solution is generally considered to have a composition similar to that of the external solution.[117] If the grafting degree and the length of the grafted chains are sufficiently high, the structure of grafted membrane can be described as two interpenetrating networks: one formed by the base polymer and the other by the functionalized grafted polymer.

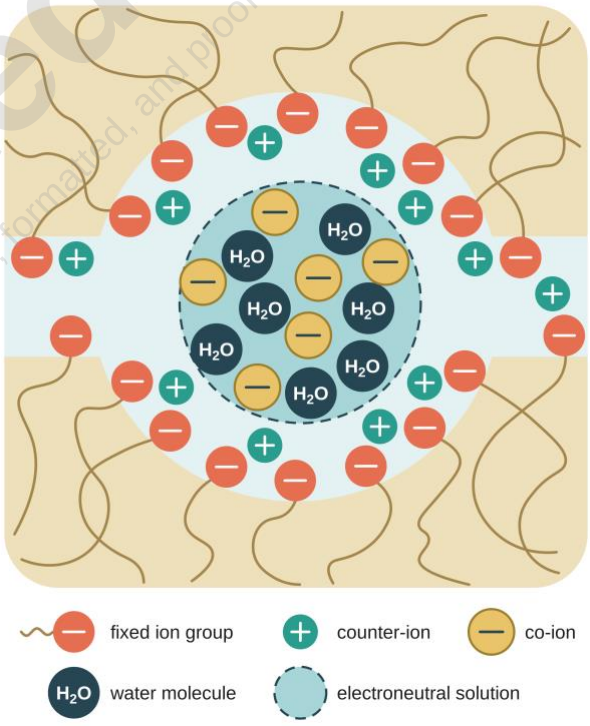


Figure 3. Schematic of the pore structure of an ion-exchange membrane showing the location of the electroneutral solution

Accepted manuscript
This manuscript will be edited, formatted, and proof read. The final version may differ from this version.

The mechanical properties of grafted membranes can be regarded as a combination of the properties of the polymers they contain.[118,119] At low degrees of grafting in particular, they are largely determined by the base film. Since a sufficiently strong polymer is typically chosen as the base, increasing the grafting degree usually reduces the membrane strength.[120] However, this decrease is not uniform. As the grafted chains grow longer, they push the base film chains apart, and the base film resists this stretching. On the other hand, the smaller the proportion of the base polymer, the lower the tensile resistance of the membrane. Consequently, membranes with high grafting degrees and high concentrations of functional groups deform more readily upon hydration. For example, the water uptake of polyethylene-based membranes has been reported to increase disproportionately with the degree of grafting of sulfonated polystyrene (Fig. 4).[121] Another contributing factor is that absorbed liquid also act as a plasticizer, which further increases elasticity and reduces strength.[122–124]

To prevent excessive hydration of the membranes, the grafted polymers are cross-linked. According to the theory of rubber elasticity, the extent to which a polymer chain can be stretched is proportional to the square root of the number of segments, which reflects the statistically expected end-to-end distance of a coiled chain.[125,126] Cross-linking agents reduce the effective distance between the "end" segments of the chains, since the positions of these segments are fixed by the cross-linking sites.[127–129] This restricts the swelling of the grafted membrane and, consequently, its water uptake.[110,130,131]

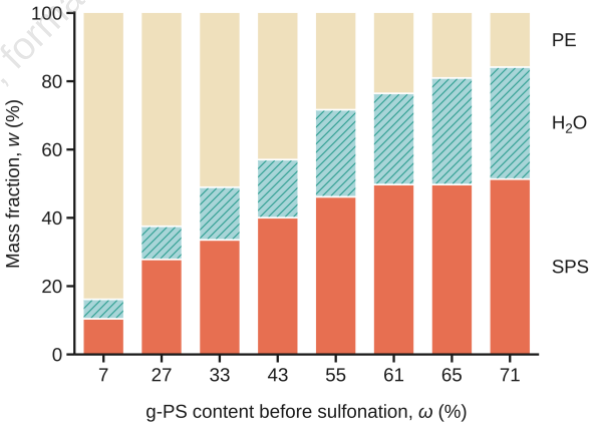


Figure 4. Composition of polyethylene (PE) membranes with grafted sulfonated polystyrene (SPS) as a function of the grafted polystyrene (g-PS) content before sulfonation, ω, at 95% relative humidity[116]

The key functional properties of ion-exchange membranes for practical applications are ionic conductivity and selectivity.[26,132,133] Both generally depend on several parameters,

Accepted manuscript
This manuscript will be edited, formatted, and proofread. The final version will be replaced with version of record.

including the ion-exchange capacity*, the internal structure of pores and channels, the degree of hydration, and the surface hydrophilicity. However, these parameters are largely interrelated, because, as noted above, ionic transport in membranes occurs through the solution inside pores and channels.[29,114,134,135] In most practical applications, membranes are in contact with water, an aqueous solution, or moisture-saturated gases, as in fuel cells. Higher hydration enlarges the pores and the connecting channels. These channels are the bottleneck for ion transport through the membrane and therefore determine its conductivity.[136,137] At the same time, higher hydration increases the volume of electroneutral solution in the pore centers, which determines the total concentration and transport rate of co-ions and thus reduces selectivity.[25] A higher ion-exchange capacity therefore leads to a higher degree of hydration and to larger pores and connecting channels.

Counterion transport occurs within a thin Debye layer along the membrane pore walls. Co-ions, having the same charge as the fixed ions, are displaced from this layer by Coulomb interactions (the so-called Donnan exclusion). Non-polar or low-polarity molecules are also largely excluded from this layer. These species can exist only in the electroneutral solution at the pore centers, and their concentration and diffusion rate determine the undesirable transport of co-ions and, in fuel cells, of gas molecules. Increased hydration results mainly from a larger volume of electroneutral solution, which widens the connecting channels. Higher hydration therefore increases the concentration and mobility of these species, which enhance ionic conductivity but reduce selectivity. This increase in hydration underlies the typical trade-off: higher conductivity of ion-exchange membranes is usually accompanied by lower selectivity† (Fig. 5).[25]

At the same time, Fig. 5 shows that the distribution of membranes by conductivity and selectivity is only a statistical trend. Increasing the grafting degree together with cross-linking maintains a high concentration of counterions, which promotes high ionic conductivity, while limits membrane swelling, thereby preserving high selectivity.[115] The upper part of Fig. 5 is dominated by homogeneous and pseudo-homogeneous ion-exchange membranes, whereas the lower part is dominated by heterogeneous ones. This difference

* Ion-exchange capacity (IEC) is the number of ionogenic functional groups per gram of dry membrane; it is expressed as mmol g^{-1}.

† Membrane selectivity is generally characterized by the potentiometric (apparent) transport number of counterions. It is determined from the membrane potential measured between two solutions of the same electrolyte with different concentrations by comparing this potential with the theoretical value for an ideally selective membrane. A transport number of 1 corresponds to ideal selectivity, whereas lower values indicate co-ion transport through the membrane.

Accepted manuscript
This manuscript will be edited, formatted, and proofread. The final version may vary from this version of record.

arises from the way heterogeneous membranes are fabricated: hot pressing or rolling a mixture of ion-exchanger particles with a binder creates micrometer-sized intergranular pores[31], and only a small fraction of the pore surface bears functional groups. Moreover, the Debye layer, which is about three orders of magnitude thinner than these pores, occupies only a very small portion of their volume. As a result, the concentrations of co-ions and non-polar molecules in these pores are very high, and the resulting secondary porosity leads to substantially lower selectivity of heterogeneous membranes.[31,115]

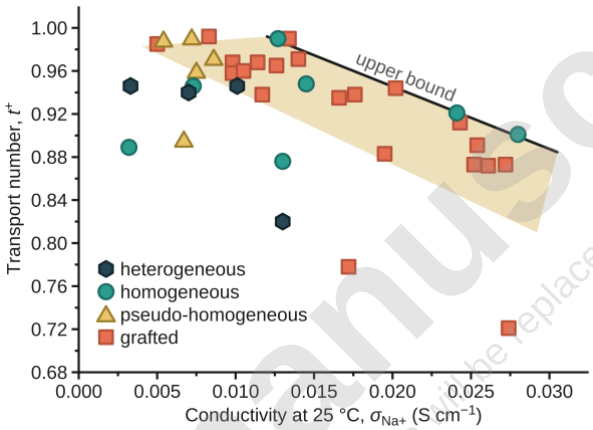


Figure 5. Potentiometric transport numbers versus ionic conductivity of ion-exchange membranes in the Na^+-form[25]

One might therefore expect that grafted membranes with a composition similar to that of heterogeneous ones would also show low selectivity. However, during grafting, the new polymer forms wherever radicals are present in the continuous base film and pushes the base chains apart as it grows, filling the resulting space. Secondary porosity is therefore absent in grafted membranes, and they can reach a selectivity as high as that of the best perfluorinated homogeneous membranes. (Fig. 5).[25,120,138,139]

3. Pore-filled membranes

3.1. Synthesis of pore-filled membranes

The widespread use of radiation-induced graft polymerization is limited by the need to activate polymer films with high-energy radiation, which is not always readily available.[40] This has driven the development of alternative fabrication methods that retain all the advantages of grafted membrane synthesis: simplicity, ease of varying the base film and the composition of the reaction mixture, and scalability. One such alternative is the pore-filling method, in which the pores of a porous base film are filled with a polymer, which may be ionogenic.[36,140,141] To produce pore-filled membranes (PFMs), the base film

Accepted manuscript
This manuscript will be edited, formatted and proofread. The file will be replaced with Version of Record.

must combine a porous structure with good mechanical stability. Suitable materials include polyethylene[142–150], polypropylene[151,152], polyimide[153,154], polyacrylonitrile[155,156], polyesters[157–159], polycarbonate[160], polybenzimidazole[161], poly(vinylidene fluoride)[162–165], polytetrafluoroethylene[166–175], and porous inorganic substrates[176–179].

Various precursors and techniques can be used to fill the base film pores. Many studies have used polyelectrolyte solutions (e.g., Nafion[149,157,161,165,180–185] and Aquivion[186]) as precursors[143,146,156,159,173,187–189], introduced by impregnation[147,173,190,191], sometimes under pressure[155] or vacuum[148,160,179,186]. However, this approach has some limitations: the ion-exchange component may gradually leach out during membrane operation, and some residual porosity may retain. Both effects lower selectivity and largely negate the advantages of such membranes over commercial heterogeneous membranes.

In contrast to grafted membranes, pore-filled membranes do not have covalent bonds between the ionogenic polymer and the hydrophobic base film. As a result, porous base films typically require preliminary modification to improve phase compatibility and prevent polyelectrolyte leaching. This can be done using plasma treatment[143,157], γ-[192] or electron beam irradiation[164,193], surfactant treatment[172,194], and other approaches[187,195].

The efficiency of pore-filling with a polymer solution is limited by two factors: the difference in polarity between the matrix and polyelectrolyte, and by steric hindrance caused by the mismatch in structure and size between the macromolecules and the pores of the base film.[196] The latter problem can be overcome by forming the new polymer phase directly within pores of the base film. This is achieved through radical polymerization of monomers pre-sorbed in the pores, initiated either thermal initiator[148,171,174,197,198] or a photoinitiator[172,194].

Optimal percolation conditions for the formation of pore-filled ion-exchange membranes appear to be achieved with a membrane whose through-pores are oriented perpendicular to the membrane plane as in track-etched membranes.[48,199] For instance, the pores of polyethylene terephthalate track-etched membranes were filled with a solution of MF-4SC, a perfluorinated sulfonic acid ionomer (an analogue of Nafion).[200] The resulting membranes showed lower conductivity than MF-4SC membranes cast from the same polymer, yet their selectivity was comparable. This decrease in conductivity is to be expected, since only about 30% of the volume can be filled with a conductive polymer, and at higher porosity track-etched membranes lose considerable mechanical strength.[48]

Accepted manuscript
This manuscript will be edited, formatted and proofread. The final version may differ from this version.

From this perspective, highly porous polymers with interconnected open pores are of particular interest.[36] Such membranes can be fabricated by several techniques. One of the most common approaches is crazing, in which a polymer is stretched in a wetting liquid, producing numerous intersecting microscopic cracks (crazes) bridged by fibrils.[201–204] In stretched polymers of this kind, the chains are largely aligned along the stretching direction. As a result, the membranes can retain quite high tensile strength even at porosities of 70–80%. Another widely used method is electrospinning, which produces highly porous mats of polymer nanofibers with diameters ranging from a few to several hundred nanometers, formed from a polymer solution or melt in an electrostatic field.[161,173,180,205–213] A less common approach is phase inversion during casting of a polymer solution.[153,159,214–216] Ion-exchange membranes are then prepared in a similar way: the pores are filled with a monomer, which is polymerized and then sulfonated or aminated. Pore-filling methods can differ considerably. For example, in addition to filling the pores with a liquid precursor, some authors employ polymerization of a monomer sorbed from the vapor phase.[217–221]

Comparing the two approaches, both offer a wide range of membrane properties and yield materials with high conductivity and selectivity comparable to those of the best perfluorinated sulfonic acid membranes. At the same time, methods for producing GMs and PFMs are simpler and more environmentally friendly. This is particularly evident for PFMs, which do not require high-energy radiation and allow a wide range of substrates to be used. However, PFMs may retain some residual secondary porosity, whereas graft polymerization prevents its formation. In any case, the transport properties of both GMs and PFMs make them excellent candidates for a variety of electromembrane technologies, some of which are discussed below. Specific examples of porous base films, ion-exchange polymers, and pore-filling methods used to prepare pore-filled membranes are given in Sections 4.1–4.4.

3.2. Properties of pore-filled membranes

The structure of pore-filled membranes is similar to that of grafted membranes. However, even when the ion-exchange polymer content is high, the base and ion-exchange polymers remain more distinctly separated. Moreover, porous films produced by plastic deformation or electrospinning contain highly stretched polymer chains with limited

Accepted manuscript
This manuscript will be edited for style and proofread. The file will be replaced with Version of Record.

capacity for further deformation.[201,202] As a result, their base is less prone to plasticization, making such membranes more rigid (less deformable) and less prone to swelling than their grafted counterparts.[222] The pore-filling method thus often improves the mechanical strength of the membrane.[152] For example, anion-exchange membranes exhibited a much higher tensile strength than a commercial membrane, despite being half as thick.[223] However, the degree of plasticization in such membranes depends on several factors, including the mutual affinity of the polymers, the nature of the solvent used to dissolve the monomer, and the processing temperature, each of which can significantly influence the crystallinity and elasticity of the resulting material.

Pore-filled membranes made from ion-exchange polymers such as Nafion are much less conductive than pure cast membranes of the same material.[200] At the same time, the pore-filling allows the use of higher-capacity polymers, such as polystyrene sulfonate, which cannot be processed into stable membranes without a plasticizer. This can even lead to higher conductivity.[152,163,192,218,222–225] The key advantages of this approach are the ability to produce thin, mechanically strong membranes and to use highly porous supports, both of which offer the potential for high ionic conductivity.[226–228]

Although highly porous base films are used, most studies report nearly complete pore-filling, with no large voids left in the resulting membranes. This may be further promoted by swelling of the ion-exchange polymer upon hydration.[222] As a result, several research groups have achieved relatively high selectivities, including selectivity for monovalent cations.[229,230]

Overall, combining grafting and pore-filling methods makes it possible to produce membranes from various polymer films and monomers. The main advantage over the conventional production of heterogeneous ion-exchange membranes is the ability to create highly selective materials without secondary porosity.

Before describing the practical applications of grafted and pore-filled membranes, it is useful to compare their properties with each other and with those of the best-known classes of widely used commercial membranes, namely, perfluorosulfonic acid (PFSA) and heterogeneous membranes (Fig. 6). As can be seen, for example, from Fig. 5, the properties of membranes even within one class can vary considerably. We therefore compared the best representatives of each membrane type that we have studied previously. The values

Accepted manuscript
This manuscript will be edited, formatted, and proofread. The final version may vary from this version of record.

given are based on our expert assessment, in which a score of 5 corresponds to the best value of a given property among all membrane types.

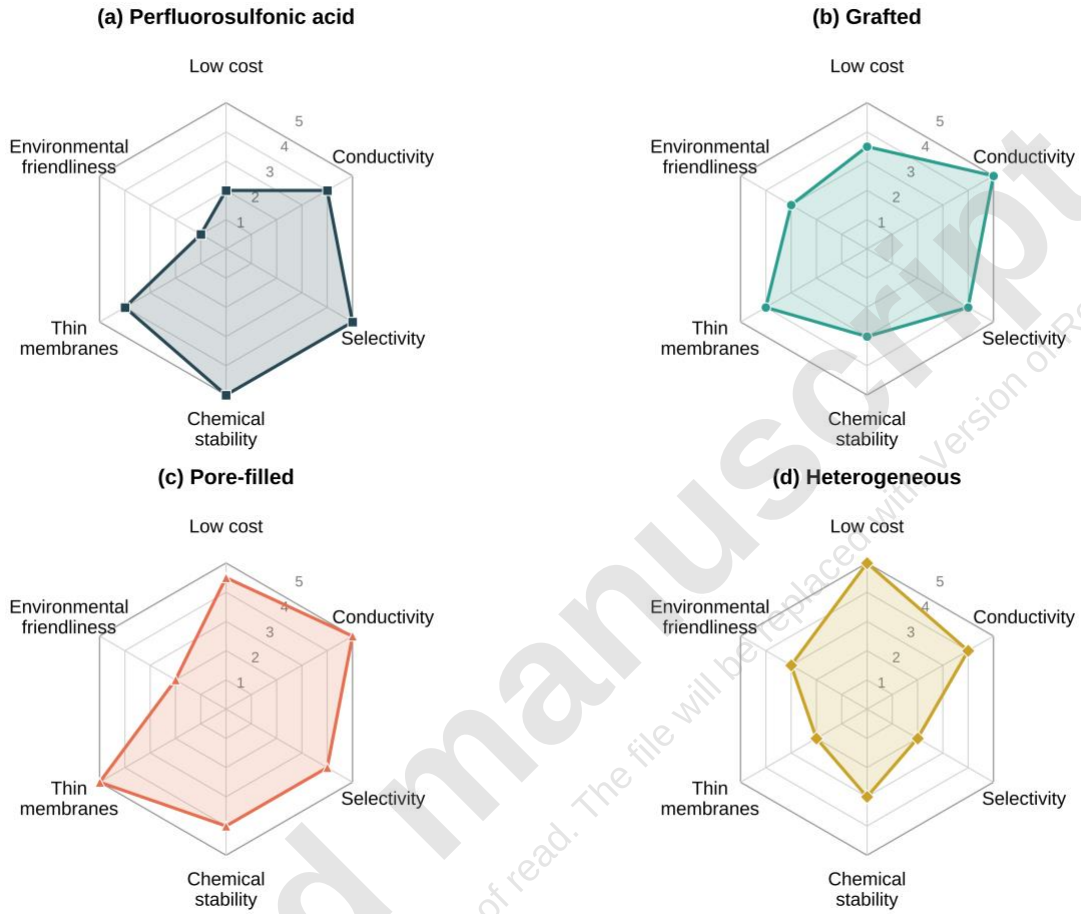


Figure 6. Comparison of the key properties (ionic conductivity, selectivity, chemical stability, possibility of producing thin membranes with acceptable mechanical properties, environmental friendliness, and low cost) of different classes of cation-exchange membranes: (a) perfluorosulfonic acid, (b) grafted, (c) pore-filled, and (d) heterogeneous. Expert assessment on a scale from 1 to 5, where 5 corresponds to the best value among all membrane types

4. Practical applications

Environmental degradation and global warming are among the major challenges facing modern society.[231,232] In this regard, much attention is being paid to renewable energy sources, such as solar and wind energy, which are expected to become the basis of the world energy supply by the middle of the 21st century. However, their integration into large-scale power generation requires energy storage systems, primarily metal-ion batteries and the hydrogen cycle.[10,233–235] Flow batteries, especially vanadium redox flow batteries, are also in growing demand.[236–239] At the same time, new technologies for converting

Accepted manuscript
This manuscript will be edited, formatted and proof read. The file will be replaced with Version of Record.

renewable energy are emerging, among which reverse electrodialysis deserves particular mention, which has been extensively studied.[240–242]

Progress in these energy storage and generation technologies is constrained either by poor membrane properties or by high membrane costs. New, relatively cheap membranes with improved properties are therefore needed, and GMs or PFMs could fill this niche in a number of applications.[37,243] Similar needs are typical for other technologies, including conventional ones that use ion-exchange membranes and are now facing new challenges. In electrodialysis, for example, there is a growing demand not only for water purification but also for the recovery of valuable components from wastewater, which requires separating ions of the same charge but different valence (e.g., mono- and divalent ions).[244–246] The following sections briefly describe the principal prospective applications of grafted and pore-filled membranes. In addition to these electromembrane processes, grafted and pore-filled membranes are used in pervaporation[247], separation of saturated and unsaturated hydrocarbons[248], potentiometric sensors[249], etc. The main applications of grafted and pore-filled membranes considered in this review are shown in Fig. 7.

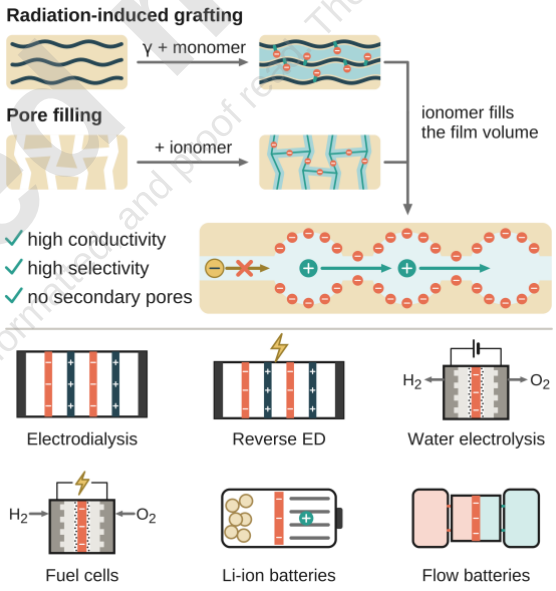


Figure 7. Schematic of the preparation of grafted and pore-filled ion-exchange membranes, their key properties, and main applications

4.1. Electrodialysis

Clean water is one of the most essential resources for quality of life and public health.[250] In recent years, membrane technologies such as reverse osmosis and electrodialysis (ED) have been replacing conventional methods of desalination and water

purification.[251–261] Electrodialysis, one of the first applications of ion-exchange membranes, has been used in water purification for over 50 years and remains the most important and commercially available process based on ion-exchange membranes.

Electrodialysis offers several advantages, including relatively low energy consumption, a simple design, reagent-free operation, and environmental friendliness.[262–270] These advantages explain why ED is widely used in modern industry, in applications such as food production[271,272], chemical production[273–275], seawater desalination[276,277], wastewater treatment[278–280], and even carbon dioxide capture[281,282].

Electrodialysis setups consist of alternating concentrate and dilute compartments separated by cation- and anion-exchange membranes (Fig. 8). Under a direct-current voltage, cations and anions from the dilute compartments move through their respective membranes into the concentrate compartments, allowing fresh water and concentrated brines to be produced simultaneously.[263,265,283] Ion-exchange membranes used in ED must have high ionic conductivity* and selectivity. Here, selectivity refers to the membrane ability to transport ions of one charge sign while blocking those of the opposite sign. It is typically characterized by transport numbers, which represent the fraction of the total current carried by cations or anions.[284–286] In addition, membranes must be chemically stable and inexpensive.[287] For this reason, ED typically relies on relatively cheap heterogeneous membranes, despite their low selectivity. In contrast, using selective homogeneous membranes such as Nafion would significantly increase the cost of the products. In this regard, developing membranes that combine high conductivity and selectivity with low cost is critical for ED.[288,289]

Accepted manuscript
This manuscript will be edited for style, and proof read. The final version may be published with Version of Record.

* In some cases, the membrane area resistance ($\Omega\ cm^2$), i.e., the electrical resistance of 1 cm^2 of the membrane, is reported instead of conductivity. It equals the ratio of the membrane thickness to its conductivity; therefore, thin membranes can have a low area resistance even at moderate conductivity.

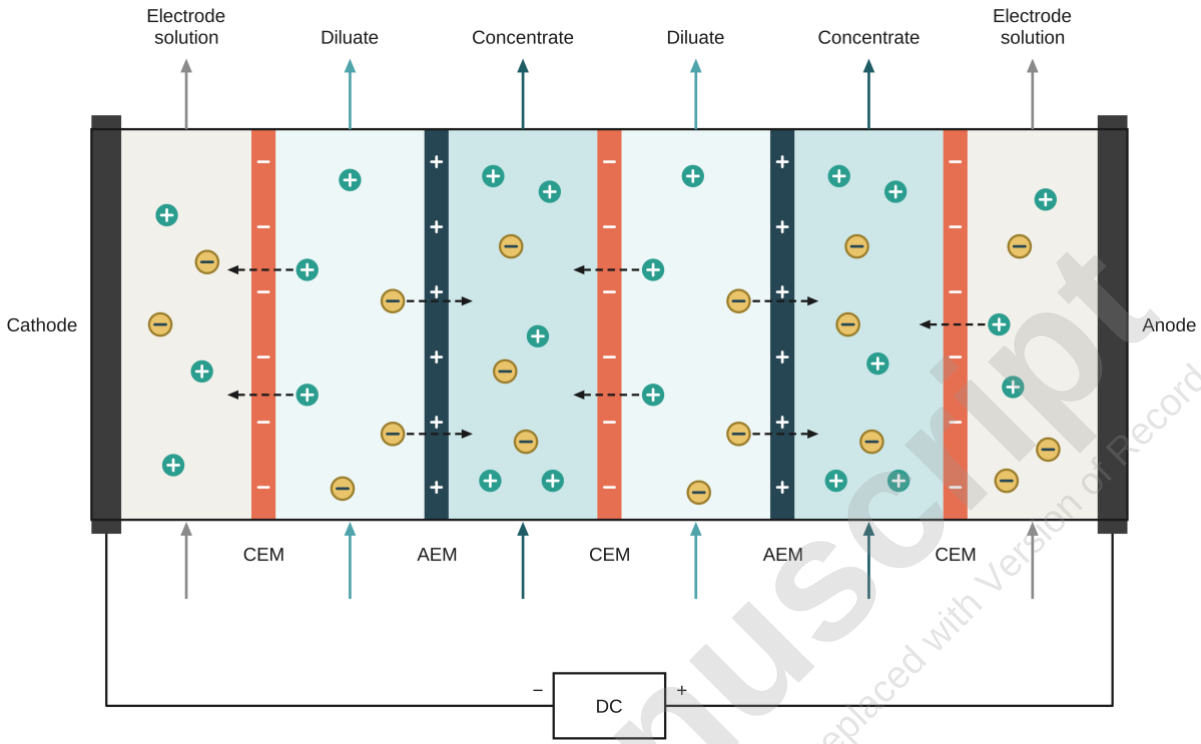


Figure 8. Schematic of an electrodialysis setup

Relatively inexpensive grafted and pore-filled membranes meet the above criteria and therefore appear to be near-ideal candidates for electrodialyzers. Their synthetic flexibility (the ability to vary both the base and incorporated polymers) allows achieving high selectivity, conductivity, and desalination efficiency. Examples of their successful use in water purification and other applications are reported elsewhere.[25,290–292] Many studies report desalination efficiencies of up to 92%, exceeding those of commercial membranes.[229] Moreover, because a rigid porous matrix and crosslinking agents can effectively limit membrane swelling, some of these materials can be fabricated as thin membranes with high ionic conductivity and good selectivity. This intensifies the electrodialysis process, improving both water purity and the degree of brine concentration.[290,293]

In recent years, considerable attention has been paid to the extraction of valuable or harmful components from brines. Examples include lithium extraction from natural brines[18,294–297] or spent batteries[298,299], seawater concentration by electrodialysis for sodium chloride production[300], acid production from hydrometallurgical waste[301–303] and other processes[15,17,304].

Solving these problems requires membranes with increased selectivity for monovalent ions.[245,305–311] Recent strategies include doping membranes with inorganic or

Accepted manuscript
This manuscript will be edited, formatted and proofread. The file will be replaced with Version of Record.

organic nanoparticles with high affinity for polyvalent ions[245,305,309,312–314] or reducing pore size to hinder transport of polyvalent ions, which have higher hydration energies and larger hydrated radii[15,315,316].

A further extension of this approach is the creation of GMs and PFMs, in which swelling is limited by a rigid matrix or by cross-linking. This effectively restricts the pore and channel sizes, thereby improving selectivity for the transport of monovalent ions.[317,318] The choice of grafted monomer (styrene vs. vinylbenzyl chloride) makes it possible to control the hydration of functional groups and, consequently, the selectivity for chloride–sulfate and nitrate–sulfate separation in grafted anion-exchange membranes.[318] For example, Ul Afsar et al. reported a very high selectivity for the separation of chloride and sulfate ions*, reaching 244 while maintaining high conductivity.[230]

Another intensively developing approach to increasing monovalent ion selectivity is the deposition of alternating layers of oppositely charged polyelectrolytes on the membrane surface.[308,319–326] The improved selectivity is attributed to electrostatic repulsion of polyvalent ions by the like-charged polyelectrolyte layers.[310] Moreover, the formation of "salt bridges" between oppositely charged functional groups leads to the formation of a thin "zero-charged" interfacial layer[317] that is more hydrophobic and has a near-zero concentration of charge carriers. The minimal water content and small transport channels in this layer hinder the transport of divalent ions, which are larger when hydrated, yielding high monovalent selectivity.[16] However, such multilayer membranes have lower ionic conductivity, which reduces the performance of electrodialysis units. To improve selectivity for monovalent ions, a single polyelectrolyte layer with a charge opposite to that of the bulk may be sufficient. This approach reduces the resistance of zero-charge regions without significantly lowering ionic conductivity. In grafted membranes, it was achieved by adjusting the functionalization conditions of the grafted polymer. For example, the resulting membranes have sulfonic acid groups only in the near-surface layer, while the membrane bulk contained quaternary amino groups.[317,327] This gave high selectivity for the chloride-sulfate pair (6.4) while maintaining high ionic conductivity (11.2 mS cm^{-1}).[317,327]

Membrane selectivity for monovalent ions can also be improved by creating a non-uniform distribution of functional groups within the matrix of grafted or pore-filled

* Permselectivity of a membrane for ion A relative to ion B with the same charge sign, $P(A/B)$, is the ratio of their transport numbers in the membrane divided by the ratio of their concentrations in the solution; values greater than 1 indicate preferential transport of ion A.

Accepted manuscript
This manuscript will be edited, formatted, and proofread. The final version may vary from the accepted manuscript.

membranes.[291,308,328–332] This strategy was recently demonstrated[67]: a low concentration of sulfonated polystyrene in a thin central region of the base film gave the grafted membrane enhanced selectivity for monovalent ions. Surface modification of cation-exchange membranes with weakly basic polyaniline increased monovalent ion selectivity further.[67] Grafting 3-bromopropyltrimethylammonium bromide onto a polyethyleneimine/trimesoyl chloride nanofiltration membrane achieved 99.2% magnesium chloride rejection while maintaining high lithium permeability.[333] Additional examples of grafted and pore-filled membranes used in electrodialysis units are summarized in Table 1.

Accepted manuscript
This manuscript will be edited, formatted, and proof read. The file will be replaced with Version of Record

Table 1. Properties and performance of some reported cation- and anion-exchange membranes (CEMs and AEMs) in electrodialysis

Base film (thickness, μm)	Grafted polymer (GD, %) / Filler	Preparation method	IEC, mmol g^{-1}	Membrane area resistance, Ω cm^2[b]	Performance	Test conditions[a]	Ref.
CEMs							
polyketone (75)	sodium styrene sulfonate (14.4–81.4)	γ-radiation-induced graft polymerization	0.43–1.10	2.2–12.0	salt removal rate 87.6 %	membrane capacitive deionization cell feed solution: 250 mg L^{-1} NaCl adsorption potential: +1.5 V (120 s) desorption potential: -1.5 V (180 s)	334
polyvinylidene fluoride (50)	polystyrene (50, 120)	post γ-radiation-induced emulsion graft polymerization	1.7–3.4	conductivity 11–28 mS cm^{-1}	P(Na/Mg) = 3.69 P(Li/Mg) = 2.36	six chamber ED stack DC 0.01 M $NaNO_3$, 0.01 M $LiNO_3$, 0.01 M $Mg(NO_3)_2$, 0.01 M $Ca(NO_3)_2$ CC 0.04 M KNO_3 EC 0.2 M K_2SO_4 current density 1.88 mA cm^{-2}	67
poly(ethylene-co-tetrafluoroethylene) (100)	ethyl styrenesulfonate (15–60.7)	post γ-radiation-induced graft polymerization	0.55–1.73	conductivity 46–225 mS cm^{-1}	salt removal rate 97.6–99.9%	three chamber ED stack DC: 0.5 M $CsNO_3$ EC: 0.5 M $CsNO_3$	335
porous bromomethylated poly(2,6-dimethyl-1,4-phenylene oxide) (ND)	sulfonated poly(2,6-dimethyl-1,4-phenylene oxide)	impregnation with polymer solution	ND	9.7–18.5	P(Na/Mg) = 0.80–1.62	four chamber ED stack DC and CC: 0.1 M NaCl and 0.1 M $MgCl_2$ EC: 0.3 M Na_2SO_4 current density: 14 mA cm^{-2}	336
porous poly(ether sulfone) (200)	sulfonated poly(ether sulfone) and ethylene glycol	asymmetric casting	0.21–0.52	3.11–10.22	NaCl removal 71.0–91.9 % current efficiency 99.8–127.5 % energy consumption 5.55–7.05 kW h kg^{-1}	four chamber ED stack DC and CC: 0.1 M NaCl CC: 0.1 M HCl EC: 0.3 M Na_2SO_4	229
porous polytetrafluoroethylene (35)	sodium 4-vinylbenzenesulfonate and N,N′-methylenebis(acrylamide)	soaking in monomer solutions followed by UV-polymerization	1.97–2.59	1.3–2.3	desalination rate 86.7–93.4% energy consumption 9.4–13.8 kW h kg^{-1} energy efficiency 70.0–94.6%	six chamber ED stack DC and CC: 0.1 M NaCl EC: 0.3 M Na_2SO_4 current density 28 mA cm^{-2}	172
porous polyvinyl chloride-SiO_2 (360±20)	potassium 3-sulfopropyl methacrylate, acrylic acid, hex-functional polyester acrylate and bi-functional epoxy acrylate oligomers	blade coating followed by UV-initiated radical crosslinking	0.29–0.31	6.15–11.02	selectivity 87.91–97.04% current efficiency 91.87–95.10% desalination rate 49–56% cell resistance 5.66–6.31 Ω	six chamber ED stack DC and CC: 5 g L^{-1} NaCl EC: 10 g L^{-1} Na_2SO_4 voltage-controlled mode (5 V)	290
anodic aluminum oxide (ND)	nanosheets of metal-hydroxide-porphin framework based on meso-tetra(4-carboxyphenyl) porphine molecules linked with nickelous hydroxide	vacuum filtering	ND	ND	Li^+ permeability 0.019 mol m^{-2} h^{-1} Na^+ permeability 0.462 mol m^{-2} h^{-1}	two chamber ED stack DC: 0.05 M NaCl and 0.05 LiCl, 0.05 M KCl and 0.05 LiCl, 0.05 M	337

Accepted manuscript
This manuscript will be edited, formatted, and proof read. The file will be replaced with Version of Record.

					K^+ permeability 0.334 mol m^{-2} h^{-1} Mg^{2+} permeability 0.067 mol m^{-2} h^{-1} Ca^{2+} permeability 0.098 mol m^{-2} h^{-1}	MgCl2 and 0.05 M LiCl, 0.05 M CaCl2 and 0.05 M LiCl CC: deionized water voltage-controlled mode (0.1, 0.5, 0.8 V)	
AEMs							
poly(ethylene-co-tetrafluoroethylene) (25)	polystyrene (25) or poly(vinylbenzyl chloride) (64, 130)	post γ-radiation-induced emulsion graft polymerization	1.01–1.90	conductivity 2.1–11.8 mS cm^{-1}	$P(NO_3/Cl)$ 1.00–1.25 $P(NO_3/SO_4)$ 1.50–2.25 $P(Cl/SO_4)$ 1.50–1.75	six chamber ED stack DC 0.014 M NaCl, 0.014 M $NaNO_3$, 0.014 M Na_2SO_4 CC 0.042 M $NaHCO_3$ EC 0.2 M Na_2SO_4 current density 1.88 mA cm^{-2}	318
polyvinylidene fluoride (50)	polystyrene (39) or poly(vinylbenzyl chloride) (18)	post γ-radiation-induced emulsion graft polymerization	0.64–1.51	conductivity 0.20–4.0 mS cm^{-1}	$P(NO_3/Cl)$ 1.25–1.60 $P(NO_3/SO_4)$ 1.88–2.10 $P(Cl/SO_4)$ 1.13–1.63	six chamber ED stack DC 0.014 M NaCl, 0.014 M $NaNO_3$, 0.014 M Na_2SO_4 CC 0.042 M $NaHCO_3$ EC 0.2 M Na_2SO_4 current density 1.88 mA cm^{-2}	318
polymethylpentene (ND)	polystyrene crosslinked with divinylbenzene (ND)	post UV-induced emulsion graft polymerization	1.8–1.9	ND	$P(Cl/SO_4)$ 0.52–5.6	four chamber ED stack DC and CC: 0.02/0.05/0.1 M XCl + 0.02/0.05/0.1 M X_2SO_4 ($X=H^+$, Na^+, Cs^+) EC: 0.2 M Na_2SO_4	317
poly(ethylene-co-tetrafluoroethylene) (100)	chloromethyl styrene (15–54.9)	post γ-radiation-induced graft polymerization	0.65–1.88	conductivity 11–31 mS cm^{-1}	salt removal rate 97.6–99.9%	three chamber ED stack DC: 0.5 M $CsNO_3$ EC: 0.5 M $CsNO_3$	335
nonwoven polyester fabric (100)	methyl methacrylate and chloromethyl styrene blended with polyvinylidene fluoride	blade coating and non-solvent induced phase inversion	1.00–1.85	2.78–3.02	energy consumption: 0.978–1.411 kW h kg^{-1} current efficiency: 66–94%	three chamber ED stack DC: 2000 mg L^{-1} NaCl CC: EC: diluted Na_2SO_4 voltage-controlled mode (10V/cell pair)	338
porous polyvinyl chloride-SiO_2 (360±20)	[2-(acryloyloxy)ethyl]trimethylammonium chloride, hydroxyethyl methacrylate, hex-functional polyester acrylate and bi-functional epoxy acrylate oligomers	blade coating followed by UV-initiated radical crosslinking	1.13–1.17	5.22–6.44	selectivity 88.30–93.72% current efficiency 91.87–95.10% desalination rate 49–56% cell resistance 5.66–6.31 Ω	six chamber ED stack DC and CC: 5 g L^{-1} NaCl EC: 10 g L^{-1} Na_2SO_4 voltage-controlled mode (5 V)	290
porous polytetrafluoroethylene (35)	ionic liquid tricapryl(methyl) ammonium chloride, poly(ethylene glycol) dimethacrylate and poly(vinylidene fluoride-co-hexafluoropropylene)	solvent casting followed by UV-polymerization	0.2–0.9	3.4–7.0	$HCrO_4^-$ flux (90.7 μmol m^{-2} s^{-1}) energy consumption (3.9 kW h kg^{-1})	four chamber ED stack DC: 250 mg L^{-1} Cr(VI) solution in 0.1 M HCl CC: 0.1 M HCl EC: 0.1 M H_2SO_4 current density: 1, 3, 5, 7, 10, 15 mA cm^{-2}	293
porous polyethylene (9 ± 2)	solution of octadecyl hydrophobic long chain modified series-connected aliphatic di-cation ionomer	impregnation with ionomer solution	1.34–2.05	1.3–2.2	current efficiency (91.3–94.4 %), NaCl flux (83.1–85.9 mg m^{-2} s^{-1}), energy consumption (1.50 – 2.20 kW h kg^{-1})	four chamber ED stack DC and CC: 0.1 M NaCl EC: 0.3 M Na_2SO_4 current density: 15 mA cm^{-2}	291

Accepted manuscript
This manuscript will be edited, formatted and proofread before it is published in its final version of Record.

porous polyethylene (9 ± 2)	solution of modified with hydrophobic side alkyls octadecyl hydrophobic chains modified linear di-cation ionomer	impregnation with ionomer solution	2.04–3.01	1.06–3.22	desalination rate 77.20% current efficiency 95.45% NaCl flux 81.02 mg m−2 s−1 energy consumption 1.61 kW h kg−1	four chamber ED stack DC and CC: 0.1 M NaCl EC: 0.3 M Na_2SO_4 current density: 15 mA cm^{-2}	339
porous polytetrafluoroethylene (ND)	poly(vinylidene fluoride-co-hexafluoropropylene) and trioctylamine	impregnation with polymer solution	ND	161.4–2259	P(Bi/Cu)=483.9 P(Bi/Ni)=40499.7 P(Bi/Co)=27663.1 P(Bi/Fe)=378.3 P(Bi/Cr)=819.1 P(Bi/Mn)=2014.9 P(Bi/Al)=505.6	four chamber ED stack DC: mixed solution containing 50 mg L^{-1} Bi(III), 50 mg L^{-1} Cu(II), 50 mg L^{-1} Ni(II), 50 mg L^{-1} Co(II), 50 mg L^{-1} Fe(III), 50 mg L^{-1} Cr(III), 50 mg L^{-1} Mn(II), 50 mg L^{-1} Al(III) and 0.3 M HCl CC: 0.3 M H_2SO_4 EC: 0.3 M Na_2SO_4 current density: 5 mA cm^{-2}	175
porous polytetrafluoroethylene (ND)	vinyl phosphonic acid and crosslinking agents (polyethyleneglycol dimethacrylate or acrylated thiourea or acrylated tannic acid)	impregnation with monomer solution followed by thermal radical polymerization	0.14–1.90	conductivity 58.3–110.6 mS cm^{-1}	removal efficiency (> 99 %)	two chamber stack DC: 1 ppm Cu(II) CC: 0.01 M H_2SO_4	340
porous polyethylene (16)	(vinylbenzyl)trimethylammonium chloride, styrene and trimethylolpropane triacrylate	impregnation with monomer solutions followed by photo-polymerization	ND	0.17	P(Cl/SO_4) = 1.32	four chamber ED stack DC: 0.01 M NaCl, 0.01 M Na_2SO_4 CC: distilled water EC: 0.1 M Na_2SO_4 was used Current density: 15 A m^{-2}	341

Note. CEMs and AEMs are cation- and anion-exchange membranes; GD is the grafting degree; IEC is the ion-exchange capacity; ED is electrodialysis; *P*(A/B) is the permselectivity of ion A relative to ion B; ND is no data reported.

[a]DC – dilute chamber, CC – concentrate chamber, EC – electrode chambers

[b] For some studies, ionic conductivity (mS cm^{-1}) is given instead of membrane area resistance.

Accepted manuscript
This manuscript will be edited, formatted, and proofread. The file will be replaced by the Version of Record.

4.2. Reverse electrodialysis

Reverse electrodialysis (RED) is the reverse of the ED process: it generates electricity by mixing saline and fresh water.[342] Its stack design (Fig. 9) is similar to that of an electrodialysis unit, with alternating cation-exchange and anion-exchange membranes that provide electrolyte flow between the separated compartments that contain salt and fresh water. At first glance, the practicality of this approach might seem questionable, given the substantial energy required for seawater desalination and industrial wastewater treatment. However, rivers inevitably flow into the sea without any practical benefit. Unlike many other renewable energy sources, RED can generate energy continuously, with far less dependence on seasonal or weather changes.[343] It is therefore reasonable to use this process to power coastal regions or to recover energy from concentrates of desalination plants.[241,242,344–348]

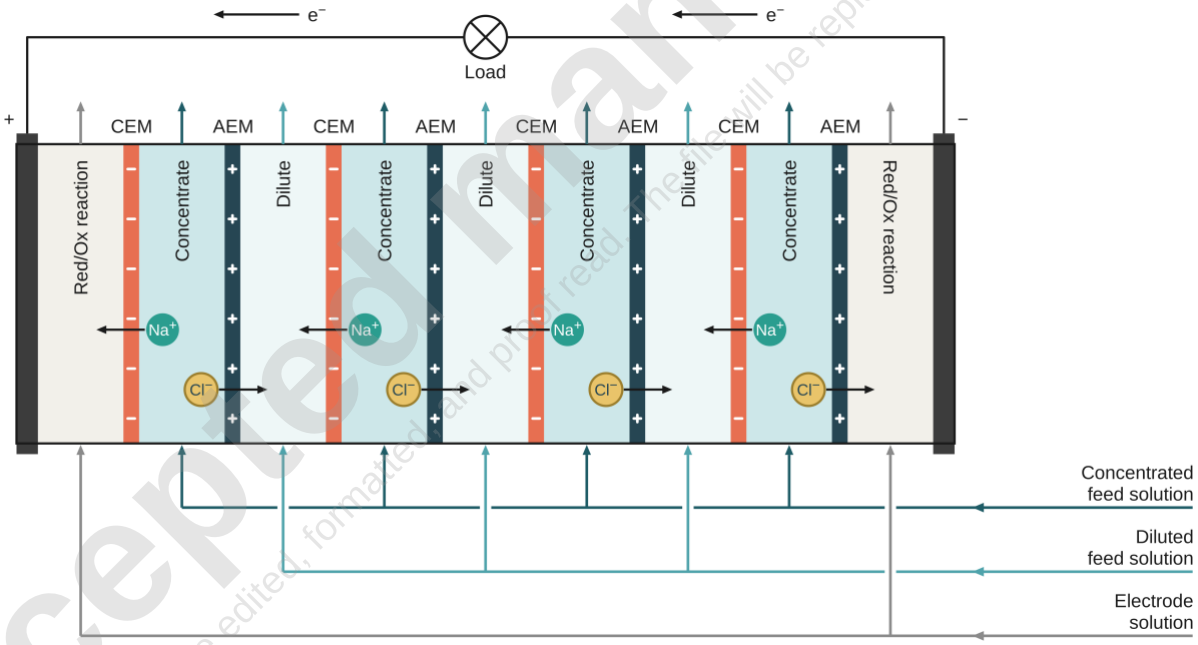


Figure 9. Schematic of the membrane–electrode stack in a reverse electrodialysis unit

The driving force in reverse electrodialysis is determined by the membrane potential, which arises as ions diffuse through the membranes from the salt water compartments into the fresh water compartments.[349–351] The maximum theoretical power of a RED cell is expressed by the following equation[241,351,352]:

$$P_{\max} = \frac{(E_{\mathrm{OCV}})^2}{4R_{\mathrm{c}}}, \qquad (1)$$

Accepted manuscript
This manuscript will be edited, formatted and proofread. The final version will be replaced with version of record.

where E_{OCV} is the open-circuit potential (also referred to as the membrane potential), and R_c is the internal resistance of the cell. The open-circuit potential can be calculated from the Nernst equation:

$$E_{OCV} = \frac{2t_{av}RT}{F} \cdot \ln\left(\frac{a_s}{a_f}\right), \quad (2)$$

where t_{av} is the average transport number of cation- and anion-exchange membranes, R is the gas constant, T is the absolute temperature, F is the Faraday constant, and a_s and a_f are the activities of sodium chloride in salt and fresh water, respectively.

The power output of RED stacks remains low. The best current systems require about 400–500 m^2 of membrane area to produce just 1 kW. Nevertheless, the volumes of water available for mixing are very large and could easily power coastal communities. One limitation is that non-selective diffusion of co-ions across the membranes reduces the membrane potential and with it, the overall power output. Membranes with high selectivity (that is, high transport numbers) and low resistance are therefore required. Although cell resistance is generally thought to be mainly determined by the membrane resistance, at low salt concentrations in fresh water, the water resistance increases and can exceed the membrane resistance.

Relatively inexpensive pseudo-homogeneous membranes, such as those from Fujifilm, Fumatech, and Neosepta, are the most widely used in RED cells, achieving a maximum power of 2.2 W m^{-2}.[341,349,353–357] To increase RED efficiency, very thin membranes are advantageous because of their lower resistance.[222] However, for most membranes, this results in a significant loss of selectivity and tends to have the opposite effect on performance.

As noted earlier, grafted and pore-filled membranes can achieve high selectivity because they have no secondary porosity. However, the water content must also be limited. This can be achieved by using low-deformable base films, keeping moderate grafting degrees, or introducing additional crosslinking into the ion-exchange polymer.[55,58,340,358] Several successful applications of grafted and pore-filled membranes in RED stacks with power densities reaching 1.5–2.4 W m^{-2} have been reported elsewhere.[58,194,222,359–364] The best results were obtained with highly selective membranes, which underscores the key role of selectivity in power generation in RED cells.[58]

It is worth noting that seawater, and especially river water, often contains large amounts of suspended and colloidal particles of both inorganic and organic origin, which

Accepted manuscript
This manuscript will be edited, formatted and proofread. This file will be replaced with Version of Record

can cause rapid membrane fouling. This, in turn, can markedly reduce the performance of a RED stack. For instance, the performance of RED stacks with Nafion 117 and Fuji-CEM-80050 membranes decreases by more than 20% in the presence of magnesium chloride.[348] Anion-exchange membranes are particularly prone to fouling, for example by humic acids and their salts. In some cases, fouling can reduce the performance of a RED unit by more than half within just a few hours of operation.[365,366] Therefore, membranes must have strong fouling resistance.[367,368] Possible mitigation approaches include using membranes selective for monovalent ions and coating membranes with polydopamine or polyaniline.[249,367,369–372] Fouling resistance can also be enhanced by doping with inorganic nanoparticles such as cerium phosphate.[373] Further examples illustrating the use of grafted and pore-filled membranes in reverse electrodialysis are given in Table 2.

Accepted manuscript
This manuscript will be edited, formatted, and proof read. The file will be replaced with Version of Record

Table 2. Properties and performance of some reported CEMs and AEMs in reverse electrodialysis

Base film (thickness, μm)	Grafted polymer (GD, %) / Filler	Preparation method	IEC, mmol g^{-1}	Membrane area resistance, Ω cm^2	Permselectivity	Performance	Test conditions	Ref.
CEMs								
polymethylpentene (50)	polystyrene crosslinked with divinylbenzene (47, 112)	post UV-induced emulsion graft polymerization	1.83–2.70	0.39–2.33	88.2–96.1	power density of 0.47–2.1 W m^{-2} current efficiency 14–88%	four cell pairs RED stack feed solutions: 0.1 M and 1 M NaCl or 0.1 M and 5 M NaCl electrode solution: 0.05 M $K_4Fe(CN)_6$ and 0.05 M $K_3Fe(CN)_6$ in 0.25 M NaCl	58
porous polyethylene (16)	2-acrylamido-2-methyl-1-propanesulfonic acid, 2-Acrylamido-2-methyl-1-propanesulfonic acid sodium salt and piperazine diacrylamide	roll-to-roll process with impregnation and photo-polymerization	1.80	0.42	95.7%	power density of 1.95 W m^{-2}	five cell pairs RED stack feed solutions: 0.017 M and 0.5 M NaCl electrode solution: 0.05 M $K_4Fe(CN)_6$ and 0.05 M $K_3Fe(CN)_6$	360
porous tri-layer of polypropylene-polyethylene-polypropylene (38)	2-acrylamido-2-methyl-1-propanesulfonic acid, 2-Acrylamido-2-methyl-1-propanesulfonic acid sodium salt and piperazine diacrylamide	roll-to-roll process with impregnation and photo-polymerization	1.562	0.82	95.9%	power density of 1.76 W m^{-2} open circuit voltage 0.724 V	five cell pairs RED stack feed solutions: 0.017 M and 0.5 M NaCl electrode solution: 0.05 M $K_4Fe(CN)_6$ and 0.05 M $K_3Fe(CN)_6$	194
porous polyethylene (16)	N,N′-ethylenebis(acrylamide) and acrylamido-2-methyl-1-propanesulfonic acid	impregnation with monomer solutions followed by photo-polymerization	1.41–1.61	0.35–0.51	97.5–99.8	power density of 2.43 W m^{-2}	five cell pairs RED stack feed solutions: 0.017 M and 0.58 M NaCl electrode solution: 0.05 M $K_4Fe(CN)_6$ and 0.05 M $K_3Fe(CN)_6$	222
porous polyethylene (16)	2-acrylamido-2-methyl-1-propanesulfonic acid, 2-acrylamido-2-methyl-1-propanesulfonic acid sodium salt, piperazine diacrylamide and multiwall carbon nanotube	impregnation with monomer solutions followed by photo-polymerization	1.75–2.03	0.39–0.46	90.3–97.8%	power density of 1.695–1.922 W m^{-2} open circuit voltage 0.726–0.736 V	five cell pairs RED stack feed solutions: 0.017 M and 0.5 M NaCl electrode solution: 0.05 M $K_4Fe(CN)_6$ and 0.05 M $K_3Fe(CN)_6$	374

Accepted manuscript
This manuscript will be edited, formatted, and proof read. The file will be replaced with Version of Record.

porous polyethylene (16)	2-acrylamido-2-methyl-1-propanesulfonic acid, 2-acrylamido-2-methyl-1-propanesulfonic acid sodium salt and piperazine diacrylamide	impregnation with monomer solutions followed by photo-polymerization	ND	ND	ND	power density of 1.794–1.870 W m^{-2}	five cell pairs RED stack feed solutions: 0.017 M and 0.5 M NaCl electrode solution: 0.05 M $K_4Fe(CN)_6$ and 0.05 M $K_3Fe(CN)_6$	364
silanized porous anodized aluminum oxide (60)	2-acrylamido-2-methyl-1-propanesulfonic acid and N,N′-methylene-bisacrylamide	impregnation with monomer solutions followed by thermal induced radical polymerization	ND	2.3–4.9	19.2–99.0%	power density of 0.017 W m^{-2}	two cell pairs RED stack feed solutions: 0.017 M and 0.51 M NaCl electrode solution: 0.51 M NaCl	375
porous polyolefin substrate (22)	vinyl sulfonic acid cross-linked with N,N′-ethylenebis(acrylamide)	impregnation with monomer solutions followed by photo-polymerization	2.64	0.34	97.8%	power density of 2.4 W m^{-2}	five cell pairs RED stack feed solutions: 0.017 M and 0.58 M NaCl electrode solution: 0.05 M $K_4Fe(CN)_6$ and 0.05 M $K_3Fe(CN)_6$ in 0.5 M Na_2SO_4 current density: 0–14 A m^{-2}	376
AEMs								
polymethylpentene (50)	polystyrene crosslinked with divinylbenzene (47, 112)	post UV-induced emulsion graft polymerization	1.71–2.15	0.64–1.09	92.9–95.2	power density of 0.47–2.1 W m^{-2} current efficiency 14–88%	four cell pairs RED stack feed solutions: 0.1 M and 1 M NaCl or 0.1 M and 5 M NaCl electrode solution: 0.05 M $K_4Fe(CN)_6$ and 0.05 M $K_3Fe(CN)_6$ in 0.25 M NaCl	58
poly(ethylene-co-tetrafluoroethylene) (50)	poly(vinylbenzyl chloride) crosslinked with divinylbenzene or N,N,N′,N′-tetramethylhexane-1,6-diamine (ND)	post electron-beam irradiation-induced emulsion graft polymerization	1.34–1.76	0.49–2.31	82.4–93.4%	ND	ND	55
porous polyethylene (16)	(3-acrylamidopropyl)trimethylammonium chloride and piperazine diacrylamide	roll-to-roll process with impregnation and photo-polymerization	1.81	0.40	92.4%	power density of 1.95 W m^{-2}	five cell pairs RED stack feed solutions: 0.017 M and 0.5 M NaCl electrode solution: 0.05 M $K_4Fe(CN)_6$ and 0.05 M $K_3Fe(CN)_6$	360

Accepted Manuscript
This manuscript will be edited, formatted, and proof read. The file will be replaced with Version of Record.

porous tri-layer of polypropylene-polyethylene-polypropylene (38)	(3-acrylamidopropyl) trimethylammonium chloride and piperazine diacrylamide	roll-to-roll process with impregnation and photo-polymerization	1.645	0.661	94.3%	power density of 1.76 W m^{-2} open circuit voltage 0.724 V	five cell pairs RED stack feed solutions: 0.017 M and 0.5 M NaCl electrode solution: 0.05 M $K_4Fe(CN)_6$ and 0.05 M $K_3Fe(CN)_6$	194
porous polyethylene (16)	(vinylbenzyl)trimethylammonium chloride, styrene and trimethylolpropane triacrylate	impregnation with monomer solutions followed by photo-polymerization	ND	0.17	99%	power density of 0.379 W m^{-2} open circuit voltage 0.708 V	five cell pairs RED stack feed solutions: 0.459 M NaCl, 0.051 M Na_2SO_4 and 0.0153 M NaCl, 0.0017 M Na_2SO_4 electrode solution: 0.05 M $K_4Fe(CN)_6$ and 0.05 M $K_3Fe(CN)_6$ in 0.25 M Na_2SO_4 current density: 0–14 A m^{-2}	341
porous polyethylene (22)	(vinylbenzyl)trimethylammonium chloride, ethylene glycol diacrylate, dopamine methacrylamide and 1,4-diazabicyclo-[2,2,2]octane	impregnation with monomer solutions followed by photo-polymerization	1.24–1.39	0.717–0.809	87.9–93.8%	power density of 1.335–1.524 W m^{-2}	five cell pairs RED stack feed solutions: 0.017 M and 0.5 M NaCl electrode solution: 0.05 M $K_4Fe(CN)_6$ and 0.05 M $K_3Fe(CN)_6$	359
porous polyethylene (16)	(vinylbenzyl)trimethylammonium chloride and N,N′-bis(acryloyl)piperazine	impregnation with monomer solutions followed by photo-polymerization	1.69	0.23	93.4%	power density of 2.43 W m^{-2}	five cell pairs RED stack feed solutions: 0.017 M and 0.58 M NaCl electrode solution: 0.05 M $K_4Fe(CN)_6$ and 0.05 M $K_3Fe(CN)_6$	222
porous polyethylene (50)	quaternary-aminated polystyrene and quaternary-aminated poly(phenylene oxide) cross-linked with 4,4′-diaminobenzophenone	impregnation with mixture of polymers	1.0–1.2	0.69–1.67	96–97%	power density of 1.82 W m^{-2} open circuit voltage 0.86 V	five cell pairs RED stack feed solutions: 0.00856 M and 0.599 M NaCl electrode solution: 0.05 M $K_4Fe(CN)_6$ and 0.05 M $K_3Fe(CN)_6$ in 0.5 M Na_2SO_4	363

Accepted manuscript
This manuscript will be edited, formatted, and proofread. The file will be replaced with Version of Record.

porous polyethylene (16)	(3-acrylamidopropyl) trimethylammonium chloride, piperazine diacrylamide and multiwall carbon nanotube	impregnation with monomer solutions followed by photo-polymerization	1.78–2.00	0.39–0.47	83.7–90.8%	power density of 1.695–1.922 W m^{-2} open circuit voltage 0.726–0.736 V	five cell pairs RED stack feed solutions: 0.017 M and 0.5 M NaCl electrode solution: 0.05 M $K_4Fe(CN)_6$ and 0.05 M $K_3Fe(CN)_6$	374
porous polyethylene (16)	(3-acrylamidopropyl) trimethylammonium chloride and piperazine diacrylamide	impregnation with monomer solutions followed by photo-polymerization	ND	ND	ND	power density of 1.794–1.870 W m^{-2}	five cell pairs RED stack feed solutions: 0.017 M and 0.5 M NaCl electrode solution: 0.05 M $K_4Fe(CN)_6$ and 0.05 M $K_3Fe(CN)_6$	364
silanized porous anodized aluminum oxide (60)	diallyldimethylammonium chloride and N,N′-methylene-bisacrylamide	impregnation with monomer solutions followed by photo-polymerization	ND	1.4–2.9	49.5–89.3%	power density of 0.017 W m^{-2}	one cell pairs RED stack feed solutions: 0.017 M and 0.51 M NaCl electrode solution: 0.51 M NaCl	375
porous polyethylene (16)	ammonium–acrylamide siloxane resin and (3-acrylamidopropyl)trimethylammonium chloride	impregnation with monomer solutions followed by photo-polymerization	1.568–2.186	0.228–0.323	85.4–95.5%	power density of 1.50 W m^{-2}	five cell pairs RED stack feed solutions: 0.017 M and 0.5 M NaCl electrode solution: 0.05 M $K_4Fe(CN)_6$ and 0.05 M $K_3Fe(CN)_6$	361
porous polyethylene (25)	vinylbenzyl chloride, 2-(dimethylamino)ethyl methacrylate, divinylbenzene and p-xylylene dichloride or 1-allyl-3-methylimidazolium bis(trifluoromethylsulfonyl)imide, 2-(dimethylamino)ethyl methacrylate, divinylbenzene and p-xylylene dichloride	impregnation with monomer solutions followed by photo-polymerization	1.74–2.42	0.54–1.81	95–97%	power density of 0.404–0.446 W m^{-2} open circuit voltage 0.740–0.756 V	five cell pairs RED Stack feed solutions: 0.017 M and 0.513 M NaCl electrode solution: 0.05 M $K_4Fe(CN)_6$ and 0.05 M $K_3Fe(CN)_6$ in 0.25 M Na_2SO_4 current density: 0–14 A m^{-2}	228
porous polyolefin substrate (22)	(vinylbenzyl)trimethylammonium chloride cross-linked with N,N-bis(acryloyl)piperazine	impregnation with monomer solutions followed by photo-polymerization	1.55	0.28	91.8%	power density of 2.4 W m^{-2}	five cell pairs RED stack feed solutions: 0.017 M and 0.58 M NaCl electrode solution: 0.05 M $K_4Fe(CN)_6$ and 0.05 M	376

Accepted Manuscript
This manuscript will be edited, formatted, and proofread. The file will be replaced with Version of Record.

							$K_3Fe(CN)_6$ in 0.5 M Na_2SO_4 current density: 0–14 A m^{-2}	

Note. GD is the grafting degree; IEC is the ion-exchange capacity; RED is reverse electrodialysis; ND is no data reported.

Accepted manuscript
This manuscript will be edited, formatted, and proof read. The file will be replaced with Version of Record.

4.3. Hydrogen energy

Using hydrogen as a fuel provides several advantages, including high energy density, high efficiency, and environmental friendliness. The growing scientific interest in hydrogen energy is largely driven by national hydrogen programs launched in several leading countries.[10,377–381] The primary objectives of these programs are hydrogen production and electricity generation through its oxidation. Currently, most hydrogen is produced by steam methane reforming.[382,383] This approach is cheaper, but it produces high emissions of carbon oxides, including carbon monoxide, which poisons catalysts of low-temperature fuel cells. Hydrogen produced this way therefore requires thorough purification to ensure efficient fuel cell operation, which significantly increases costs. Water electrolysis powered by renewable energy is one of the most promising routes to hydrogen production, as it fits well within a carbon-free economy.[384–386] Electrolysis has considerable potential, even though hydrogen produced in this way is currently 2–4 times more expensive than hydrogen from natural gas.[387] There are four main methods of water electrolysis: (1) proton exchange membrane electrolysis, (2) alkaline electrolysis, (3) high-temperature solid oxide electrolysis, and (4) microbial electrolysis.[386,388–392] Alkaline electrolysis uses a porous separator filled with a concentrated alkali solution as an electrolyte. Although this technology is easy to implement and industrially mature, it has several disadvantages, including low current efficiency and the use of carcinogenic separator materials, such as asbestos.[392,393] High-temperature electrolyzers based on ceramic membranes, by contrast, have a significantly lower level of technological readiness.[392] Moreover, their implementation is complicated by the high operating temperatures and long start-up times, which severely limit their practical application.

Given the main topic of this review, the discussion below focuses mainly on low-temperature electrolysis: proton-exchange membrane (PEM) water electrolysis and anion-exchange membrane (AEM) water electrolysis. Compared with the technologies described above, these processes are easier to operate, produce hydrogen more efficiently, and consume less energy.[394–396] In essence, they differ only in the type of membrane used, which is either cation-exchange or anion-exchange. In both cases, hydrogen is produced at the cathode and oxygen at the anode, but the ions that carry the current through the membrane differ (Fig. 10).

Accepted manuscript
This manuscript will be edited, formatted, and proofread. The final version may vary from this version.

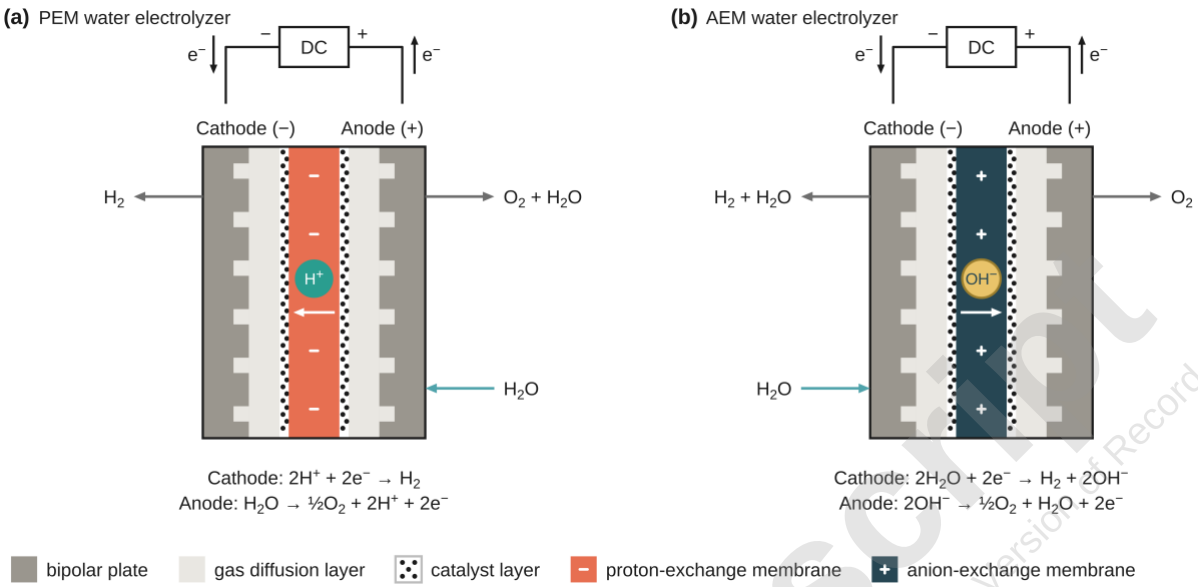


Figure 10. Schematic of the operation of PEM (a) and AEM (b) water electrolyzers

PEM water electrolysis requires materials with high chemical stability, which is why expensive noble metal-based electrocatalysts and perfluorinated membranes such as Nafion are typically used.[397,398] Because the operating potential is lower in an alkaline medium, AEM water electrolysis does not rely on costly noble metal-based electrocatalysts and allows the use of non-perfluorinated ion-exchange membranes.[399–401] However, a disadvantage of AEM water electrolysis is that the kinetics of the hydrogen evolution reaction is a 2–3 orders of magnitude slower.[402–404] PEM water electrolyzers, by contrast, offer high performance and safe operation.[405–407]

Electrolyzers require membranes with high proton or hydroxide conductivity and low gas crossover.[408] Grafted and pore-filled membranes generally meet these requirements. However, the high overvoltage in electrolyzers creates a large potential difference across the membranes, causing degradation of the base polymer, the grafted polymer or both. Nevertheless, GMs and PFMs can be successfully used in both PEM[409,410] and AEM[223,395,411] water electrolyzers. In PEM electrolyzers, pore-filled membranes based on perfluorinated cation-exchange membranes are the more common choice, whereas AEM electrolyzers typically use composite membranes with inorganic fillers to improve stability. The use of perfluorinated polymers for the fabrication of grafted and pore-filled membranes for electrolyzers is a promising way to improve stability, despite their significantly higher cost. Additional examples of grafted and pore-filled membranes used in electrolysis units are summarized in Table 3.

Accepted manuscript
This manuscript will be edited, formatted, and proofread. There may be changes before it is published in its final form.

Table 3. Properties and performance of some reported ion-exchange membranes in water electrolysis

Base film (thickness, μm)	Grafted polymer (GD, %) / Filler	Preparation method	IEC, mmol g^{-1}	Conductivity, mS cm^{-1}[a]	Performance	Test conditions	Ref.
CEMs							
poly(ethylene-co-tetrafluoroethylene) (50)	copolymers of styrene and acrylonitrile (40, 41) or styrene, acrylonitrile and 1,3-diisopropenylbenzene (39, 41)	post electron-beam irradiation-induced dispersion graft polymerization	1.15–1.29	membrane area resistance 100–140 mΩ cm^2	cell voltage 1.47 V (100 mA cm^{-2}, 80 °C)	feed: H_2O temperature: 80 °C anode: Ti porous sinter, IrO_2 cathode: carbon paper, Pt/C	412
poly(ethylene-co-tetrafluoroethylene) (50)	copolymers of styrene and acrylonitrile (40), styrene, acrylonitrile and 1,3-diisopropenylbenzene (40),α-methylstyrene and acrylonitrile (40),α-methylstyrene, acrylonitrile and 1,3-diisopropenylbenzene (40)	post electron-beam irradiation-induced dispersion graft polymerization	1.20–1.65	ND	ND	feed: H_2O temperature: 80 °C anode: Ti porous sinter, IrO_2 cathode: carbon paper, Pt/C	413
porous polysulfone (ND)	commercial Aquivion® dispersion	two-side casting of polymer solution	ND	150–320 (in-plane, 80 °C, RH=95%)	cell voltage 1.436 V (0.2 A cm^{-2}, 80 °C), 1.57 V (1 A cm^{-2}, 80 °C), 1.76 V (2 A cm^{-2}, 80 °C), 1.390 V (0.2 A cm^{-2}, 120 °C), 1.515 V (1 A cm^{-2}, 120 °C), 1.631 V (2 A cm^{-2}, 120 °C)	feed: H_2O temperature: 80/120 °C anode: $Ir_{0.7}Ru_{0.3}O_X$, Nafion® ionomer cathode: Pt/C, Aquivion® ionomer	398
porous polytetrafluoroethylene (ND)	commercial Aquivion® dispersion	impregnation with polymer solution	ND	2 (in-plane, 80 °C, RH=20%) 170 (in-plane, 80 °C, RH=120%)	cell voltage 1.8 V (5 A cm^{-2}, 80 °C)	feed: H_2O temperature: 30–90 °C anode: $IrRuO_X$, Aquivion® ionomer cathode: Pt/C, Aquivion® ionomer	410
poly(ether-ether-ketone) mesh (50, 72)	sulfonated poly(phenylene sulfone)	two-side casting of polymer solution	1.92, 2.36	128	cell voltage 1.8 V (3.2 A cm^{-2}, 80 °C)	feed: H_2O temperature: 80 °C anode: IrO_2, Nafion® ionomer cathode: Pt/C, Nafion® ionomer	414
AEMs							
polyethylene (75)	vinylbenzyl chloride (65.6)	γ-radiation-induced graft polymerization	2.3	90 (through-plane, 50 °C, RH=100%)	cell voltage 1.65 V (100 mA cm^{-2}, 60 °C)	feed: 0.01/0.1/1 M NaOH temperature: 20–80 °C anode: Ti fiber felt, lab-made ionomer, lab-made $NiCo_2O_4$ or commercial catalysts	415

Accepted manuscript
This manuscript will be edited, formatted, and proof read. The file will be replaced with Version of Record.

						cathode: carbon mesh, Pt/C, lab-made ionomer	
polyethylene (25, 50, 125)	vinylbenzyl chloride (48–120)	post electron-beam irradiation-induced emulsion graft polymerization	1.69–2.70	115–188 (in-plane, OH^-, 60 °C, RH=90%)	cell voltage 1.67–1.74 V (0.5 A cm^{-2}), 1.78–1.92 V (1 A cm^{-2})	feed: 1 M KOH temperature: 60 °C anode: bare metal stainless steel felt cathode: Ni felt, Pt/C, AEMION ® ionomer	71
poly(ethylene-co-tetrafluoroethylene) (25, 50)	vinylbenzyl chloride (52–81)	post electron-beam irradiation-induced emulsion graft polymerization	1.75–2.16	121–163 (in-plane, OH^-, 60 °C, RH=90%)	cell voltage 1.67–1.69 V (0.5 A cm^{-2}), 1.79–1.82 V (1 A cm^{-2})	feed: 1 M KOH temperature: 60 °C anode: bare metal stainless steel felt cathode: Ni felt, Pt/C, AEMION ® ionomer	71
porous polybenzimidazole (22)	bromomethylated poly(terphenylene)	two-side casting of polymer solution	1.57	30–50 (through-plane, KOH aqueous solution, RT) 49–65 (in-plane, DI water)	cell voltage 1.98V (0.25 A cm^{-2}, 1 M KOH)	feed: 0.01/0.1/1 M KOH temperature: 50 °C anode: $Ni_XFe_YO_Z$, lab-made ionomer cathode: Mo_2C, lab-made ionomer	416
porous polyethylene (25)	(3-acrylamidopropyl) trimethylammonium chloride or (vinylbenzyl)trimethylammonium chloride cross-linked with 1,4-bis(acryloyl)piperazine or trimethylolpropane trimethacrylate	impregnation with monomer solution followed by photo-polymerization	1.43–1.80	39–62 (1 M KOH aqueous solution, RT)	current density 0.477–0.583 A cm^{-2} (1.75 V)	feed: 1 M KOH temperature: 60 °C anode: IrO_2, Nafion D521 ionomer cathode: Pt/C, Nafion D2021 ionomer	223
porous polyethylene (25)	poly(biphenyl piperidinium)	impregnation with polymer solution	0.75–1.88	5–15 (in-plane, OH^-, 30 °C) 17–42 (in-plane, OH^-, 80 °C)	current density 0.23–0.8 A cm^{-2} (1.8 V, 80 °C)	feed: 1 M KOH temperature: 50–80 °C anode: lab-made Ni/Fe catalyst, lab-made ionomer cathode: Pt/C, lab-made ionomer	150
porous polypropylene (95)	(vinylbenzyl) trimethylammonium chloride cross-linked with 1,3,5-triacryloylhexahydro-1,3,5-triazine or trimethylolpropane trimethacrylate	impregnation with monomer solution followed by photo-polymerization	1.54–1.57	71.4–98.7 (OH^-, 60 °C, 1 M KOH aqueous solution)	current density 0.285–0.339 A cm^{-2} (1.9 V, 60 °C)	feed: 1 M KOH temperature: 60 °C anode: IrO_2, PiperION® ionomer cathode: Pt/C, PiperION® ionomer	417
porous polytetrafluoroethylene (20, 50, 100)	vinylbenzyl chloride and 1-vinylimidazole aminated with 1,2-dimethylimidazole	impregnation with monomer solution followed by thermal induced radical polymerization	1.3–2.5	7.5–39.5 (in-plane, OH^-, 25 °C) 18.4–79.1 (in-plane, OH^-, 80 °C)	current density 1.03–1.9 A cm^{-2} (2.0 V, 60 °C), 1.31–2.4 A cm^{-2} (2.0 V, 80 °C)	feed: 1 M KOH temperature: 60/80 °C anode: IrO_2, PiperION® ionomer cathode: PtRu/C, PiperION® ionomer	174

Accepted manuscript
This manuscript will be edited, formatted, and proof read. The final version replaced with Version of Record.

porous polytetrafluoroethylene (38)	1,3,5-tris(bromomethyl)benzene and 4,4′-trimethylenebis(1-methylpiperidine	impregnation with monomer solution	1.5, 2.2	69 (in-plane, OH^-, 25 °C) 138 (in-plane, OH^-, 80 °C)	current density 0.9 A cm^{-2} (1.8 V, 80 °C, $NiFe_2O_4$/NiFeCo/ Nafion ionomer), 3.0 A cm^{-2} (2 V, 80 °C, $NiFe_2O_4$/NiFeCo/ Nafion ionomer), 6.24 A cm^{-2} (1.8 V, 80 °C, IrO_2/PtRu/C/lab-made ionomer), 11.85 A cm^{-2} (2 V, 80 °C, IrO_2/PtRu/C/lab-made ionomer)	feed: 5 wt.% KOH temperature: 60/80 °C anode: IrO_2 or $NiFe_2O_4$, lab-made ionomer or Nafion® ionomer cathode: PtRu/C or NiFeCo, lab-made ionomer or Nafion® ionomer	418

Note. GD is the grafting degree; IEC is the ion-exchange capacity; RH is relative humidity; RT is room temperature; DI water is deionized water; ND is no data reported.

[a] For some studies, membrane area resistance is given instead of conductivity.

Accepted manuscript
This manuscript will be edited, formatted, and proof read. The file will be replaced with the Version of Record.

Fuel cells are electrochemical devices that generate electricity by oxidizing hydrogen[419] or hydrogen-containing fuels such as methanol[420] or formic acid[421] with oxygen. Compared with conventional internal combustion engines, they offer higher efficiency and are more environmentally friendly because the only byproduct is water (or water and carbon dioxide when methanol or formic acid is used).[422]

The basic design of a fuel cell is generally similar to that of an electrolyzer (Fig. 11), but the processes are reversed. In a proton-exchange membrane fuel cell (PEMFC), for instance, hydrogen is dissociatively adsorbed on the anode catalyst and splits into protons and electrons, giving the anode a negative charge. Driven by the electrochemical potential gradient, protons migrate through the membrane to the cathode, where they combine with oxygen to form water.[423,424] A positive charge remains on the cathode, which generates an open-circuit voltage of approximately 1 V.

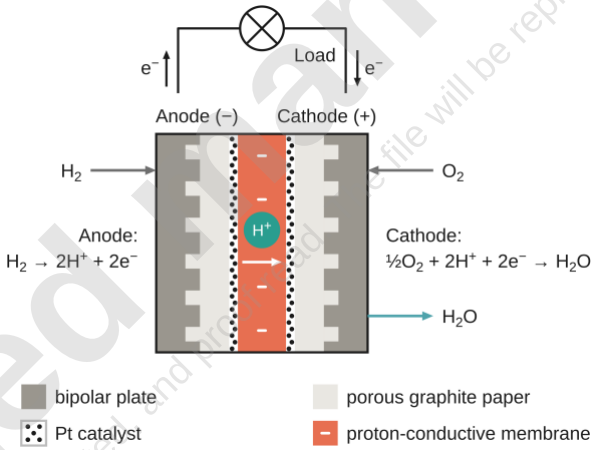


Figure 11. Schematic of the operation of a hydrogen–oxygen PEM fuel cell

The requirements for membranes used in fuel cells are similar to those for electrolyzers: high ionic conductivity and low permeability to the feed gases or liquids such as oxygen, hydrogen, or methanol. Fuel cells operate at a much lower potential difference than electrolyzers do, so the stability requirements are less demanding. However, unlike electrolyzers, fuel cells need external humidification of the feed gases (especially hydrogen), because membrane conductivity drops sharply as humidity decreases.[29,240] Moreover, protons moving from the anode to the cathode carry several water molecules with them (typically about three)[425,426], which dehydrates the anode side and reduces conductivity unless the hydrogen is humidified. Finally, most membranes cannot be used in fuel cells at temperatures above 90 °C, because they lose water and, consequently, ionic conductivity. Higher operating temperatures are nevertheless desirable because they

Accepted manuscript
This manuscript will be edited, formatted and proofread before it is published in its final version. The file will be replaced with the final version of record.

increase membrane ionic conductivity and mitigate CO poisoning when the hydrogen was produced from carbon-containing sources.[427,428] Membranes that retain high conductivity at low humidity and high temperatures are therefore needed. Ion-exchange membranes with high ion-exchange capacity meet these requirements.[391,429] This suggests that grafted and pore-filled membranes, for example those containing high-capacity polystyrene sulfonate, are promising candidates for fuel cell applications.

Perfluorinated sulfonic acid membranes of the Nafion type or its short-side-chain analogue Aquivion, which has higher conductivity, are currently the most widely used in PEMFCs.[430–432] However, their high cost drives efforts to replace them by grafted and pore-filled membranes, which not only achieve high conductivity and selectivity but can also be produced as thin membranes.

Numerous studies have examined various types of fuel cells that use grafted and pore-filled membranes, most of them focusing on PEMFCs.[59,141,147,219,433–436] The highest power density reported so far is 1.2 W cm^{-2} at 80 °C and 20% relative humidity.[437] Comparing results across studies is difficult because the experimental conditions, cell design, gas flow rates, catalyst loadings, and other parameters vary considerably. Many researchers therefore benchmark their results against Nafion-based fuel cells operated under similar conditions. Notably, PEMFCs with grafted or pore-filled membranes perform as well as, or even better than, those with Nafion.[59,147]

Direct methanol fuel cells have attracted less research interest[141,146,157,164,190,221,438–440], primarily because of their lower performance: methanol oxidation products adsorb strongly onto the catalyst, reducing both electrochemical efficiency and power output[441,442]. Nevertheless, grafted and pore-filled membranes are promising for this application, as they typically show lower methanol permeability and deliver power comparable to that of Nafion-based direct methanol fuel cells.[221,438] This behavior is attributed to the dense matrix, which limits membrane swelling and thus reduce the content of electroneutral solution in the pores.

Anion-exchange membrane fuel cells (AEMFCs) have recently attracted significant research interest.[443] As in alkaline electrolyzers, their lower operation potential allows the use of non-platinum catalysts and less expensive, non-perfluorinated membranes.[444–446] However, AEMFC power output remained low for many years. Recent advances in materials and process optimization have markedly increased peak power densities,

Accepted manuscript
This manuscript will be edited for style and proofread. The final version may be replaced with Version of Record.

reaching 2–3 W cm^{-2}.[447–451] Despite the promise of grafted and pore-filled membranes, only a few studies have demonstrated their successful use in AEMFCs.[95,216,452,453] This may be due to two factors: the limited demand for AEMFCs, which stems from their modest performance, and the risk of alkaline degradation for some membranes. In any case, the stability of grafted and pore-filled membranes is likely to be the most critical factor for their use in fuel cells and electrolyzers. Additional examples of grafted and pore-filled membranes used in fuel cells are summarized in Table 4.

Accepted manuscript
This manuscript will be edited, formatted, and proof read. The file will be replaced with Version of Record.

Table 4. Properties and performance of some reported ion-exchange membranes in fuel cells

Base film (thickness, μm)	Grafted polymer (GD, %) / Filler	Preparation method	IEC, mmol g^{-1}	Conductivity, mS cm^{-1}	Performance	Test conditions	Ref.
CEMs							
poly(ethylene-co-tetrafluoroethylene) (25)	1-vinylimidazole and 4-vinylpyridine (6–59)	post γ-radiation-induced graft polymerization	ND	3–50	0.237 W cm^{-2} (110 °C, RH=60%)	H_2/O_2, 80/100/110 °C, RH=20/60/80/100 % anode: Pt commercial electrode cathode: Pt commercial electrode	102
poly(ethylene-co-tetrafluoroethylene) (50)	4-vinylpyridine, 1-vinylimidazole or binary mixture (59–83) doped with phosphoric acid	post electron-beam irradiation-induced graft polymerization	ND	33.4–75.4 (H^+, 120 °C)	open circuit voltage 0.96–0.97 V (RH=0%), 0.95–0.98 V (RH=20%) peak power density 0.131–0.226 W cm^{-2} (RH=0%), 0.147–0.278 W cm^{-2} (RH=20%)	H_2/O_2, 120 °C, RH=0/20 % anode: Pt/Vulcan XC72 cathode: Pt/Vulcan XC72	454
poly(ethylene-co-tetrafluoroethylene) (50)	4-vinylpyridine (50), N-vinylformamide (70–80) or 1-vinylimidazole (80–120) doped with phosphoric acid	post electron-beam irradiation-induced graft polymerization	ND	20–100 (120 °C, RH<2%)	peak power density 0.075–0.15 W cm^{-2}	H_2/O_2, total pressure 3 bar, 120 °C, RH=0% anode: carbon black and Pt catalyst cathode: carbon black and Pt catalyst	455
poly(tetrafluoroethylene-co-hexafluoropropylene) (50)	4-vinylpyridine (50) doped with phosphoric acid	post electron-beam irradiation-induced graft polymerization	ND	40 (120 °C, RH<2%)	ND	H_2/O_2, total pressure 3 bar, 120 °C, RH=0% anode: carbon black and Pt catalyst cathode: carbon black and Pt catalyst	455
poly(ethylene-co-tetrafluoroethylene) (25)	4-vinyl pyridine or crosslinked with divinylbenzene (34–57) doped with phosphoric acid	post γ-radiation-induced graft polymerization	ND	10–30 (H^+, 120 °C, RH=10%) 35–75 (H^+, 120 °C, RH=50%)	peak power density 0.093 W cm^{-2} (80 °C), 0. 11 W cm^{-2} (100 °C), 0.081 W cm^{-2} (120 °C)	H_2/O_2, backpressure 1 barg, 80/100/120 °C, RH=50% anode: commercial PTFE treated electrodes with Pt cathode: commercial PTFE treated electrodes with Pt	456
poly(ethylene-co-tetrafluoroethylene) (25)	styrene crosslinked with 1,3-diisopropenylbenzene (23.8–27.2)	post electron-beam irradiation-induced dispersion graft polymerization	1.61–1.79	41.2–81.7 (in-plane, RT) 18.3–107.5 (through-plane, RT)	high frequency resistance 0.057–0.093 Ω cm^2 ohmic resistance 0.05–0.087 Ω cm^2 H_2 crossover 0.58–0.97 mA cm^{-2}	H_2/O_2, 80 °C, RH=100% anode: commercial electrodes with Pt cathode: commercial electrodes with Pt	457
poly(ethylene-co-tetrafluoroethylene) (25)	styrene (20.8) or binary mixture with methacrylonitrile (27.1, 27.4)	post electron-beam irradiation-induced dispersion graft polymerization	1.14–1.46	42–69 (RT)	ohmic resistance 0.08–0.132 Ω cm^2 polarization resistance 0.153–0.216 Ω cm^2 H_2 permeation 0.31–0.53 mA cm^{-2}	H_2/O_2, 80 °C, RH=100% anode: commercial electrodes with Pt cathode: commercial electrodes with Pt	65
poly(ethylene-co-tetrafluoroethylene) (25)	styrene (25–128), methacrylonitrile (9–45), acrylonitrile (3.6) and comonomers of styrene	post electron-beam irradiation-induced	1.0–1.8	40–147 (RT)	ohmic resistance 0.054–0.067 Ω cm^2	H_2/O_2, 80 °C, RH=100% anode: commercial electrodes with Pt	458

Accepted manuscript
This manuscript will be edited, formatted, and proof read. The file will be replaced with Version of Record.

	with methacrylonitrile (7–63) or acrylonitrile (19–98)	dispersion graft polymerization			polarization resistance 0.133–0.534 Ω cm^2 H_2 crossover 0.24–0.45 mA cm^{-2}	cathode: commercial electrodes with Pt	
poly(tetrafluoroethylene-co-hexafluoropropylene) (25)	styrene crosslinked with divinylbenzene (18.0, 18.2)	post electron-beam irradiation-induced dispersion graft polymerization	1.33–1.36	41–72 (RT)	ohmic resistance 0.098 Ω cm^2	H_2/O_2, 80 °C, backpressure 1 barg, RH=100% anode: commercial electrodes with Pt cathode: commercial electrodes with Pt	459
poly(tetrafluoroethylene-co-hexafluoropropylene) (25)	α-methylstyrene and methacrylonitrile crosslinked with divinylbenzene (34.5, 36.0)	post electron-beam irradiation-induced dispersion graft polymerization	1.28–1.38	89–98 (RT)	ohmic resistance -0.125–0.175 Ω cm^2	H_2/O_2, backpressure 1 barg, 80 °C, RH=100% anode: commercial electrodes with Pt cathode: commercial electrodes with Pt	459
polymethylpentene (ND)	styrene crosslinked with divinylbenzene (47, 112)	post ultraviolet irradiation-induced graft polymerization	1.91–2.90	3.5–21 (30 °C, RH=95%) 0.23–0.95 (30 °C, RH=32%)	peak power density 0.097–0.183 W cm^{-2}	H_2/O_2, 30 °C, RH=100% anode: commercial Pt electrodes on carbon black with Nafion® ionomer cathode: commercial Pt electrodes on carbon black with Nafion® ionomer	59
polyvinylidene fluoride (50)	styrene crosslinked with divinylbenzene (24, 27)	post γ-radiation-induced emulsion graft polymerization	1.82–1.83	47–71 (30 °C, RH=100%) 18–25 (30 °C, RH=95%) 0.42–0.44 (30 °C, RH=30%) 85–132 (80 °C, RH=100%)	peak power density 0.269–0.356 W cm^{-2}	H_2/O_2, 65 °C, RH=100% anode: lab-made Pt/carbon nanotubes with Nafion® ionomer cathode: lab-made Pt/carbon nanotubes with Nafion® ionomer	436
poly(ethylene-co-tetrafluoroethylene) (50)	glycidyl methacrylate and hydroxyethyl methacrylate crosslinked with N,N′-methylenebis(acrylamide) (225, 284)	post electron-beam irradiation-induced graft polymerization	ND	45–62 (30 °C) 67–77 (60 °C)	peak power density 0.118 W cm^{-2} (30 °C), 0.128 W cm^{-2} (40 °C), 0.129 W cm^{-2}, 0.134 W cm^{-2} (50 °C)	H_2/O_2, 30/40/50 °C, RH=100% anode: commercial electrodes with Pt cathode: commercial electrodes with Pt	460
poly(ethylene-co-tetrafluoroethylene) (50)	acrylic acid and 2-acrylamido-2-methylpropane sulfonic acid (205, 500)	post electron-beam irradiation-induced graft polymerization	4.64–5.71	42–70 (30 °C) 49–81 (60 °C)	ND	H_2/O_2, 40/50 °C, RH=100% anode: commercial electrodes with Pt cathode: commercial electrodes with Pt	461
polyvinylidene fluoride (50)	acrylic acid and 2-acrylamido-2-methylpropane sulfonic acid (305, 421)	post electron-beam irradiation-induced graft polymerization	ND	40–45 (30 °C) 47–58 (60 °C)	peak power density 0.105–0.124 W cm^{-2} (40 °C), 0.122–0.132 W cm^{-2} (50 °C)	H_2/O_2, 40/50 °C, RH=100% anode: commercial electrodes with Pt cathode: commercial electrodes with Pt	461
porous polytetrafluoroethylene (15, 30)	perfluorosulfonated (Nafion 117) ionomer	impregnation with ionomer solution	ND	ND	open circuit voltage 0.956–0.975 V H_2 crossover 0.60–0.74 mA cm^{-2}	H_2/O_2, 80 °C, RH=100% anode: lab-made Pt/C, Nafion ionomer	462

Accepted manuscript
This manuscript will be edited, formatted, and proof read. The final version will be replaced with Version of Record.

						cathode: lab-made Pt/C, Nafion ionomer	
porous polytetrafluoroethylene (ND)	perfluorosulfonated (Nafion®) ionomer	impregnation with ionomer solution	ND	43–62 (60 °C)	open circuit voltage 0.932–0.954 V H_2 crossover 1.05–2.27 mA cm^{-2}	H_2/air, 60 °C, RH=100% anode: Pt/C, Nafion® ionomer cathode: Pt/C, Nafion® ionomer	463
porous polytetrafluoroethylene (ND)	short side chain (Aquivion™) perfluorosulfonated acid ionomer	impregnation with ionomer solution under vacuum	ND	115 (60 °C, RH=100%) 22 (60 °C, RH=25%) 179 (120 °C, RH=100%) 43 (120 °C, RH=25%)	open circuit voltage 0.654 V (60 °C), 0.59 V (120 °C) H_2 crossover 1.04 mA cm^{-2} (60 °C)	H_2/air, 60/80/100/120 °C, RH=25% anode: Pt/C, Nafion® ionomer cathode: Pt/C, Nafion® ionomer	186
composite nanofiber mat of silica/sulfonated poly(ether ether ketone) (45)	perfluorosulfonated (Nafion®) ionomer	impregnation with ionomer solution	ND	70 (75 °C, RH=100%) 78 (90 °C, RH=100%) 26 (110 °C, RH=60%) 13 (120 °C, RH=40%)	peak power density 0.85 W cm^{-2} (75 °C, RH=100%), 0.78 W cm^{-2} (90 °C, RH=100%), 0.25 W cm^{-2} (110 °C, RH=60%), 0.17 W cm^{-2} (120 °C, RH=40%)	H_2/O_2, 75/90/110/120 °C, RH=40/60/100% anode: Pt/C, Nafion® ionomer cathode: Pt/C, Nafion® ionomer	464
porous polytetrafluoroethylene (15)	end-group cross-linkable sulfonated fluorinated biphenol	lab-scale continuous casting process	0.72–1.51	15–75 (in-plane, RT)	peak power density 0.9–1.2 W cm^{-2}	H_2/O_2, 60 °C, RH=100% anode: Pt/C, Nafion® ionomer cathode: Pt/C, Nafion® ionomer	465
porous polyethylene (16)	sulfonated poly (2,6-dimethyl-1,4-phenylene oxide)	lab-scale continuous casting process	0.92–2.23	4.3–255 (through-plane, RT) 30–140 (in-plane, RT)	peak power density 0.17–0.28 W cm^{-2}	H_2/O_2, 30 °C, RH=100% anode: Pt/C, Nafion® ionomer cathode: Pt/C, Nafion® ionomer	146
porous cross-linked benzoxazine-benzimidazole copolymer (15–20)	sulfonated poly(arylene ether sulfone)	impregnation with polymer solution	ND	3.1–6.5 (120 °C, RH=40%)	peak power density 0.17 W cm^{-2}	H_2/air, 120 °C, RH=40% anode: Pt/C, Aquivion™ ionomer cathode: Pt/C, Aquivion™ ionomer	434
porous polyethylene (6)	low equivalent weight perfluorosulfonic acid polymer	impregnation with polymer solution	ND	20 (in-plane, 80 °C, RH=30%) 200 (in-plane, 80 °C, RH=90%)	peak power density 1.2 W cm^{-2} (80 °C, RH=20%), 1.0 W cm^{-2} (100 °C, RH=20%)	H_2/O_2, 80/90/100 °C, RH=20/30/60% anode: Pt/C, low equivalent weight perfluorosulfonic acid ionomer cathode: Pt/C, low equivalent weight perfluorosulfonic acid ionomer	147
porous polyethylene (6)	low equivalent weight perfluorosulfonic acid polymer	impregnation with polymer solution	ND	ND	peak power density 1.2 W cm^{-2} (80 °C, RH=20%)	H_2/O_2, 80 °C, RH=20/30/60%	437

Accepted manuscript
This manuscript will be edited, formatted, and proof read. The final version may replace this version of Record.

						anode: Pt/C, low equivalent weight perfluorosulfonic acid ionomer cathode: Pt/C, low equivalent weight perfluorosulfonic acid ionomer	
porous polytetrafluoroethylene (30)	2-acrylamido-2-methylpropanesulfonic acid and 1H,1H,5H-octafluoropentyl methacrylate cross-linked with trimethylolpropane triacrylate	impregnation with monomer solutions followed by photo-polymerization	1.10–1.32	39–53 (in-plane, 70 °C, RH=100%)	peak power density 0.334–0.340 W cm^{-2}	H_2/air, 70 °C, RH=100% anode: Pt/C, Nafion D521 ionomer cathode: Pt/C, Nafion D521 ionomer	440
porous polytetrafluoroethylene (ND)	perfluorosulfonated (Nafion®) ionomer	impregnation with ionomer solution	ND	125–158 (80 °C, RH=100%) 112–141 (120 °C, RH=100%)	peak power density 0.59–1.12 W cm^{-2} (80 °C, RH=100%), 0.59–1.0 W cm^{-2} (100 °C, RH=100%), 0.15 W cm^{-2} (120 °C, RH=100%)	H_2/O_2, 80/100/120 °C, RH=100% anode: Pt/C and PtCo/C, low equivalent weight perfluorosulfonic acid ionomer cathode: Pt/C and PtCo/C, low equivalent weight perfluorosulfonic acid ionomer	435
porous cross-aligned polytetrafluoroethylene (ND)	perfluorosulfonated (Nafion®) ionomer	impregnation with ionomer solution	ND	88 (20 °C) 210 (80 °C)	peak power density 0.85 W cm^{-2} (1.5 barg, RH=100%), 0.7 W cm^{-2} (1 barg, RH=50%)	H_2/air, backpressure 1/1.5 barg, 80 °C, RH=50/100% anode: Pt/C, Nafion® ionomer cathode: Pt/C, Nafion® ionomer	173
AEMs							
polyethylene (25)	vinylbenzyl chloride (ND)	post electron-beam irradiation-induced dispersion graft polymerization	2.49	130 (OH^-, 40 °C) 290 (OH^-,110 °C)	peak power density 2.1 W cm^{-2} (0.51 V) open circuit voltage 1.02 V current density 574 mA cm^{-2} (0.8 V)	H_2/O_2, backpressure 1.5 barg, 110 °C, RH=95% anode: PtRu/C, Fumion® ionomer, Vulcan XC 72 cathode: Pt/C, Fumion® ionomer	450
polyethylene (25)	vinylbenzyl chloride (102, 143)	post electron-beam irradiation-induced dispersion graft polymerization	2.63, 2.87	64, 76 (Cl^-, 80 °C) 145 (OH^-, 80 °C)	peak power density 0.96 W cm^{-2} (60 °C, O_2, Pt/C), 1.45 W cm^{-2} (80 °C, O_2, Pt/C), 0.63 W cm^{-2} (80 °C, air, Pt/C), 0.9 W cm^{-2} (80 °C, O_2, Ag/C)	H_2/O_2 or air, 60/80 °C, RH=68/100 % anode: PtRu/C, lab-made ionomer cathode: Pt/C or Ag/C, lab-made ionomer	93
poly(ethylene-co-tetrafluoroethylene) (25)	vinylbenzyl chloride (79)	post electron-beam irradiation-induced dispersion graft polymerization	2.05	63 (Cl^-, 80 °C)	peak power density 0.91 W cm^{-2} (60 °C, O_2, Pt/C), 1.21 W cm^{-2} (80 °C, O_2, Pt/C)	H_2/O_2, 60/80 °C, RH=68/100 % anode: PtRu/C, lab-made ionomer cathode: Pt/C, lab-made ionomer	93
polyethylene (15)	vinylbenzyl chloride (92–121)	post electron-beam irradiation-induced	1.88–2.54	63 (Cl^-, 80 °C)	peak power density 2.02 W cm^{-2} (O_2, Pt/C), 1.62 W cm^{-2} (O_2, Ag/C),	H_2/O_2 or air, 80 °C, RH=92%	448

Accepted manuscript
This manuscript will be edited, formatted, and proof read. The final version replaced with Version of Record.

		dispersion graft polymerization		208 (OH^-, 80 °C)	1.26 W cm^{-2} (O_2, FeCoPc/C), 0.85 W cm^{-2} (air, Pt/C), 0.68 W cm^{-2} (air, Ag/C), 0.37 W cm^{-2} (air, FeCoPc/C)	anode: PtRu/C, lab-made ionomer cathode: Pt/C or Ag/C or FeCoPc/C, lab-made ionomer	
poly(ethylene-co-tetrafluoroethylene) (12.7)	vinylbenzyl chloride (70)	post electron-beam irradiation-induced dispersion graft polymerization	2.11	23.8 (Cl^-, 25 °C) 57.8 (Cl^-, 70 °C)	peak power density 1.57 W cm^{-2} (O_2, Pt/C), 1.11 W cm^{-2} (O_2, Ag/C), 0.65 W cm^{-2} (air, Pt/C), 0.70 W cm^{-2} (air, Ag/C)	H_2/O_2 or air, 70 °C, RH=84% anode: PtRu/C, lab-made ionomer cathode: Pt/C or Ag/C, lab-made ionomer	466
polyethylene (25)	vinylbenzyl chloride (80–220)	γ-radiation-induced graft polymerization with a reversible addition–fragmentation chain-transfer agent	1.6–3.1	80–116 (OH^-, 30 °C) 153–230 (OH^-, 80 °C)	peak power density 0.9–1.3 W cm^{-2}	H_2/O_2, 80 °C, RH=100% anode: PtRu/C, lab-made ionomer cathode: Pt/C, lab-made ionomer	72
polyethylene (30–130)	vinylbenzyl chloride (32.0–74.6)	γ-radiation-induced graft polymerization	1.4–3.2	50–120 (OH^-, 70 °C)	peak power density 0.319–0.363 W cm^{-2} (40 °C, O_2), 0.359–0.608 W cm^{-2} (50 °C, O_2), 0.242–0.284 W cm^{-2} (40 °C, air), 0.236–0.262 W cm^{-2} (50 °C, air)	H_2/O_2 or air, 40/50 °C, RH=100% anode: Pt/C, poly(vinylbenzyl chloride) ionomer cathode: Pt/C, poly(vinylbenzyl chloride) ionomer	467
polyethylene (40, 50)	vinylbenzyl chloride (26–68)	γ-radiation-induced graft polymerization	1.22–2.13	40–320 (in-plane, OH^-, 20–80 °C) 34–110 (through-plane, OH^-, 20–80 °C)	peak power density 0.648 W cm^{-2} (20 °C, O_2), 0.718 W cm^{-2} (50 °C, O_2), 0.823 W cm^{-2} (60 °C, O_2), 0.424 W cm^{-2} (40 °C, air 1 barg), 0.451 W cm^{-2} (50 °C, air 1 barg), 0.471 W cm^{-2} (60 °C, air 1 barg)	H_2/O_2 or air 1 barg, 20/40/50/60 °C, RH=100% anode: Pt/C, poly(vinylbenzyl chloride) ionomer cathode: Pt/C, poly(vinylbenzyl chloride) ionomer	109
polyethylene (10)	vinylbenzyl chloride (171, 185)	post electron-beam irradiation-induced dispersion graft polymerization	2.7–2.8	35–105 (OH^-, 25–80 °C)	peak power density 2.84 W cm^{-2}	H_2/O_2, backpressure 100 kPa, 80 °C, RH=100% anode: PtRu/C, Vulcan XC-72R, lab-made ionomer cathode: Pt/C, lab-made ionomer	468
polyethylene (10, 15)	vinylbenzyl chloride (125, 165)	post electron-beam irradiation-induced dispersion graft polymerization	2.44, 2.54	100, 121 (OH^-, 25 °C) 208, 214 (OH^-, 80 °C)	peak power density 2.01, 2.55 W cm^{-2} (Pt/C), 1.72 W cm^{-2} (Ag/C)	H_2/O_2, 80 °C, RH=92% anode: PtRu/C, Vulcan XC-72R, lab-made ionomer cathode: Pt/C or Ag/C, lab-made ionomer	68
poly(ethylene-co-tetrafluoroethylene) (25)	vinylbenzyl chloride (20–89)	post electron-beam irradiation-induced dispersion/emulsion graft polymerization	0.87–2.13	16–68 (Cl^-, 80 °C)	peak power density 0.91, 1.16 W cm^{-2}	H_2/O_2, 60 °C, RH=100% anode: PtRu/C, lab-made ionomer cathode: Pt/C, lab-made ionomer	94

Accepted manuscript
This manuscript will be edited, formatted, and proofread. The file will be replaced with the version of record.

poly(ethylene-co-tetrafluoroethylene) (25)	vinylbenzyl chloride (ND)	post electron-beam irradiation-induced emulsion graft polymerization	2.22	190 (OH^-, 80 °C) 201 (OH^-, 105 °C)	peak power density 1.14 W cm^{-2}	H_2/O_2, backpressure 1.4 barg, 105 °C, RH=95% anode: PtRu/C, Fumion® ionomer, Vulcan XC 72 cathode: N-doped-C, Fumion® ionomer	451
poly(ethylene-co-tetrafluoroethylene) (25)	vinylbenzyl chloride (52–143) aminated with N-methylpiperidine	post electron-beam irradiation-induced emulsion graft polymerization	1.72–2.62	113.5–146 (OH^-, 40 °C)	peak power density 1.25 W cm^{-2} (60 °C), 1.35 W cm^{-2} (70 °C)	H_2 backpressure 0.2 barg /O_2, 60/70 °C, RH=95% anode: PtRu/C, Fumion® ionomer, Vulcan XC 72 cathode: Pt/C, Fumion® ionomer	469
poly(ethylene-co-tetrafluoroethylene) (50)	vinylbenzyl chloride (ND) aminated with trimethylamine/N-methylpiperidine/4-methylmorpholine/1-methylpyrrolidine/1-methylpiperazine/1,4-dimethylpiperazine	post electron-beam irradiation-induced dispersion graft polymerization	1.08–1.82	5.4–20 (through-plane, Cl^-, 25 °C) 27–52 (in-plane, Cl^-, 90 °C) 132–159 (in-plane, OH^-, 80 °C)	peak power density 0.36–0.63 W cm^{-2} (0 backpressure), 0.47–0.80 W cm^{-2} (0.1 MPa backpressure)	H_2/O_2, backpressure 0 or 0.1 MPa, 60 °C, RH=100% anode: PtRu/C, lab-made ionomer cathode: Pt/C, lab-made ionomer	95
porous polyethylene (20)	vinylbenzyl chloride cross-linked with divinylbenzene and quaternized with trimethylamine/trimethylamine/1,4-diazabicyclo[2.2.2]octane/N,N,N,N-tetramethylethylenediamine/tris(2,4,6-trimethoxyphenyl)-phosphine	impregnation with monomer solution followed by thermal induced radical polymerization	0.44–1.35	5.4–38.1 (in-plane, OH^-)	peak power density 0.081–0.090 W cm^{-2}	H_2/O_2, 60 °C, RH=100% anode: Pt/C, commercial ionomer AS-4 cathode: Pt/C, commercial ionomer AS-4	470
porous polyethylene (ND)	vinylbenzyl chloride	impregnation with monomer solution and γ-radiation-induced radical polymerization	1.25–1.96	73–126 (in-plane, OH^-, 80 °C)	peak power density 0.038–0.127 W cm^{-2}	H_2/O_2, 80 °C, RH=100% anode: Pt/C, lab-made ionomer cathode: Pt/C, lab-made ionomer	471
porous polytetrafluoroethylene (80)	N,N′-dimethylaminoethyl methacrylate cross-linked with divinylbenzene quaternized with p-xylylene dichloride	impregnation with monomer solutions followed photo-polymerization	1.24–1.95	11–128 (in a 1.0 M KOH aqueous solution, RT)	open circuit voltage 0.90–0.97 V peak power density 0.008–0.069 W cm^{-2}	HCOOK&KOH/HCOOK&KOH&O_2, 60 °C, RH=100% anode: Pd/C, commercial ionomer AS-4 cathode: Pt/C, commercial ionomer AS-4	227
porous bromomethylated poly (2,6-dimethyl-1,4-phenylene oxide) (60)	methyl methacrylate and 2-(dimethylamino) ethyl methacrylate	impregnation with polymer solution	0.87–0.97	26.5–39.8 (in-plane, OH^-, 30 °C)	peak power density 0.150–0.315 W cm^{-2}	H_2/O_2, 60 °C, RH=100% anode: PtRu/C, lab-made ionomer cathode: Pt/C, lab-made ionomer	216
porous hydrophobic polytetrafluoroethylene (80)	N,N’-dimethylaminoethyl methacrylate cross-linked with divinylbenzene quaternized with p-xylylene dichloride	impregnation with monomer solution followed by photo-polymerization	1.46	10 (in a 1.0 M KOH aqueous solution, RT)	peak power density 0.1 W cm^{-2}	N_2H_4&KOH/N_2H_4&KOH&O_2, 60 °C, RH=100% anode: lab-made Ni/C, commercial ionomer AS-4	472

Accepted manuscript
This manuscript will be edited, formatted and proof read. The final version may be replaced with version of Record.

						cathode: Pt/C, commercial ionomer AS-4	
porous hydrophilic polytetrafluoroethylene (35)	N,N'-dimethylaminoethyl methacrylate cross-linked with divinylbenzene quaternized with p-xylylene dichloride	impregnation with monomer solution followed by photo-polymerization	1.42	19 (in a 1.0 M KOH aqueous solution, RT)	peak power density 0.4 W cm^{-2}	N_2H_4&KOH/ N_2H_4&KOH&O_2, 60 °C, RH=100% anode: lab-made Ni/C, commercial ionomer AS-4 cathode: Pt/C, commercial ionomer AS-4	[472]
porous polyamide (ND)	vinylbenzyl chloride cross-linked with 1,8-octanediamine and quaternized with trimethyl amine or 1,2-dimethylimidazole	post electron-beam irradiation-induced radical polymerization	1.86–2.05	34.7–48.3 (30 °C, OH^-, RH=90%) 109.5–130.1 (80 °C, OH^-, RH=90%)	ND	H_2/O_2, 80 °C, RH=90% anode: commercial catalyst and ionomer cathode: commercial catalyst and ionomer	[193]
porous polypropylene (ND)	vinylbenzyl chloride cross-linked with 1,8-octanediamine and quaternized with trimethyl amine or 1,2-dimethylimidazole	post electron-beam irradiation-induced radical polymerization	1.94–2.03	41.3–48.4 (30 °C, OH^-, RH=90%) 127.5–148.6 (80 °C, OH^-, RH=90%)	peak power density 0.190–0.440 W cm^{-2}	H_2/O_2, 80 °C, RH=90% anode: commercial catalyst and ionomer cathode: commercial catalyst and ionomer	[193]
porous hydrophobic polyethylene (80)	acrylated poly(2,6-dimethyl-1,4-phenylene oxide) cross-linked with N,N,N'N'-tetramethyl-1,6-hexanediamine	impregnation with polymer solution by centrifugal force	2.05–2.65	30.7–47.7 (25 °C, OH^-, DI water) 50.8–87.1 (80 °C, OH^-, DI water) 49.5–79.3 (80 °C, OH^-, RH=95%)	open circuit voltage 0.96 V peak power density 0.239 W cm^{-2}	H_2/O_2, 60 °C, RH=100% anode: Pt/C, commercial ionomer Sustainion XB-7 cathode: Pt/C, commercial ionomer Sustainion XB-7	[453]
porous polyethylene (4, 10)	vinylbenzyl chloride cross-linked with divinylbenzene and quaternized with N-methyl-piperidine	vacuum-assisted impregnation with monomer solution followed thermal induced radical polymerization	1.51–1.58	63.2–105.9 (in-plane, 80 °C, OH^-)	peak power density 0.709–1.014 W cm^{-2} (O_2), 0.534 W cm^{-2} (air)	H_2/O_2 or air, backpressure 0.15 MPa, 65 °C, RH=100% anode: PtRu/C, lab-made ionomer cathode: Pt/C, lab-made ionomer	[148]

Note. GD is the grafting degree; IEC is the ion-exchange capacity; RH is relative humidity; RT is room temperature; DI water is deionized water; ND is no data reported.

Accepted manuscript
This manuscript will be edited, formatted, and proof read. The final version replaced with Version of Record.

4.4. Energy storage devices

Lithium-ion batteries (LIBs) have become an integral part of modern life, powering everything from portable electronics and cordless tools to electric vehicles and home and grid energy storage. The demand for higher energy density has driven a recent trend toward lithium metal anodes, which do not operate stably with liquid electrolytes. Considerable interest has therefore arisen in all-solid-state batteries that use solid electrolytes. The principal advantages of these systems include high lithium-ion transport numbers and the ability to suppress dendrite growth.[473–477]

Among solid electrolytes, polymer electrolytes are particularly attractive because of their low interfacial resistance with electrode materials (Fig. 12).[478–484] The most common are polar polymers that contain lithium salts and are solvated (plasticized) with aprotic solvents. Ion-exchange membranes in their lithium form can also serve as solid electrolytes; they are typically solvated with aprotic organic solvents to achieve sufficient conductivity.[11,485–489]

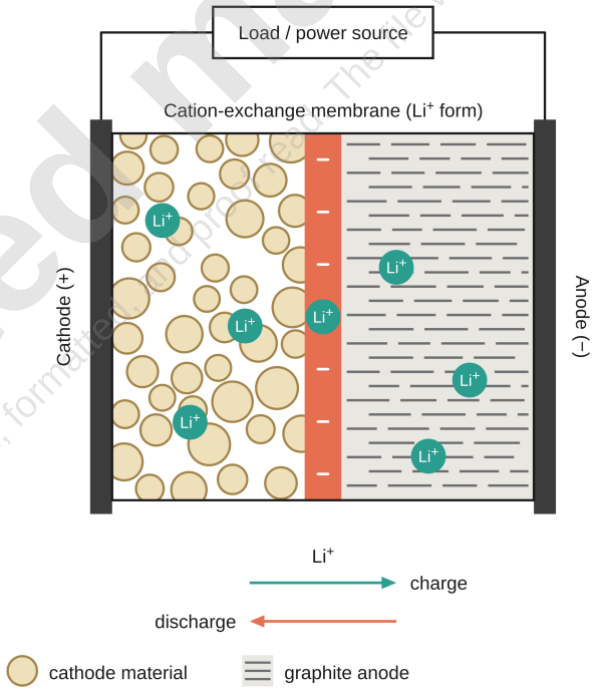


Figure 12. Schematic of a lithium-ion battery operation

Perfluorinated membranes have received the most attention for LIB applications[490–494], whereas only a few studies have explored grafted or pore-filled membranes in LIBs. Nevertheless, such research is now beginning to appear in studies of polymer electrolytes.[123] For example, a PVDF-based electrolyte with a lithium [(4-styrenesulfonyl)(fluorosulfonyl)imide] copolymer swollen in ethylene

Accepted manuscript
This manuscript will be edited, formatted and proofread. The file will be replaced with Version of Record

carbonate/dimethyl carbonate showed an ionic conductivity of 5.8×10^{-3} S cm^{-1} at 28 °C and a Li^+ transport number of 0.91.[495] Solid and gel polymer electrolytes based on oxidized starch grafted with poly[poly(ethylene glycol) methyl ether methacrylate] exhibit ionic conductivity up to $5.5\cdot10^{-3}$ S cm^{-1}, lithium transport numbers of 0.6–0.9, and an electrochemical stability window of 4.4–4.9 V depending on composition.[496] A battery based on these materials delivered a discharge capacity of 180 mA h g^{-1} at 0.2 C, retaining 75% of its capacity after 100 cycles. Additional examples of grafted and pore-filled membranes used in lithium-ion batteries are summarized in Table 5.

Accepted manuscript
This manuscript will be edited, formatted, and proof read. The file will be replaced with Version of Record

Table 5. Properties and performance of some grafted and pore-filled ion-exchange membranes in lithium-ion batteries

Base film (thickness, μm)	Grafted polymer (GD, %) / Filler	Preparation method	IEC, mmol g^{-1}	Conductivity, mS cm^{-1}	Performance	Test conditions	Ref.
CEMs							
polyvinylidene fluoride (80)	styrene (5–50) and electrolyte: 1 M $LiPF_6$ in 1:1 ethylene carbonate -diethylcarbonate	γ-radiation-induced graft polymerization	ND	$4.3 \cdot 10^{-3}$–1.6	ND	ND	[497]
porous polyethylene separator (ND)	glycidyl methacrylate (ND) and electrolyte: 1 M $LiPF_6$ in 1:1 ethylene carbonate -diethylcarbonate	post electron-beam irradiation-induced graft polymerization	ND	ND	discharge capacity 145 mA h g^{-1} (C/5), 130 mA h g^{-1} (C/2)	anode: mesocarbon microbeads cathode: $LiCoO_2$ cut-off voltages: 4.2 V/ 2.8 V C/5 or C/2 rate	[498]
porous polyethylene separator (25)	methyl methacrylate (27–168) and electrolyte: 1 M $LiPF_6$ in 1:1 ethylene carbonate -diethylcarbonate	electron-beam irradiation-induced graft polymerization	ND	0.91–1.01 (20 °C)	oxidation stability 4.6 V discharge capacity 131–134 mA h g^{-1} (C/5), 138.48 mA h g^{-1} (C/10)	anode: mesocarbon microbeads, PVDF binder, acetylene black cast on copper foil cathode: $LiCoO_2$, PVDF binder, acetylene black cast on aluminum foil cut-off voltages: 4.2 V/ 2.8 V C/5 or C/10 rate	[499]
porous polyvinylidene fluoride (ND)	styrene (20–120) and electrolyte: 1 M $LiClO_4$ in γ-butyrolactone	γ-radiation-induced graft polymerization	ND	0.75–2.50 (RT)	ND	ND	[500]
porous polyvinylidene fluoride (110)	styrene (8–46) and electrolyte: 1 M $LiPF_6$ in 1:1 ethylene carbonate -diethylcarbonate	electron-beam irradiation-induced graft polymerization	ND	1.91	ND	ND	[501]
microporous polyethylene separator (12)	methyl methacrylate (5–127) and electrolyte: 1 M $LiClO_4$ in 1:1 ethylene carbonate -diethylcarbonate	post γ-radiation-induced graft polymerization	ND	0.15–2.0	ND	ND	[502]
microporous polyethylene separator (20)	methyl methacrylate (8–262) and electrolyte: 1 M $LiClO_4$ in 1:1 ethylene carbonate -diethylcarbonate	post γ-radiation-induced graft polymerization	ND	1.04–1.30	oxidation stability 5 V discharge capacity 131–134 mA h g^{-1} (C/5), 138.48 mA h g^{-1} (C/10)	anode: lithium metal cathode: stainless steel cut-off voltages: 6 V / 3 V	[503]
porous tri-layer of polypropylene-polyethylene-polypropylene (25)	methyl methacrylate (36.8) and electrolyte: 1 M $LiPF_6$ in 1:1 ethylene carbonate -diethylcarbonate	post γ-radiation-induced graft polymerization	ND	0.91–1.38	oxidation stability 4.6 V discharge capacity 127–130 mA h g^{-1}	anode: lithium metal cathode: $LiCoO_2$ cut-off voltages: 4.2 V / 2.8 V C/5 rate	[504]
porous polyethylene separator (25)	acrylamide (5.1–33.6) and electrolyte: 1 M $LiPF_6$ in 1:1 ethylene carbonate -diethylcarbonate	γ-radiation-induced graft polymerization	ND	0.76 (30 °C)	discharge capacity 121.9 mA h g^{-1}	anode: lithium metal cathode: $LiCoO_2$ cut-off voltages: 4.15 V / 2.8 V C/10 rate	[505]

Accepted manuscript
This manuscript will be edited, formatted, and proofread. The file will be replaced with Version of Record.

microporous polyethylene separator (25)	poly(ethylene oxide), poly(ethylene glycol dimethacrylate) and electrolyte: 1 M $LiPF_6$ in 1:1 ethylene carbonate – diethylcarbonate or 1 M $LiBF_4$ in 1:1 ethylene carbonate – diethylcarbonate	impregnation with polymer solution	ND	0.6–2.2 ($LiPF_6$, RT) 0.4–1.0 ($LiBF_4$, RT)	oxidation stability 4.3 V ($LiPF_6$), 4.5 V ($LiBF_4$) discharge capacity 142 mA h g^{-1} ($LiBF_4$) Coulombic efficiency 93% ($LiBF_4$)	anode: mesophase carbon fiber, PVDF binder and super-P carbon cast on copper foil cathode: $LiCoO_2$, PVDF binder and super-P carbon cast on aluminum foil cut-off voltages: 4.2 V / 2.8 V C/10 rate	506
porous polytetrafluoroethylene (12)	poly(ethylene glycol), lithium bis(trifluoromethanesulfonyl)imide, and 1-butyl-1-methylpyrrolidinium bis(fluorosulfonyl)imide	impregnation with polymer solution	ND	0.12–0.52	discharge capacity 89.09–126.53 mA h g^{-1} (C/10)	anode: lithium metal cathode: $LiCoO_2$, conductive graphite and PVDF binder cast on aluminum foil cut-off voltages: 4.15 V / 2.8 V C/10, C/2, C or 2C rate	507
AEM							
porous polypropylene separator (25)	poly(diallyldimethylammonium bis(trifluoromethanesulfonyl)imide)	coating with polymer solution	ND	1.61	Coulombic efficiency 96%	anode: lithium foil cathode: Cu foil	508

Note. GD is the grafting degree; IEC is the ion-exchange capacity; RT is room temperature; ND is no data reported.

Accepted manuscript
This manuscript will be edited, formatted, and proof read. The file will be replaced with the version of record.

Flow batteries, particularly vanadium redox flow batteries, are another important class of energy storage devices. These batteries are larger and less energy-dense than LIBs, but their stability makes them attractive for stationary energy storage. Their operation principle is similar to that of LIBs, but charge is balanced by proton transport through the membrane between two compartments fed from tanks containing vanadium ions in different oxidation states (V^{2+}/V^{3+} and VO^{2+}/VO_2^{+}) (Fig. 13). During discharge, vanadium ions are reduced in the compartments where their oxidation state is higher, whereas in the compartments with vanadium ions in a lower oxidation state, they are oxidized (the processes are reversed during charging). Membranes for such systems require high proton conductivity, low permeability to vanadium ions, and high chemical stability.[509,510] Grafted and pore-filled membranes have several advantages over the commonly used Nafion membranes, including lower cost, smaller thickness, and reduced vanadium crossover due to their limited pore volume.[37,511] Through structural optimization, some membranes achieved vanadium ion permeability an order of magnitude lower than that of Nafion. Together with high proton conductivity and the ability to produce thin membranes while maintaining mechanical strength, this has made grafted and pore-filled membranes a common choice for flow battery applications.[163,220,224,225,512–514]

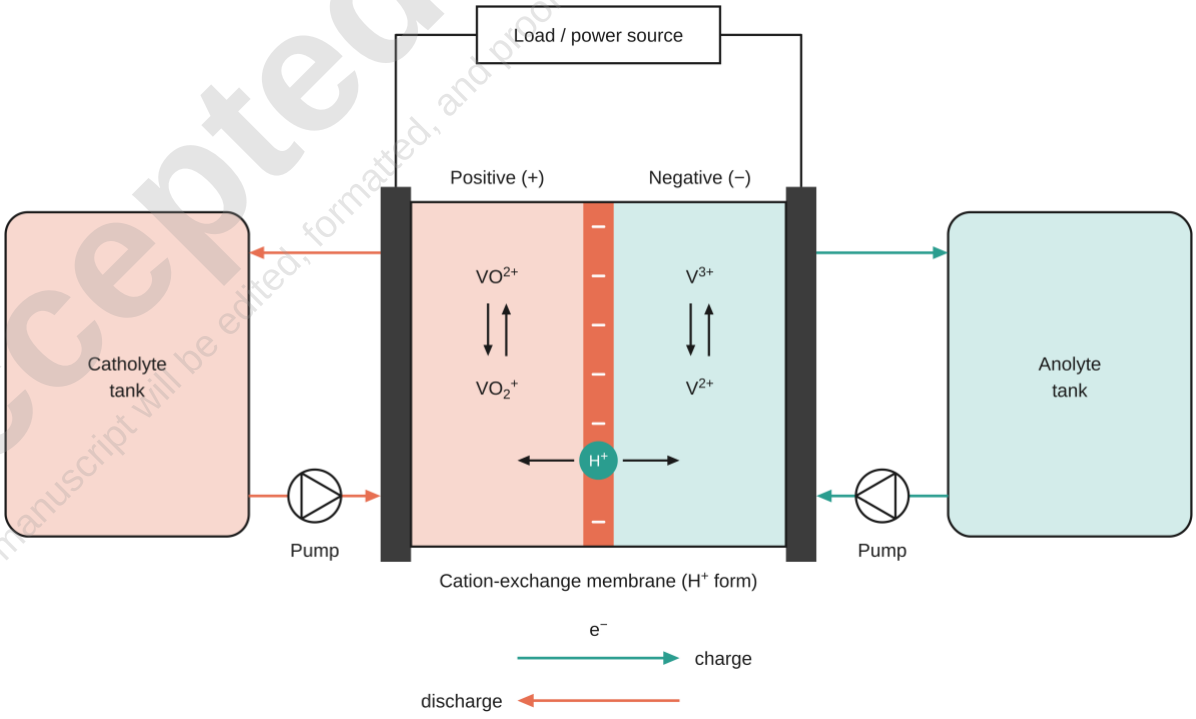


Figure 13. Schematic of the operation of a vanadium redox flow battery

Accepted manuscript
This manuscript will be edited, formatted, and proofread before the final version is published with Version of Record

Flow batteries based on pore-filled membranes achieved Coulombic efficiencies* of 94–97%, compared to 92.5% for Nafion membranes.[513] Among the pore-filled membranes tested, the best performance was shown by a membrane with a high degree of cross-linking (10% divinylbenzene).[513] This suggests that the restriction of pore size, which determines membrane selectivity, plays a key role in this application. At the same time, flow batteries with grafted membranes achieved even higher Coulombic efficiency of 98.2–98.6%, owing to low vanadium permeability ($(1–5)\cdot10^{-7}$ cm min^{-1}).[515,516] An even lower vanadium permeability ($5.3\cdot10^{-8}$ cm min^{-1}) was reported for another grafted membrane, although the Coulombic efficiency of the flow battery based on it was somewhat lower (97.8%).[517] The best samples achieve energy efficiencies of 83–84%, which are among the highest values reported for flow batteries and make these membranes strong candidates for stationary energy storage. Table 6 summarizes the characteristics of several grafted and pore-filled membranes used in redox flow batteries.

Accepted manuscript
This manuscript will be edited, formatted, and proof read. The file will be replaced with version of record.

* Coulombic efficiency is the ratio of the charge delivered by a battery during discharge to the charge consumed during charging; in vanadium flow batteries, it decreases primarily due to crossover of vanadium ions through the membrane. Voltage efficiency is the ratio of the average discharge voltage to the average charge voltage and depends primarily on the cell resistance. The energy efficiency is the product of the Coulombic and voltage efficiencies.

Table 6. Properties and performance of some grafted and pore-filled ion-exchange membranes in redox flow batteries

Base film (thickness, μm)	Grafted polymer (GD, %) / Filler	Preparation method	IEC, mmol g^{-1}	Conductivity, mS cm^{-1}[a]	Performance	Test conditions	Ref.
CEMs							
polytetrafluoroethylene (70)	styrene (5–60) or copolymer of styrene and maleic anhydride (5–110)	γ-radiation-induced graft polymerization	1.0–3.5	membrane area resistance 0.66–14 Ω cm^2	ND	electrolyte solution: 1 M $VOSO_4$ in 2 M H_2SO_4	518
polyvinylidene fluoride (20)	styrene and dimethylaminoethyl methacrylate (11.6–26.1)	γ-radiation-induced graft polymerization	0.83	19–52	open circuit voltage 1.2 V	electrodes: graphite carbon positive half: 1.5 M V(II)/V(III) in 2.5 M H_2SO_4 negative half: 1.5 M V(IV)/V(V) in 2.5 M H_2SO_4	519
poly(ethylene-co-tetrafluoroethylene) (25)	styrene and dimethylaminoethyl methacrylate (12.3–23.1)	γ-radiation-induced graft polymerization	0.95–1.06	39–48	open circuit voltage 1.3 V coulombic efficiency: 95.6% voltage efficiency: 78.6% energy efficiency: 75.1%	electrodes: graphite carbon positive half: 1.5 M V(II)/V(III) in 2.5 M H_2SO_4 negative half: 1.5 M V(IV)/V(V) in 2.5 M H_2SO_4 charge/discharge: 1.6 V/0.8 V current density: 40 mA cm^{-2}	520
poly(ethylene-co-tetrafluoroethylene) (50)	2-hydroxyethyl methacrylate and glycidyl methacrylate (150–226)	post electron-beam irradiation-induced graft polymerization	2.05–2.41	20–45 (30 °C)	peak power density 0.315–0.387 W cm^{-2} coulombic efficiency: 72–85% voltage efficiency: 62.5–72.5% energy efficiency: 57.5–62.5%	electrodes: carbon felt positive and negative half: 1.6 M V(II)/V(III) in 4 M H_2SO_4 charge/discharge: 1.8 V/0.6 V	521
poly(ethylene-co-tetrafluoroethylene) (50)	glycidyl methacrylate and hydroxyethyl methacrylate cross-linked with N,N′-methylenebis(acrylamide) (230)	post electron-beam irradiation-induced graft polymerization	2.24	45–62 (30 °C) 67–77 (60 °C)	peak power density 0.474 W cm^{-2} coulombic efficiency: 85%	positive and negative half: 1.6 M V(II)/V(III) in 4 M H_2SO_4 charge/discharge: 1.8 V/0.6 V	460
polyvinylidene fluoride (25)	α-methyl styrene and dimethylaminoethyl methacrylate (9–56)	γ-radiation-induced graft polymerization	1.2	54	open circuit voltage 1.4 V	electrodes: graphite carbon	522

Accepted manuscript
This manuscript will be edited, formatted, and proofread. The file will be replaced with version of Record.

						positive half: 1.5 M V(IV)/V(V) in 3 M H_2SO_4 negative half: 1.5 M V(II)/V(III) in 3 M H_2SO_4 charge/discharge: 1.6 V/0.8 V current density: 40 mA cm^{-2}	
porous polytetrafluoroethylene (ND)	sulfonated poly(ether ether ketone)	impregnation with polymer solution	ND	membrane area resistance 0.57 Ω cm^2	coulombic efficiency: 93% voltage efficiency: 89.6% energy efficiency: 83.7%	electrodes: carbon felt positive half: 1.5 M V(IV)/V(V) in 3 M H_2SO_4 negative half: 1.5 M V(II)/V(III) in 3 M H_2SO_4 charge/discharge: 1.65 V/0.8 V current density: 80 mA cm^{-2}	188
porous polytetrafluoroethylene (ND)	perfluorosulfonated (Nafion®) ionomer	impregnation with polymer solution	0.69	68.1	coulombic efficiency: 94% voltage efficiency: 90.0% energy efficiency: 85.5%	electrodes: graphite felt positive half: 1.5 M V(IV)/V(V) in 2.5 M H_2SO_4 negative half: 1.5 M V(II)/V(III) in 2.5 M H_2SO_4 charge/discharge: 1.65 V/0.8 V	182
porous polytetrafluoroethylene (ND)	sulfonated poly(ether ether ketone) and microporous Engelhard titanosilicate-10	impregnation with polymer solution	ND	34.3–42.6 (in-plane)	coulombic efficiency: 92.5–99.4% voltage efficiency: 85–90% energy efficiency: 82–88%	electrodes: carbon felt positive and negative half: 2 M V(IV)/V(III) in 2 M H_2SO_4 charge/discharge: 1.6 V/0.8 V current density: 80 mA cm^{-2}	523
porous perfluorosulfonated (Nafion®) film (40)	polybenzimidazole	spraying	ND	0.04–1.5 (in 2 M H_2SO_4)	coulombic efficiency: 96–97.5% voltage efficiency: 66–79.5% energy efficiency: 64–78%	electrodes: carbon felt positive and negative half: 1.5 M V(IV) in 2 M H_2SO_4 charge/discharge: 1.6 V/0.8 V current density: 80 mA cm^{-2}	514
porous polyvinylidene fluoride (125)	polybenzimidazole	spraying	ND	membrane area resistance 0.124 Ω cm^2	coulombic efficiency: 97.7–98.4%	electrodes: carbon felt positive and negative half: 1.5 M V(IV) in 2 M H_2SO_4	524

Accepted manuscript
This manuscript will be edited, formatted, and proof read before the file will be replaced with Version of Record.

					voltage efficiency: 85.3–86.5% energy efficiency: 83.3–85.1%	charge/discharge: 1.7 V/0.8 V current density: 80 mA cm^{-2}	
porous polypropylene (60)	styrene and 2-vinyl benzimidazole	impregnation with polymer solution	1.12	32.01	peak power density 0.348 W cm^{-2} coulombic efficiency: 90.5–98.5% voltage efficiency: 79–91% energy efficiency: 77.81–82.35%	positive and negative half: 1 M V(IV)/V(III) in 2 M H_2SO_4 charge/discharge: 1.6 V/1.0 V current density: 20–200 mA cm^{-2}	525
porous polyvinylidene fluoride (125)	perfluorosulfonated (Nafion®) ionomer	impregnation with polymer solution	ND	16–98	coulombic efficiency: 91.3–93.8% voltage efficiency: 60–75% energy efficiency: 56.3–71.3%	electrodes: carbon felt positive half: 1.5 M V(IV) in 2.5 M H_2SO_4 negative half: 1.5 M V(II) in 2.5 M H_2SO_4 charge/discharge: 1.7 V/1.0 V Current density: 50–120 mA cm^{-2}	163
surface treated porous polytetrafluoroethylene (ND)	sulfonated poly(arylene ether ketone)	impregnation with polymer solution	1.15–2.09	41.3–53.1	coulombic efficiency: 96.3–98.3% voltage efficiency: 70.5–88.1% energy efficiency: 69.3–85.1%	electrodes: carbon felt positive half: 1.5 M V(IV) in 3 M H_2SO_4 negative half: 1.5 M V(III) in 3 M H_2SO_4 charge/discharge: 1.7 V/1.0 V Current density: 20–80 mA cm^{-2}	224
porous polyethylene (25)	styrene and 1H,1H,5H-octafluoropentyl methacrylate cross-linked with divinylbenzene	impregnation with monomer solutions followed by thermal induced radical polymerization	1.96–2.74	1.52–4.31 (in 0.5 M NaCl)	coulombic efficiency: 92.4–94.8% voltage efficiency: 92.1–93.5% energy efficiency: 86.3–87.6%	electrodes: carbon felt positive half: 2 M V(IV) in 2 M H_2SO_4 negative half: 2 M V(III) in 2 M H_2SO_4 charge/discharge: 1.9 V/0.9 V Current density: 20 mA cm^{-2}	511
hydrophilic porous polytetrafluoroethylene (40)	sulfonated poly (ether ether ketone) and sulfonated poly (ether ether ketone) blended with metal–organic framework UiO-66-NH_2	asymmetrical casting of polymer solutions	ND	233.3–356.7 (in-plane)	coulombic efficiency: 95.92%	electrodes: graphite felt positive and negative half: 1.7 M V(IV)/V(III) in 4.7 M H_2SO_4	169

Accepted manuscript
This manuscript will be edited, formatted, and proof read. The file will be replaced with Version of Record.

					voltage efficiency: 75.6% energy efficiency: 69.66%	charge/discharge: 1.65 V/0.8 V Current density: 80–200 mA cm^{-2}	
AEM							
poly(ethylene-co-tetrafluoroethylene) (100)	vinylbenzyl trimethyl ammonium chloride and 2-hydroxyl ethyl methacrylate (91.7)	γ-radiation-induced graft polymerization	0.80	ND	coulombic efficiency: 88% voltage efficiency: 79% energy efficiency: 70%	electrodes: graphite carbon positive half: 1.5 M V(II)/V(III) in 2.5 M H_2SO_4 negative half: 1.5 M V(IV)/V(V) in 2.5 M H_2SO_4 charge/discharge: 1.6 V/0.8 V Current density: 20–60 mA cm^{-2}	88
poly(ethylene-co-tetrafluoroethylene) (50)	dimethylaminoethyl methacrylate (5–52)	γ-radiation-induced graft polymerization	0.4–1.96	membrane area resistance 2.3–18 Ω cm^2	open circuit voltage 1.3 V	electrodes: graphite carbon positive half: 1.5 M V(II)/V(III) in 3 M H_2SO_4 negative half: 1.5 M V(IV)/V(V) in 3 M H_2SO_4 charge/discharge: 1.7 V/0.8 V Current density: 20 mA cm^{-2}	526
porous polyethylene (20)	vinylbenzyl chloride cross-linked with divinylbenzene and aminated with pyridine	impregnation with monomer solutions followed by thermal induced radical polymerization	0.32–0.95	membrane area resistance 0.05–0.42 Ω cm^2	coulombic efficiency: 95.6% voltage efficiency: 94.3% energy efficiency: 90.2%	electrodes: graphite felt positive and negative half: 1 M V(IV)/V(III) in 2.5 M H_2SO_4 charge/discharge: 1.65 V/0.8 V	513
porous polyethylene (20)	vinylbenzyl chloride cross-linked with divinylbenzene and quaternized with trimethylamine, triethylamine, 1,4-diazabicyclo[2.2.2]octane, N,N,N,N-tetramethylethylenediamine or tris(2,4,6-trimethoxyphenyl)-phosphine	impregnation with monomer solutions followed by thermal induced radical polymerization	0.44–1.35	5.4–38.1 (in-plane, OH^-)	voltage efficiency: 95.7% energy efficiency: 58.2%	electrodes: graphite felt positive and negative half: 0.01 M $V(acac)_3$ and 0.1 M $TEABF_4$ in CH_3CN charge/discharge: 2.5 V/1.8 V	470
porous polytetrafluoroethylene (80)	N,N′-dimethylaminoethyl methacrylate cross-linked with divinylbenzene and quaternized with p-xylylene dichloride	impregnation with monomer solutions followed by photo-polymerization	1.24–1.95	11–128 (in a 1.0 M KOH aqueous solution, RT)	coulombic efficiency: 90.6–98.47% voltage efficiency: 83.72–87.97%	electrodes: carbon felt positive half: 2 M V(IV) in 3 M H_2SO_4 negative half: 2 M V(III) in 3 M H_2SO_4 charge/discharge: 1.9 V/0.9 V	227

Accepted manuscript
This manuscript will be edited, formatted, and proof read. The file will be replaced with version of record.

					energy efficiency: 77.51–85.50%		
hydrophobic porous polytetrafluoroethylene (80)	N,N'-dimethylaminoethyl methacrylate cross-linked with divinylbenzene quaternized with p-xylylene dichloride	impregnation with monomer solutions followed by photo-polymerization	1.46	10 (in a 1.0 M KOH aqueous solution, RT)	coulombic efficiency: 97.2% voltage efficiency: 89.4% energy efficiency: 86.9%	electrodes: carbon felt positive half: 2 M V(IV) in 3 M H_2SO_4 negative half: 2 M V(III) in 3 M H_2SO_4 charge/discharge: 1.9 V/0.9 V	[472]
hydrophilic porous polytetrafluoroethylene (35)	N,N'-dimethylaminoethyl methacrylate cross-linked with divinylbenzene quaternized with p-xylylene dichloride	impregnation with monomer solutions followed by photo-polymerization	1.42	19 (in a 1.0 M KOH aqueous solution, RT)	coulombic efficiency: 90.9% voltage efficiency: 91.3% energy efficiency: 83.0%	electrodes: carbon felt positive half: 2 M V(IV) in 3 M H_2SO_4 negative half: 2 M V(III) in 3 M H_2SO_4 charge/discharge: 1.9 V/0.9 V	[472]
porous polyethylene (25)	vinylbenzene chloride and 2-(dimethylamino)ethyl methacrylate or 1-allyl-3-methylimidazolium bis(trifluoromethylsulfonyl)imide and 2-(dimethylamino)ethyl methacrylate and cross-linked with divinylbenzene quaternized with p-xylylene dichloride	impregnation with monomer solutions followed by photo-polymerization	1.74–2.42	membrane area resistance 0.54–1.81 Ω cm^2	coulombic efficiency: 93.5–99.3% voltage efficiency: 78.0–90.5% energy efficiency: 74.6–87.4%	electrodes: carbon felt positive half: 2 M V(IV) in 3 M H_2SO_4 negative half: 2 M V(III) in 3 M H_2SO_4 charge/discharge: 1.9 V/0.8 V current density: 20 mA cm^{-2}	[228]
porous polypropylene (60)	4-vinyl pyridine cross-linked with divinylbenzene and quaternized with methyl iodide	impregnation with monomer solution followed by thermal induced radical polymerization	1.4	65	peak power density 0.34 W cm^{-2} coulombic efficiency: 88–99% voltage efficiency: 70–86% energy efficiency: 69–76%	electrodes: graphite felt positive half: 1 M V(IV) in 2 M H_2SO_4 negative half: 1 M V(III) in 2 M H_2SO_4 charge/discharge: 1.8 V/0.8 V current density: 50–150 mA cm^{-2}	[527]
porous polyethylene (25)	vinylbenzyl chloride and 1H,1H,5H-octafluoropentyl methacrylate cross-linked with divinylbenzene	impregnation with monomer solution followed by thermal induced radical polymerization	1.34–2.02	1.58–3.97 (in 0.5 M NaCl)	coulombic efficiency: 93.3–96.4% voltage efficiency: 92.1–93.5%	electrodes: carbon felt positive half: 2 M V(IV) in 2 M H_2SO_4 negative half: 2 M V(III) in 2 M H_2SO_4	[511]

Accepted manuscript
This manuscript will be edited, formatted, and proofread. The file will be replaced with Version of Record.

					energy efficiency: 86.3–87.6%	charge/discharge: 1.9 V/0.9 V Current density: 20 mA cm^{-2}	
surface treated porous polytetrafluoroethylene (ND)	imidazolium grafted poly(arylene ether ketone)	impregnation with polymer solution	1.06–1.26	5.6–6.4	coulombic efficiency: 96.5–98.4% voltage efficiency: 80.8–88.9% energy efficiency: 79.5–85.8%	electrodes: carbon felt positive half: 1.5 M V(IV) in 3 M H_2SO_4 negative half: 1.5 M V(III) in 3 M H_2SO_4 charge/discharge: 1.65 V/0.8 V Current density: 40–100 mA cm^{-2}	225

Note. GD is the grafting degree; IEC is the ion-exchange capacity; RT is room temperature; acac is acetylacetonate; $TEABF_4$ is tetraethylammonium tetrafluoroborate; ND is no data reported.

[a] For some studies, membrane area resistance is given instead of conductivity.

Accepted manuscript
This manuscript will be edited, formatted, and proof read. The final version will be replaced with Version of Record.

5. Conclusion

Modern technologies demand new, highly efficient ion-exchange membranes, and for many applications, relatively inexpensive materials are preferred. Ion conductivity and selectivity are the key performance parameters, but their best combinations are often achieved with expensive homogeneous membranes. In recent years, grafted and pore-filled membranes have become promising alternatives in many applications. Ionic conductivity and selectivity can be tuned over a broad range, and an optimal balance for a given application achieved, by varying the degree of grafting, the degree of crosslinking, and the functional group concentration. The wide choice of base films available for grafting or pore-filling makes it possible to produce thin membranes with sufficient strength, which is a significant advantage in many applications.

This unique combination of properties makes grafted and pore-filled membranes highly promising materials for a wide range of practical applications. They demonstrate excellent performance in electrodialysis and electromembrane energy generation devices such as fuel cells, reverse electrodialysis stacks, and flow batteries. The availability of inexpensive precursors for their synthesis could help significantly reduce the cost of the generated energy. Together with the environmental friendliness of these electromembrane technologies, this opens up broad prospects for their use in the face of rising environmental standards. Less research has been devoted to grafted and pore-filled membranes in electrolyzers and lithium-ion batteries, because many of these membranes are currently unstable at high voltage or when exposed to the reactive oxygen radicals generated during the operation of these devices.

The applications of grafted and pore-filled membranes considered in this review are summarized in Fig. 7. Table 7 lists the main requirements for membranes in these applications and the membrane types most suitable for them. In general, both types of membranes can be used in all these applications, and the choice between them is determined by the required balance of selectivity, conductivity, mechanical strength, and stability under operating conditions.

Table 7. Requirements for ion-exchange membranes in the applications considered and the most suitable membranes for them

Application (section)	Main requirements for the membrane	Most suitable membranes
electrodialysis (4.1)	high counterion selectivity and low area resistance; selectivity for monovalent ions for the recovery of valuable components; chemical stability; low cost	heterogeneous membranes, GMs, PFMs

Accepted manuscript
This manuscript will be edited, formatted, and proofread. The final version may differ from this version.

reverse electrodialysis (4.2)	high selectivity (transport numbers close to 1) and low area resistance, which favors thin membranes; fouling resistance; low cost, since about 400–500 m^2 of membrane is needed per 1 kW	PFMs, GMs, PFSA
water electrolysis (4.3)	high proton (PEM) or hydroxide (AEM) conductivity; low gas crossover; high chemical stability at large potential differences	PFSA, PFMs, GMs
fuel cells (4.3)	high ionic conductivity at low humidity and elevated temperatures; low permeability to hydrogen, oxygen, and methanol; high chemical stability	PFSA, PFMs, GMs
lithium-ion batteries (4.4)	high Li^+ conductivity in the solvated state and high Li^+ transport numbers; wide electrochemical stability window; suppression of dendrite growth	PFSA, PFMs
vanadium redox flow batteries (4.4)	high proton conductivity; low permeability to vanadium ions; high chemical stability; low cost	PFSA, PFMs, GMs

Future advances in grafted and pore-filled membranes will focus on finding combinations of reagents and synthesis routes that produce low cost membranes with a good balance of mechanical and transport properties. At the same time, the degradation of these membranes must be studied in aggressive chemical environments, in fouling-prone natural waters, and under high potential differences. The goal of such studies should be to develop strategies for improving membrane stability and ensuring long-term, efficient operation of devices based on these membranes.

Funding: *This work was financially supported by the Russian Science Foundation, grant No. 25-63-00033.*

Declaration of generative AI and AI-assisted technologies in the manuscript preparation process: *During the preparation of this manuscript, the authors followed the VALENCE recommendations*[528] *and used Claude (Anthropic) for the following purposes: translating parts of the manuscript; language editing; checking the manuscript against the journal's Guide for Authors. After using this tool, the authors reviewed, edited, verified and approved the entire text. The AI tool was not used as a source of scientific conclusions and is not an author or co-author. The authors take full responsibility for the scientific content of the publication.*

Accepted manuscript
This manuscript will be edited, formatted, and proofread. The file will be replaced with Version of Record.

6. List of abbreviations and symbols

Abbreviations

AEM — anion-exchange membrane

AEMFC — anion-exchange membrane fuel cell

CC — concentrate chamber

CEM — cation-exchange membrane

DC — dilute chamber

DI — deionized

EC — electrode chamber

ED — electrodialysis

GD — grafting degree

GM — grafted membrane

IEC — ion-exchange capacity

LIB — lithium-ion battery

ND — no data reported

PEM — proton-exchange membrane

PEMFC — proton-exchange membrane fuel cell

PFM — pore-filled membrane

PFSA — perfluorosulfonic acid

PTFE — polytetrafluoroethylene

PVDF — polyvinylidene fluoride

RED — reverse electrodialysis

RH — relative humidity

RT — room temperature

UV — ultraviolet

Symbols

a_f — activity of NaCl in fresh water

a_s — activity of NaCl in salt water

E_{OCV} — open-circuit potential (membrane potential)

F — Faraday constant

P(A/B) — permselectivity of ion A relative to ion B

P_{max} — maximum theoretical power of a reverse electrodialysis cell

Accepted manuscript
This manuscript will be edited, formatted, and proof read. The file will be replaced with Version of Record.

R — universal gas constant

R_c — internal resistance of the cell

T — absolute temperature

t_{av} — average transport number of cation- and anion-exchange membranes

ΔS — entropy change

Accepted manuscript
This manuscript will be edited, formatted, and proof read. The file will be replaced with Version of Record.

7. References

1. A. Alabi, A. AlHajaj, L. Cseri, G. Szekely, P. Budd, L. Zou. *npj Clean Water*, **1** (1), 10 (2018); https://doi.org/10.1038/s41545-018-0009-7
2. P.Yu. Apel, O.V. Bobreshova, A.V. Volkov, V.V. Volkov, V.V. Nikonenko, I.A. Stenina, A.N. Filippov, Yu.P. Yampolskii, A.B. Yaroslavtsev. *Membr. Membr. Technol.*, **1** (2), 45 (2019) [*Мембраны и мембранные технологии*, **9** (2), 59 (2019)]; https://doi.org/10.1134/S2517751619020021
3. S. Jiang, H. Sun, H. Wang, B.P. Ladewig, Z. Yao. *Chemosphere*, **282**, 130817 (2021); https://doi.org/10.1016/j.chemosphere.2021.130817
4. T.N. Dharmapriya, H.-Y. Shih, P.-J. Huang. *Polymers*, **14** (7), 1442 (2022); https://doi.org/10.3390/polym14071442
5. A. Boubakri. *Desalin. Water Treat.*, **320**, 100700 (2024); https://doi.org/10.1016/j.dwt.2024.100700
6. Y. Cai, M. Fang, X. Tan, B. Hu, X. Wang. *Sep. Purif. Technol.*, **350**, 127975 (2024); https://doi.org/10.1016/j.seppur.2024.127975
7. Y. Bozorov, K. Turaev, R. Alikulov, M. Karimov, B. Muminov, E. Berdimurodov, I. Eliboev, M. Demir, A.S. Yusuff, N. Elangovan. *Chemosphere*, **377**, 144327 (2025); https://doi.org/10.1016/j.chemosphere.2025.144327
8. H.A. Miller, K. Bouzek, J. Hnat, S. Loos, C.I. Bernäcker, T. Weißgärber, L. Röntzsch, J. Meier-Haack. *Sustainable Energy Fuels*, **4** (5), 2114 (2020); https://doi.org/10.1039/C9SE01240K
9. S.S. Kumar, H. Lim. *Sustainable Energy Fuels*, **7** (15), 3560 (2023); https://doi.org/10.1039/D3SE00336A
10. I.A. Stenina, A.B. Yaroslavtsev. *Membr. Membr. Technol.*, **6** (1), 15 (2024) [*Мембраны и мембранные технологии*, **14** (1), 19 (2024)]; https://doi.org/10.1134/S2517751624010050
11. D.Yu. Voropaeva, I.A. Stenina, A.B. Yaroslavtsev. *Russ. Chem. Rev.*, **93** (6), RCR5126 (2024) [*Успехи химии*, **93** (6), RCR5126 (2024)]; https://doi.org/10.59761/RCR5126
12. U.K. Ghorui, G. Sivaguru, U.B. Teja, A. M, S. Ramakrishna, S. Ghosh, G.K. Dalapati, S. Chakrabortty. *ACS Appl. Energy Mater.*, **7** (18), 7649 (2024); https://doi.org/10.1021/acsaem.4c01585

Accepted manuscript
This manuscript will be edited, formatted, and proofread. The file will be replaced with Version of Record.

13. J. Zheng, J. Yan, Y. Dong, S. Chen, F. Gong, Y. Yang, J. Wang, L. Wang, X. Wang. *Int. J. Hydrogen Energy*, **169**, 151191 (2025); https://doi.org/10.1016/j.ijhydene.2025.151191
14. H. Altinisik, C. Celebi, A. Ozden, Y. Devrim, C. Ozgur Colpan. *Renewable Sustainable Energy Rev.*, **226**, 116277 (2026); https://doi.org/10.1016/j.rser.2025.116277
15. X. Xu, Q. He, G. Ma, H. Wang, N. Nirmalakhandan, P. Xu. *Desalination*, **428**, 146 (2018); https://doi.org/10.1016/j.desal.2017.11.015
16. I. Stenina, D. Golubenko, V. Nikonenko, A. Yaroslavtsev. *Int. J. Mol. Sci.*, **21** (15), 5517 (2020); https://doi.org/10.3390/ijms21155517
17. P. Nativ, O. Leifman, O. Lahav, R. Epsztein. *Desalination*, **520**, 115364 (2021); https://doi.org/10.1016/j.desal.2021.115364
18. A.B. Botelho Junior, K. Abels, D.C.R. Espinosa, W.A. Tarpeh. *J. Electrochem. Soc.*, **172** (2), 023501 (2025); https://doi.org/10.1149/1945-7111/adad46
19. V. Atanasov, J. Kerres. *Eur. Polym. J.*, **63**, 168 (2015); https://doi.org/10.1016/j.eurpolymj.2014.12.017
20. L.M. Robeson. *J. Membr. Sci.*, **62** (2), 165 (1991); https://doi.org/10.1016/0376-7388(91)80060-J
21. L.M. Robeson. *J. Membr. Sci.*, **320** (1–2), 390 (2008); https://doi.org/10.1016/j.memsci.2008.04.030
22. H.B. Park, J. Kamcev, L.M. Robeson, M. Elimelech, B.D. Freeman. *Science*, **356** (6343), eaab0530 (2017); https://doi.org/10.1126/science.aab0530
23. E. Chernova, D. Petukhov, O. Boytsova, A. Alentiev, P. Budd, Y. Yampolskii, A. Eliseev. *Sci. Rep.*, **6** (1), 31183 (2016); https://doi.org/10.1038/srep31183
24. B. Comesaña-Gándara, J. Chen, C.G. Bezzu, M. Carta, I. Rose, M.-C. Ferrari, E. Esposito, A. Fuoco, J.C. Jansen, N.B. McKeown. *Energy Environ. Sci.*, **12** (9), 2733 (2019); https://doi.org/10.1039/C9EE01384A
25. D.V. Golubenko, G. Pourcelly, A.B. Yaroslavtsev. *Sep. Purif. Technol.*, **207**, 329 (2018); https://doi.org/10.1016/j.seppur.2018.06.041
26. D. Kitto, J. Kamcev. *ACS Energy Lett.*, **9** (4), 1346 (2024); https://doi.org/10.1021/acsenergylett.4c00301

Accepted manuscript
This manuscript will be edited, formatted, and proof read. The final version may differ from this version of Record.

27. M. Chen, H. Jiang, T. Luo, J. Wu, X. Wang, W. Tang. *Desalination*, **614**, 119154 (2025); https://doi.org/10.1016/j.desal.2025.119154
28. K.A. Mauritz, R.B. Moore. *Chem. Rev.*, **104** (10), 4535 (2004); https://doi.org/10.1021/cr0207123
29. I.A. Prikhno, E.Yu. Safronova, I.A. Stenina, P.A. Yurova, A.B. Yaroslavtsev. *Membr. Membr. Technol.*, **2** (4), 265 (2020) [*Мембраны и мембранные технологии*, **10** (4), 273 (2020)]; https://doi.org/10.1134/S2517751620040095
30. Y. Ke, W. Yuan, F. Zhou, W. Guo, J. Li, Z. Zhuang, X. Su, B. Lu, Y. Zhao, Y. Tang, Y. Chen, J. Song. *Renewable Sustainable Energy Rev.*, **145**, 110860 (2021); https://doi.org/10.1016/j.rser.2021.110860
31. N.A. Kononenko, M.A. Fomenko, Yu.M. Volfkovich. *Adv. Colloid Interface Sci.*, **222**, 425 (2015); https://doi.org/10.1016/j.cis.2014.07.009
32. V.I. Vasilieva, E.E. Meshcheryakova, I.V. Falina, N.A. Kononenko, M.A. Brovkina, E.M. Akberova. *Membr. Membr. Technol.*, **5** (3), 139 (2023) [*Мембраны и мембранные технологии*, **13** (3), 163 (2023)]; https://doi.org/10.1134/S2517751623030083
33. V.I. Zabolotsky, V.V. Nikonenko. *J. Membr. Sci.*, **79** (2–3), 181 (1993); https://doi.org/10.1016/0376-7388(93)85115-D
34. K. Khoiruddin, D. Ariono, S. Subagjo, I.G. Wenten. *J. Phys. Conf. Ser.*, **1090**, 012045 (2018); https://doi.org/10.1088/1742-6596/1090/1/012045
35. K.L. Lim, C.Y. Wong, W.Y. Wong, K.S. Loh, S. Selambakkannu, N.A.F. Othman, H. Yang. *Membranes*, **11** (6), 397 (2021); https://doi.org/10.3390/membranes11060397
36. X. Wang, N. Wang, X. Li, Q.-F. An. *Adv. Membr.*, **1**, 100005 (2021); https://doi.org/10.1016/j.advmem.2021.100005
37. N.A.H.M. Yusoff, M.M. Nasef, S. Sarip, M.A. Suhot, T. Matsuura. *Results Eng.*, **28**, 107921 (2025); https://doi.org/10.1016/j.rineng.2025.107921
38. A. Bhattacharya. *Prog. Polym. Sci.*, **29** (8), 767 (2004); https://doi.org/10.1016/j.progpolymsci.2004.05.002
39. S. Alkan Gürsel, L. Gubler, B. Gupta, G.G. Scherer. In *Fuel Cells I*. (Ed. G.G. Scherer). (Advances in Polymer Science. Vol. 215). (Berlin: Springer, 2008). P. 157; https://doi.org/10.1007/12_2008_153

Accepted manuscript
This manuscript will be edited for style and proof read. The file will be replaced with Version of Record.

40. M.M. Nasef, O. Güven. *Prog. Polym. Sci.*, **37** (12), 1597 (2012); https://doi.org/10.1016/j.progpolymsci.2012.07.004
41. G. Shao, A. Li, Y. Liu, B. Yuan, W. Zhang. *Macromolecules*, **57** (3), 830 (2024); https://doi.org/10.1021/acs.macromol.3c01631
42. M. Nasef. *Prog. Polym. Sci.*, **29** (6), 499 (2004); https://doi.org/10.1016/j.progpolymsci.2004.01.003
43. V. Sproll, G. Nagy, U. Gasser, J.P. Embs, M. Obiols-Rabasa, T.J. Schmidt, L. Gubler, S. Balog. *Macromolecules*, **49** (11), 4253 (2016); https://doi.org/10.1021/acs.macromol.6b00180
44. A. Nasir, A. Raza, M. Tahir, T. Yasin. *Mater. Chem. Phys.*, **246**, 122807 (2020); https://doi.org/10.1016/j.matchemphys.2020.122807
45. M. Tahir, A. Raza, A. Nasir, T. Yasin. *Radiat. Phys. Chem.*, **179**, 109259 (2021); https://doi.org/10.1016/j.radphyschem.2020.109259
46. R.F. Khedr. *Polymers*, **15** (3), 686 (2023); https://doi.org/10.3390/polym15030686
47. Q. Zhang, S. Zhang, S. Chen, P. Li, T. Qin, S. Yuan. *J. Colloid Interface Sci.*, **322** (2), 421 (2008); https://doi.org/10.1016/j.jcis.2008.03.049
48. P. Apel. *Radiat. Meas.*, **34** (1–6), 559 (2001); https://doi.org/10.1016/S1350-4487(01)00228-1
49. T. Takeda, M. Tamada, N. Seko, Y. Ueki. *Radiat. Phys. Chem.*, **79** (3), 223 (2010); https://doi.org/10.1016/j.radphyschem.2009.08.042
50. K. Akamatsu, T. Saito, H. Ohashi, X. Wang, S. Nakao. *Ind. Eng. Chem. Res.*, **60** (42), 15248 (2021); https://doi.org/10.1021/acs.iecr.1c02462
51. T. Friedrich, D. Timm, S. Glass, E.S. Schneider, V. Filiz, W. Maison. *Langmuir*, **42** (1), 949 (2026); https://doi.org/10.1021/acs.langmuir.5c05068
52. P. Suresh, M.M. Sibley, A.C. Che, L.M. Ward, S.T. Weinman, C.E. Duval. *J. Membr. Sci.*, **731**, 124243 (2025); https://doi.org/10.1016/j.memsci.2025.124243
53. B.L. Svarfvar, K.B. Ekman, M.J. Sundell, J.H. Näsman. *Polym. Adv. Technol.*, **7** (11), 839 (1996); https://doi.org/10.1002/(SICI)1099-1581(199611)7:11<839::AID-PAT592>3.0.CO;2-T
54. M. Nasef, H. Saidi, K.M. Dahlan. *Chin. J. Polym. Sci.*, **28** (5), 761 (2010); https://doi.org/10.1007/s10118-010-9138-2

Accepted manuscript
This manuscript will be edited, formatted and proof read before it will be replaced with Version of Record

55. R. Bance-Soualhi, M. Choolaei, S.A. Franklin, T.R. Willson, J. Lee, D.K. Whelligan, C. Crean, J.R. Varcoe. *J. Mater. Chem. A*, **9** (38), 22025 (2021); https://doi.org/10.1039/D1TA05166K
56. A. Ashfaq, M.-C. Clochard, X. Coqueret, C. Dispenza, M.S. Driscoll, P. Ulański, M. Al-Sheikhly. *Polymers*, **12** (12), 2877 (2020); https://doi.org/10.3390/polym12122877
57. J. Ma, J. Peng, M. Zhai. In *Radiation Technology for Advanced Materials: From Basic to Modern Applications*. (Eds G. Wu, M. Zhai, M. Wang). (London: Academic Press, 2019). P. 207; https://doi.org/10.1016/B978-0-12-814017-8.00007-X
58. D.V. Golubenko, B. Van Der Bruggen, A.B. Yaroslavtsev. *J. Power Sources*, **511**, 230460 (2021); https://doi.org/10.1016/j.jpowsour.2021.230460
59. D.V. Golubenko, E.V. Gerasimova, A.B. Yaroslavtsev. *Int. J. Hydrogen Energy*, **46** (32), 16999 (2021); https://doi.org/10.1016/j.ijhydene.2021.01.102
60. A.K. Das, M. Bhushan, V.K. Shahi. *J. Membr. Sci.*, **580**, 134 (2019); https://doi.org/10.1016/j.memsci.2019.01.056
61. M. Ponomar, V. Ruleva, V. Sarapulova, N. Pismenskaya, V. Nikonenko, A. Maryasevskaya, D. Anokhin, D. Ivanov, J. Sharma, V. Kulshrestha, B. Améduri. *Int. J. Mol. Sci.*, **25** (1), 598 (2024); https://doi.org/10.3390/ijms25010598
62. K.W. Kang, C.W. Hwang, T.S. Hwang. *Macromol. Res.*, **23** (12), 1126 (2015); https://doi.org/10.1007/s13233-015-3153-7
63. E.A. Hegazy. *J. Polym. Sci., Polym. Chem. Ed.*, **22** (2), 493 (1984); https://doi.org/10.1002/pol.1984.170220219
64. T.R. Dargaville, G.A. George, D.J.T. Hill, A.K. Whittaker. *Prog. Polym. Sci.*, **28** (9), 1355 (2003); https://doi.org/10.1016/S0079-6700(03)00047-9
65. H. Ben Youcef, L. Gubler, S.A. Gürsel, D. Henkensmeier, A. Wokaun, G.G. Scherer. *Electrochem. Commun.*, **11** (5), 941 (2009); https://doi.org/10.1016/j.elecom.2009.02.047
66. C. Hu, Y.J. Lee, J.Y. Sohn, H. Hwang, S.W. Jung, Y.M. Lee. *J. Power Sources*, **599**, 234228 (2024); https://doi.org/10.1016/j.jpowsour.2024.234228
67. P. Yurova, A. Manin, I. Stenina, A. Yaroslavtsev. *J. Macromol. Sci., Part A*, **62** (8), 669 (2025); https://doi.org/10.1080/10601325.2025.2536029

Accepted manuscript
This manuscript will be edited for style and proofread. The file will be replaced with Version of Record.

68. L. Wang, X. Peng, W.E. Mustain, J.R. Varcoe. *Energy Environ. Sci.*, **12** (5), 1575 (2019); https://doi.org/10.1039/C9EE00331B
69. S.A. Franklin, C. Crean, J.R. Varcoe. *RSC Appl. Polym.*, **4** (1), 320 (2026); https://doi.org/10.1039/D5LP00277J
70. Y.-J. Choi, M.-S. Kang, S.-H. Kim, J. Cho, S.-H. Moon. *J. Membr. Sci.*, **223** (1–2), 201 (2003); https://doi.org/10.1016/S0376-7388(03)00339-9
71. A.L.G. Biancolli, B. Chen, A.S. Menandro, F.C. Fonseca, E.I. Santiago, S. Holdcroft. *J. Mater. Chem. A*, **12** (32), 21442 (2024); https://doi.org/10.1039/D4TA02354D
72. Y. Kodama, A.S. Barbosa, B.P.S. Santos, M. Linardi, E.I. Santiago. *React. Funct. Polym.*, **218**, 106526 (2026); https://doi.org/10.1016/j.reactfunctpolym.2025.106526
73. T.A. Sherazi, J. Yong Sohn, Y. Moo Lee, M.D. Guiver. *J. Membr. Sci.*, **441**, 148 (2013); https://doi.org/10.1016/j.memsci.2013.03.053
74. S. Hasegawa, S. Takahashi, H. Iwase, S. Koizumi, N. Morishita, K. Sato, T. Narita, M. Ohnuma, Y. Maekawa. *Polymer*, **52** (1), 98 (2011); https://doi.org/10.1016/j.polymer.2010.11.009
75. M. Barsbay, O. Güven. *Radiat. Phys. Chem.*, **160**, 1 (2019); https://doi.org/10.1016/j.radphyschem.2019.03.002
76. A.J. Samaniego, A.K. Arabelo, M. Sarker, F. Mojica, J. Madrid, P.A. Chuang, J. Ocon, R. Espiritu. *J. Appl. Polym. Sci.*, **138** (10), 49947 (2021); https://doi.org/10.1002/app.49947
77. R. Rohani, M.M. Nasef, H. Saidi, K.Z.M. Dahlan. *Chem. Eng. J.*, **132** (1–3), 27 (2007); https://doi.org/10.1016/j.cej.2007.01.011
78. M.M. Nasef. *Chem. Rev.*, **114** (24), 12278 (2014); https://doi.org/10.1021/cr4005499
79. J. Zu, F. Tang, L. He, L. Fu. *RSC Adv.*, **8** (46), 25966 (2018); https://doi.org/10.1039/C8RA03472A
80. Honglong. Wang, Lu. Xu, Rong. Li, Lijuan. Pang, Jiangtao. Hu, Mouhua. Wang, Guozhong. Wu. *Appl. Surf. Sci.*, **382**, 162 (2016); https://doi.org/10.1016/j.apsusc.2016.03.175
81. A.M. Abdel Ghaffar, M.B. El-Arnaouty, M.E. Aboulfotouh, N.H. Taher, A.A. Taha. *Radiat. Eff. Defects Solids*, **169** (9), 741 (2014); https://doi.org/10.1080/10420150.2013.870175

Accepted manuscript
This manuscript will be edited, formatted, and proofread. The file will be replaced with a version of record.

82. H. Oraby, M.M. Senna, M. Elsayed, M. Gobara. *J. Appl. Polym. Sci.*, **134** (41), 45410 (2017); https://doi.org/10.1002/app.45410
83. M.M. Nasef, H. Saidi, K.Z.M. Dahlan. *J. Membr. Sci.*, **339** (1–2), 115 (2009); https://doi.org/10.1016/j.memsci.2009.04.037
84. C. Li, L. Wang, X. Wang, M. Kong, Q. Zhang, G. Li. *J. Membr. Sci.*, **527**, 35 (2017); https://doi.org/10.1016/j.memsci.2016.12.065
85. R. Hajj, B. Otazaghine, R. Sonnier, R. El Hage, S. Rouif, M. Nakhl, J.-M. Lopez-Cuesta. *Polym. Degrad. Stab.*, **166**, 86 (2019); https://doi.org/10.1016/j.polymdegradstab.2019.05.025
86. M.M. Nasef, A.A. Aly, H. Saidi, A. Ahmad. *Radiat. Phys. Chem.*, **80** (11), 1222 (2011); https://doi.org/10.1016/j.radphyschem.2011.06.014
87. S.M. Kolhe, A. Kumar. *Radiat. Phys. Chem.*, **76** (5), 901 (2007); https://doi.org/10.1016/j.radphyschem.2006.09.004
88. N.-S. Kwak, J.S. Koo, T.S. Hwang. *Macromol. Res.*, **20** (2), 205 (2012); https://doi.org/10.1007/s13233-012-0032-3
89. C. Na, H. Park. *J. Appl. Polym. Sci.*, **132** (12), app.41674 (2015); https://doi.org/10.1002/app.41674
90. M.H. Ur Rehman, D. Sebastián, P.F. Napal, I. Nicotera, C. Simari. *J. Phys. Chem. C*, **129** (7), 3382 (2025); https://doi.org/10.1021/acs.jpcc.4c07502
91. T. Zhou, R. Shao, S. Chen, X. He, J. Qiao, J. Zhang. *J. Power Sources*, **293**, 946 (2015); https://doi.org/10.1016/j.jpowsour.2015.06.026
92. A. Zaouak, C. Belgacem, N. Ahlem. *Chem. Afr.*, **7** (6), 3387 (2024); https://doi.org/10.1007/s42250-024-00986-3
93. L. Wang, J.J. Brink, Y. Liu, A.M. Herring, J. Ponce-González, D.K. Whelligan, J.R. Varcoe. *Energy Environ. Sci.*, **10** (10), 2154 (2017); https://doi.org/10.1039/C7EE02053H
94. L. Wang, E. Magliocca, E.L. Cunningham, W.E. Mustain, S.D. Poynton, R. Escudero-Cid, M.M. Nasef, J. Ponce-González, R. Bance-Souahli, R.C.T. Slade, D.K. Whelligan, J.R. Varcoe. *Green Chem.*, **19** (3), 831 (2017); https://doi.org/10.1039/C6GC02526A
95. J. Ponce-González, D.K. Whelligan, L. Wang, R. Bance-Soualhi, Y. Wang, Y. Peng, H. Peng, D.C. Apperley, H.N. Sarode, T.P. Pandey, A.G. Divekar, S. Seifert, A.M.

Accepted manuscript
This manuscript will be edited, formatted, and proof read. The file will be replaced with Version of Record

Herring, L. Zhuang, J.R. Varcoe. *Energy Environ. Sci.*, **9** (12), 3724 (2016); https://doi.org/10.1039/C6EE01958G

96. B.P.S. Santos, A.S. Barbosa, Y. Kodama, T.B. De Queiroz, E.I. Santiago. *J. Membr. Sci.*, **687**, 122071 (2023); https://doi.org/10.1016/j.memsci.2023.122071
97. M.M. Nasef, E. Shamsaei, H. Saidi, A. Ahmad, K.Z.M. Dahlan. *J. Appl. Polym. Sci.*, **128** (1), 549 (2013); https://doi.org/10.1002/app.38157
98. P.R.S. Reddy, G. Agathian, A. Kumar. *Radiat. Phys. Chem.*, **73** (3), 169 (2005); https://doi.org/10.1016/j.radphyschem.2004.08.006
99. G.A. Mahmoud. *J. Appl. Polym. Sci.*, **104** (5), 2769 (2007); https://doi.org/10.1002/app.25883
100. J.-Y. Sohn, H.-J. Sung, J. Shin, B.-S. Ko, J.-M. Song, Y.-C. Nho. *Macromol. Res.*, **20** (9), 912 (2012); https://doi.org/10.1007/s13233-012-0131-1
101. K. Yoshimura, A. Hiroki, A. Radulescu, Y. Noda, S. Koizumi, Y. Zhao, Y. Maekawa. *Macromolecules*, **57** (5), 1998 (2024); https://doi.org/10.1021/acs.macromol.3c01897
102. N. Rajabalizadeh Mojarrad, S. Sadeghi, B. Yarar Kaplan, E. Güler, S. Alkan Gürsel. *ACS Appl. Energy Mater.*, **3** (1), 532 (2020); https://doi.org/10.1021/acsaem.9b01777
103. J.E. Coughlin, A. Reisch, M.Z. Markarian, J.B. Schlenoff. *J. Polym. Sci., Part A: Polym. Chem.*, **51** (11), 2416 (2013); https://doi.org/10.1002/pola.26627
104. Y. Lei, Y. Luo, F. Chen, L. Mei. *Polymers*, **6** (7), 1914 (2014); https://doi.org/10.3390/polym6071914
105. Ngadiwiyana, Ismiyarto, Gunawan, R. Purbowatiningrum, N.B.A. Prasetya, T.D. Kusworo, H. Susanto. *J. Phys. Conf. Ser.*, **1025**, 012133 (2018); https://doi.org/10.1088/1742-6596/1025/1/012133
106. B. Gupta, F.N. Büchi, M. Staub, D. Grman, G.G. Scherer. *J. Polym. Sci., Part A: Polym. Chem.*, **34** (10), 1873 (1996); https://doi.org/10.1002/(SICI)1099-0518(19960730)34:10<1873::AID-POLA4>3.0.CO;2-Q
107. S. Alkan Gürsel, Z. Yang, B. Choudhury, M.G. Roelofs, G.G. Scherer. *J. Electrochem. Soc.*, **153** (10), A1964 (2006); https://doi.org/10.1149/1.2335626
108. D.V. Golubenko, B. Van Der Bruggen, A.B. Yaroslavtsev. *J. Appl. Polym. Sci.*, **137** (19), 48656 (2020); https://doi.org/10.1002/app.48656
109. M. Mamlouk, J.A. Horsfall, C. Williams, K. Scott. *Int. J. Hydrogen Energy*, **37** (16), 11912 (2012); https://doi.org/10.1016/j.ijhydene.2012.05.117

Accepted manuscript
This manuscript will be edited for style and proof read. The final version may be replaced with Version of Record

110. A. Chakraborty, I. Salam, M. Choolaei, J. Lee, C. Crean, D.K. Whelligan, R. Bance-Soualhi, J.R. Varcoe. *Mater. Adv.*, **4** (9), 2099 (2023); https://doi.org/10.1039/D3MA00082F
111. T. Hamada, K. Yoshimura, K. Takeuchi, S. Watanabe, Y. Zhao, A. Hiroki, T. Hagiwara, H. Shishitani, S. Yamaguchi, H. Tanaka, A. Radulescu, K. Ohwada, Y. Maekawa. *Macromol. Chem. Phys.*, **222** (11), 2100028 (2021); https://doi.org/10.1002/macp.202100028
112. B. Govind, S. Rattan, P. Singhal, B. Ameduri, A. Tyagi, A. Modak. *Chem. Eng. Technol.*, **48** (3), e202400279 (2025); https://doi.org/10.1002/ceat.202400279
113. V.V. Nikonenko, N.D. Pismenskaya, A.G. Istoshin, V.I. Zabolotsky, A.A. Shudrenko. *Chem. Eng. Process. Process Intensif.*, **47** (7), 1118 (2008); https://doi.org/10.1016/j.cep.2007.12.005
114. B. Auclair, V. Nikonenko, C. Larchet, M. Métayer, L. Dammak. *J. Membr. Sci.*, **195** (1), 89 (2002); https://doi.org/10.1016/S0376-7388(01)00556-7
115. I.A. Stenina, A.B. Yaroslavtsev. *Membranes*, **11** (3), 198 (2021); https://doi.org/10.3390/membranes11030198
116. D.V. Golubenko, E.Y. Safronova, A.B. Ilyin, N.V. Shevlyakova, V.A. Tverskoi, L. Dammak, D. Grande, A.B. Yaroslavtsev. *Mater. Chem. Phys.*, **197**, 192 (2017); https://doi.org/10.1016/j.matchemphys.2017.05.015
117. M.A. Andreeva, V.V. Gil, N.D. Pismenskaya, L. Dammak, N.A. Kononenko, C. Larchet, D. Grande, V.V. Nikonenko. *J. Membr. Sci.*, **549**, 129 (2018); https://doi.org/10.1016/j.memsci.2017.12.005
118. Y. Zhu, R. Weidisch, S.P. Gido, G. Velis, N. Hadjichristidis. *Macromolecules*, **35** (15), 5903 (2002); https://doi.org/10.1021/ma020345x
119. L. Zhang, J. Lin, S. Lin. *Soft Matter*, **5** (1), 173 (2009); https://doi.org/10.1039/B811677F
120. T.D. Tap, D.D. Khiem, L.L. Nguyen, N.Q. Hien, L.Q. Luan, P.B. Thang, S. Sawada, S. Hasegawa, Y. Maekawa. *Radiat. Phys. Chem.*, **151**, 186 (2018); https://doi.org/10.1016/j.radphyschem.2018.06.033
121. E.Y. Safronova, D.V. Golubenko, N.V. Shevlyakova, M.G. D'yakova, V.A. Tverskoi, L. Dammak, D. Grande, A.B. Yaroslavtsev. *J. Membr. Sci.*, **515**, 196 (2016); https://doi.org/10.1016/j.memsci.2016.05.006

Accepted manuscript
This manuscript will be edited, formatted, and proofread before it will be replaced with Version of Record.

122. J. Chattopadhyay, T.S. Pathak, D.M.F. Santos. *Polymers*, **15** (19), 3907 (2023); https://doi.org/10.3390/polym15193907
123. R.P. S., V. Prasannavenkadesan, V. Katiyar, A.S. Achalkumar. *RSC Appl. Polym.*, **3** (3), 499 (2025); https://doi.org/10.1039/D4LP00325J
124. Z. Siddiquee, H. Lee, W. Xu, T. Kyu, A. Jákli. *Batteries*, **11** (3), 106 (2025); https://doi.org/10.3390/batteries11030106
125. F. Hanke, H.J. Kreuzer. *Phys. Rev. E*, **72** (3), 031805 (2005); https://doi.org/10.1103/PhysRevE.72.031805
126. M. Mackley. *Rheol. Acta*, **49** (5), 443 (2010); https://doi.org/10.1007/s00397-010-0435-z
127. R. Wang, D. Ren, X. Sun, W. Liang, K. Wang. *J. Appl. Polym. Sci.*, **136** (16), 47542 (2019); https://doi.org/10.1002/app.47542
128. X. Xiong, S. Wang, L. Xue, H. Wang, J. Cui. *ACS Appl. Mater. Interfaces*, **14** (6), 8473 (2022); https://doi.org/10.1021/acsami.1c23954
129. A.Y. Siavoshani, Z. Fan, M. Yang, S. Liu, M.-C. Wang, J. Liu, W. Xu, J. Wang, S. Lin, S.-Q. Wang. *Soft Matter*, **20** (38), 7657 (2024); https://doi.org/10.1039/D4SM00794H
130. X. Zhou, Y. Zheng, H. Zhang, L. Yang, Y. Cui, B.P. Krishnan, S. Dong, M. Aizenberg, X. Xiong, Y. Hu, J. Aizenberg, J. Cui. *Nat. Commun.*, **14** (1), 3302 (2023); https://doi.org/10.1038/s41467-023-38768-z
131. M.A. Hickner, H. Ghassemi, Y.S. Kim, B.R. Einsla, J.E. McGrath. *Chem. Rev.*, **104** (10), 4587 (2004); https://doi.org/10.1021/cr020711a
132. G. Pourcelly. *Desalination*, **147** (1–3), 359 (2002); https://doi.org/10.1016/S0011-9164(02)00609-4
133. M.A. Shehzad, A. Yasmin, X. Ge, L. Wu, T. Xu. *Adv. Mater. Technol.*, **6** (10), 2001171 (2021); https://doi.org/10.1002/admt.202001171
134. S. Koter, A. Narębska. *Electrochim. Acta*, **32** (3), 455 (1987); https://doi.org/10.1016/0013-4686(87)85013-2
135. L. Wu, H. Jiang, T. Luo, X. Wang. *Membranes*, **13** (10), 811 (2023); https://doi.org/10.3390/membranes13100811

Accepted manuscript
This manuscript will be edited, formatted, and proofread. The final version may differ from this version of Record.

136. V.I. Volkov, A.V. Chernyak, D.V. Golubenko, V.A. Tverskoy, G.A. Lochin, E.S. Odjigaeva, A.B. Yaroslavtsev. *Membranes*, **10** (10), 272 (2020); https://doi.org/10.3390/membranes10100272
137. J. Kamcev. *J. Polym. Sci.*, **59** (21), 2510 (2021); https://doi.org/10.1002/pol.20210304
138. E.-S.A. Hegazy, H.A. Abd El-Rehim, A.M.I. Ali, H.G. Nowier, H.F. Aly. *Nucl. Instrum. Methods Phys. Res., Sect. B*, **151** (1–4), 393 (1999); https://doi.org/10.1016/S0168-583X(99)00107-X
139. H. Fan, Y. Huang, N.Y. Yip. *Front. Environ. Sci. Eng.*, **17** (2), 25 (2023); https://doi.org/10.1007/s11783-023-1625-0
140. J. Ran, L. Wu, Y. He, Z. Yang, Y. Wang, C. Jiang, L. Ge, E. Bakangura, T. Xu. *J. Membr. Sci.*, **522**, 267 (2017); https://doi.org/10.1016/j.memsci.2016.09.033
141. A.N. Ponomarev, E.F. Abdrashitov, D.A. Kritskaya, V.Ch. Bokun, E.A. Sanginov, Yu.A. Dobrovol'skii. *Russ. J. Electrochem.*, **53** (6), 589 (2017) [*Электрохимия*, **53** (6), 666 (2017)]; https://doi.org/10.1134/S1023193517060143
142. T. Yamaguchi, H. Kuroki, F. Miyata. *Electrochem. Commun.*, **7** (7), 730 (2005); https://doi.org/10.1016/j.elecom.2005.04.030
143. A. Navarro, C. Del Río, J.L. Acosta. *J. Polym. Sci., Part B: Polym. Phys.*, **46** (16), 1684 (2008); https://doi.org/10.1002/polb.21505
144. H. Wei, Y. Liu, W. Xu, J. Liu, C. Yan, X. Che, J. Yang, J. Tong, W. Xiao. *J. Electrochem. Soc.*, **166** (14), A3207 (2019); https://doi.org/10.1149/2.0271914jes
145. Y. Kim, H. Kim, J.G. Park, M.-G. Kim, S. Shiori, J. Lee, Y.-G. Jung, S. Yang. *J. Membr. Sci.*, **712**, 123241 (2024); https://doi.org/10.1016/j.memsci.2024.123241
146. J.-H. Lee, J.-Y. Lee, J.-H. Kim, J. Joo, S. Maurya, M. Choun, J. Lee, S.-H. Moon. *J. Membr. Sci.*, **501**, 15 (2016); https://doi.org/10.1016/j.memsci.2015.11.023
147. Y. Oshiba, J. Tomatsu, T. Yamaguchi. *J. Power Sources*, **394**, 67 (2018); https://doi.org/10.1016/j.jpowsour.2018.05.013
148. W. Yuan, L. Zeng, Y. Li, J. Wang, X. Wang, Q. Liao, L. Li, Z. Wei. *Small*, **18** (10), 2105499 (2022); https://doi.org/10.1002/smll.202105499
149. J. Saleem, P. Gao, J. Barford, G. McKay. *J. Mater. Chem. A*, **1** (45), 14335 (2013); https://doi.org/10.1039/c3ta13855k
150. W. Zou, K. Peng, R. Ling, Q. Li, Y. Liu, T. Xu, Z. Yang. *AIChE J.*, **71** (6), e18769 (2025); https://doi.org/10.1002/aic.18769

Accepted manuscript
This manuscript will be edited, formatted, and proofread before it is published in its final version of Record.

151. M. Mohammadi, S. Mehdipour-Ataei. *Int. J. Energy Res.*, **45** (3), 4224 (2021); https://doi.org/10.1002/er.6086
152. H. Asgari, F. Ghavipanjeh, M.R. Sabour, D. Emadzadeh. *Sci. Rep.*, **14** (1), 6399 (2024); https://doi.org/10.1038/s41598-024-56961-y
153. T.H. Nguyen, C. Wang, X. Wang. *J. Membr. Sci.*, **342** (1–2), 208 (2009); https://doi.org/10.1016/j.memsci.2009.06.042
154. T. Wang, F. Sun, H. Wang, S. Yang, L. Fan. *Polymer*, **53** (15), 3154 (2012); https://doi.org/10.1016/j.polymer.2012.05.049
155. N. Wang, S. Ji, J. Li, R. Zhang, G. Zhang. *J. Membr. Sci.*, **455**, 113 (2014); https://doi.org/10.1016/j.memsci.2013.12.023
156. D.M. Yu, S. Yoon, T.-H. Kim, J.Y. Lee, J. Lee, Y.T. Hong. *J. Membr. Sci.*, **446**, 212 (2013); https://doi.org/10.1016/j.memsci.2013.06.028
157. A.L. Mong, S. Yang, D. Kim. *J. Membr. Sci.*, **543**, 133 (2017); https://doi.org/10.1016/j.memsci.2017.07.060
158. C. Zhang, X. Yue, J. Luan, N. Lu, Y. Mu, S. Zhang, G. Wang. *ACS Appl. Energy Mater.*, **3** (7), 7180 (2020); https://doi.org/10.1021/acsaem.0c01212
159. C. Zhang, X. Yue, Y. Yang, N. Lu, S. Zhang, G. Wang. *J. Power Sources*, **450**, 227664 (2020); https://doi.org/10.1016/j.jpowsour.2019.227664
160. J.M. Gohil, D.G. Karamanev. *J. Power Sources*, **243**, 603 (2013); https://doi.org/10.1016/j.jpowsour.2013.06.001
161. S.-H. Wang, H.-L. Lin. *J. Power Sources*, **257**, 254 (2014); https://doi.org/10.1016/j.jpowsour.2014.01.104
162. S. Alwin, S.D. Bhat, A.K. Sahu, A. Jalajakshi, P. Sridhar, S. Pitchumani, A.K. Shukla. *J. Electrochem. Soc.*, **158** (2), B91 (2011); https://doi.org/10.1149/1.3518774
163. U. Dalal, M. Kapoor, A. Verma. *Energy Fuels*, **37** (17), 13457 (2023); https://doi.org/10.1021/acs.energyfuels.3c01932
164. M.M. Nasef, N.A. Zubir, A.F. Ismail, K.Z.M. Dahlan, H. Saidi, M. Khayet. *J. Power Sources*, **156** (2), 200 (2006); https://doi.org/10.1016/j.jpowsour.2005.05.053
165. S.W. Choi, Y.-Z. Fu, Y.R. Ahn, S.M. Jo, A. Manthiram. *J. Power Sources*, **180** (1), 167 (2008); https://doi.org/10.1016/j.jpowsour.2008.02.042
166. T. Yamaguchi, F. Miyata, S. Nakao. *J. Membr. Sci.*, **214** (2), 283 (2003); https://doi.org/10.1016/S0376-7388(02)00579-3

Accepted manuscript
This manuscript will be edited, formatted, and proofread. The final version will be replaced with Version of Record.

167. S. Narayanaru, S. Miyanishi, H. Kuroki, A. M. Gopinathan, T. Yamaguchi. *Adv. Energy Sustainability Res.*, **7** (1), e202500437 (2026); https://doi.org/10.1002/aesr.202500437

168. J.-H. Kim, S. Ryu, S. Maurya, J.-Y. Lee, K.-W. Sung, J.-S. Lee, S.-H. Moon. *RSC Adv.*, **10** (9), 5010 (2020); https://doi.org/10.1039/C9RA08616A

169. P. Zeng, Y. Su, B. Huang, F. Sun, F. Zhao, Y. Guo. *Int. J. Hydrogen Energy*, **120**, 365 (2025); https://doi.org/10.1016/j.ijhydene.2025.03.311

170. Q. Guo, Y. Huang, M. Xu, Q. Huang, J. Cheng, S. Yu, Y. Zhang, C. Xiao. *J. Membr. Sci.*, **664**, 121115 (2022); https://doi.org/10.1016/j.memsci.2022.121115

171. J. Shin, B. Chang, J. Kim, S. Lee, D. Suh. *J. Membr. Sci.*, **251** (1–2), 247 (2005); https://doi.org/10.1016/j.memsci.2004.09.050

172. B. Wang, J. Yan, H. Wang, R. Li, R. Fu, C. Jiang, V. Nikonenko, N. Pismenskaya, Y. Wang, T. Xu. *Chem. Eng. Sci.*, **287**, 119782 (2024); https://doi.org/10.1016/j.ces.2024.119782

173. C.-K. Hwang, K.A. Lee, J. Lee, Y. Kim, H. Ahn, W. Hwang, B.-K. Ju, J.Y. Kim, S.Y. Yeo, J. Choi, Y.-E. Sung, I.-D. Kim, K.R. Yoon. *Nano Energy*, **101**, 107581 (2022); https://doi.org/10.1016/j.nanoen.2022.107581

174. J.Y. Eo, T.K. Lee, G. Kim, B.R. Park, G.S. Chai, S.J. Yoo, J.H. Kim, J.-H. Kim. *J. Power Sources*, **652**, 237638 (2025); https://doi.org/10.1016/j.jpowsour.2025.237638

175. B. Wang, Z. Cui, R. Li, Z. Wang, W. Fu, J. Yan, C. Jiang, L. Wu, Y. Wang, T. Xu. *J. Membr. Sci.*, **736**, 124700 (2025); https://doi.org/10.1016/j.memsci.2025.124700

176. T. Kai, T. Yamaguchi, S. Nakao. *Ind. Eng. Chem. Res.*, **39** (9), 3284 (2000); https://doi.org/10.1021/ie9904100

177. B. Yameen, A. Kaltbeitzel, G. Glasser, A. Langner, F. Müller, U. Gösele, W. Knoll, O. Azzaroni. *ACS Appl. Mater. Interfaces*, **2** (1), 279 (2010); https://doi.org/10.1021/am900690x

178. P. Bocchetta, F. Conciauro, F. Di Quarto. *J. Solid State Electrochem.*, **11** (9), 1253 (2007); https://doi.org/10.1007/s10008-007-0280-x

179. R. Gloukhovski, V. Freger, Y. Tsur. *Fuel Cells*, **16** (4), 434 (2016); https://doi.org/10.1002/fuce.201500166

Accepted manuscript
This manuscript will be edited for style and proof read. The file will be replaced with Version of Record.

180. H.-L. Lin, S.-H. Wang, C.-K. Chiu, T.L. Yu, L.-C. Chen, C.-C. Huang, T.-H. Cheng, J.-M. Lin. *J. Membr. Sci.*, **365** (1–2), 114 (2010); https://doi.org/10.1016/j.memsci.2010.08.045
181. K. Ramya, G. Velayutham, C.K. Subramaniam, N. Rajalakshmi, K.S. Dhathathreyan. *J. Power Sources*, **160** (1), 10 (2006); https://doi.org/10.1016/j.jpowsour.2005.12.082
182. X. Teng, J. Dai, J. Su, Y. Zhu, H. Liu, Z. Song. *J. Power Sources*, **240**, 131 (2013); https://doi.org/10.1016/j.jpowsour.2013.03.177
183. Z. Wang, H. Tang, J. Li, A. Jin, Z. Wang, H. Zhang, M. Pan. *Int. J. Hydrogen Energy*, **38** (11), 4725 (2013); https://doi.org/10.1016/j.ijhydene.2013.01.176
184. H.-Y. Li, Y.-Y. Lee, J.-Y. Lai, Y.-L. Liu. *J. Membr. Sci.*, **466**, 238 (2014); https://doi.org/10.1016/j.memsci.2014.04.057
185. L. Yang, H. Li, F. Ai, X. Chen, J. Tang, Y. Zhu, C. Wang, W.Z. Yuan, Y. Zhang. *J. Power Sources*, **243**, 392 (2013); https://doi.org/10.1016/j.jpowsour.2013.06.056
186. P. Xiao, J. Li, H. Tang, Z. Wang, M. Pan. *J. Membr. Sci.*, **442**, 65 (2013); https://doi.org/10.1016/j.memsci.2013.04.014
187. C. Bi, H. Zhang, S. Xiao, Y. Zhang, Z. Mai, X. Li. *J. Membr. Sci.*, **376** (1–2), 170 (2011); https://doi.org/10.1016/j.memsci.2011.04.017
188. W. Wei, H. Zhang, X. Li, Z. Mai, H. Zhang. *J. Power Sources*, **208**, 421 (2012); https://doi.org/10.1016/j.jpowsour.2012.02.047
189. S. Mollá, V. Compañ. *J. Membr. Sci.*, **492**, 123 (2015); https://doi.org/10.1016/j.memsci.2015.05.055
190. H.-L. Lin, T.L. Yu, L.-N. Huang, L.-C. Chen, K.-S. Shen, G.-B. Jung. *J. Power Sources*, **150**, 11 (2005); https://doi.org/10.1016/j.jpowsour.2005.02.016
191. K. Kim, S.-W. Choi, J.O. Park, S.-K. Kim, M.-Y. Lim, K.-H. Kim, T. Ko, J.-C. Lee. *J. Membr. Sci.*, **536**, 76 (2017); https://doi.org/10.1016/j.memsci.2017.04.058
192. D.V. Golubenko, P.A. Yurova, A.V. Desyatov, I.A. Stenina, S.A. Kosarev, A.B. Yaroslavtsev. *Membr. Membr. Technol.*, **4** (6), 398 (2022) [*Мембраны и мембранные технологии*, **12** (6), 452 (2022)]; https://doi.org/10.1134/S2517751622060026
193. E. Abouzari-Lotf, M.V. Jacob, H. Ghassemi, M. Zakeri, M.M. Nasef, Y. Abdolahi, A. Abbasi, A. Ahmad. *Sci. Rep.*, **11** (1), 3764 (2021); https://doi.org/10.1038/s41598-021-83161-9

Accepted manuscript
This manuscript will be edited for style and proof read. The file will be replaced with Version of Record.

194. S. Yang, Y.-W. Choi, J. Choi, N. Jeong, H. Kim, H. Jeong, S.Y. Byeon, H. Yoon, Y.H. Kim. *J. Membr. Sci.*, **584**, 181 (2019); https://doi.org/10.1016/j.memsci.2019.04.075
195. H. Tang, M. Pan, S.P. Jiang, X. Wang, Y. Ruan. *Electrochim. Acta*, **52** (16), 5304 (2007); https://doi.org/10.1016/j.electacta.2007.02.031
196. R. Gloukhovski, V. Freger, Y. Tsur. *Rev. Chem. Eng.*, **34** (4), 455 (2018); https://doi.org/10.1515/revce-2016-0065
197. D.-H. Kim, J.-H. Park, S.-J. Seo, J.-S. Park, S. Jung, Y.S. Kang, J.-H. Choi, M.-S. Kang. *J. Membr. Sci.*, **447**, 80 (2013); https://doi.org/10.1016/j.memsci.2013.07.017
198. S. Jiang, B.P. Ladewig. *J. Mater. Chem. A*, **7** (29), 17400 (2019); https://doi.org/10.1039/C9TA06248C
199. T. Ma, J. Janot, S. Balme. *Small Methods*, **4** (9), 2000366 (2020); https://doi.org/10.1002/smtd.202000366
200. M.A. Ponomar, V.V. Sarapulova, V.V. Gulyaeva, P.Yu. Apel, N.D. Pismenskaya. *Eurasian J. Chem.*, **30** (3), 65 (2025); https://doi.org/10.31489/2959-0663/3-25-2
201. A. Shiohara, B. Prieto-Simon, N.H. Voelcker. *J. Mater. Chem. B*, **9** (9), 2129 (2021); https://doi.org/10.1039/D0TB01727B
202. A.Yu. Larysheva, A.A. Zvonova, P.M. Tyubaeva, D.V. Bagrov, L.M. Larysheva, O.V. Arzhakova. *Polym. Sci., Ser. A*, **65** (3), 274 (2023) [*Высокомолек. соединения, Сер. А*, **65** (3), 205 (2023)]; https://doi.org/10.1134/S0965545X23700840
203. A.Yu. Larysheva, L.M. Larysheva, F.V. Drozdov, O.V. Arzhakova, A.M. Muzafarov. *Chin. J. Polym. Sci.*, **40** (10), 1307 (2022); https://doi.org/10.1007/s10118-022-2765-6
204. O.V. Arzhakova, A.A. Dolgova, E.G. Rukhlya, A.L. Volynskii. *Polymer*, **161**, 151 (2019); https://doi.org/10.1016/j.polymer.2018.12.018
205. F.E. Ahmed, B.S. Lalia, R. Hashaikeh. *Desalination*, **356**, 15 (2015); https://doi.org/10.1016/j.desal.2014.09.033
206. J. Cui, F. Li, Y. Wang, Q. Zhang, W. Ma, C. Huang. *Sep. Purif. Technol.*, **250**, 117116 (2020); https://doi.org/10.1016/j.seppur.2020.117116
207. J. Lopez-Polo, C. Muñoz-Shugulí, M. Patiño Vidal, C. Patiño Vidal. *Trends Food Sci. Technol.*, **143**, 104253 (2024); https://doi.org/10.1016/j.tifs.2023.104253

Accepted manuscript
This manuscript will be edited for style and proof read. The file will be replaced with Version of Record.

208. A.O. Vorobyev, D.E. Kulbakin, S.G. Chistyakov, A.D. Mitrichenko, G.E. Dubinenko, I.O. Akimchenko, A.S. Gogolev, E.L. Choynzonov, V.M. Bouznik, E.N. Bolbasov. *Russ. J. Phys. Chem. B*, **17** (6), 1316 (2023) [*Хим. физика*, **42** (11), 9 (2023)]; https://doi.org/10.1134/S1990793123060106

209. S.I. Goreninskii, E.Yu. Melnik, E.V. Plotnikov, D.D. Eskova, A.V. Zvyagin, E.N. Bolbasov, S.I. Tverdokhlebov. *Polymer*, **311**, 127549 (2024); https://doi.org/10.1016/j.polymer.2024.127549

210. S.I. Goreninskii, D.V. Sidelev, S. Rutkowski, A.A. Laushkina, O.V. Kukartceva, A.Yu. Fedotkin, A.I. Mishanin, A.S. Golovkin, E.N. Bolbasov, A.B. Yaroslavtsev. *Colloids Surf., A*, **735**, 139480 (2026); https://doi.org/10.1016/j.colsurfa.2026.139480

211. U.V. Chernova, E.Yu. Varakuta, A.D. Koniaeva, A.E. Leyman, S.A. Sagdullaeva, E. Plotnikov, E.Yu. Melnik, T.-H. Tran, S. Rutkowski, V.L. Kudryavtseva, V.M. Buznik, E. Bolbasov. *ACS Appl. Mater. Interfaces*, **16** (16), 20245 (2024); https://doi.org/10.1021/acsami.4c01867

212. A. Piskunova, N. Khomutov, A. Ashikhmin, V. Chobotova, A. Di Martino, E. Melnik, E. Bolbasov, M. Piskunov, P. Strizhak. *Ind. Eng. Chem. Res.*, **64** (27), 13795 (2025); https://doi.org/10.1021/acs.iecr.5c01016

213. D. Ji, Y. Lin, X. Guo, B. Ramasubramanian, R. Wang, N. Radacsi, R. Jose, X. Qin, S. Ramakrishna. *Nat. Rev. Methods Primers*, **4** (1), 1 (2024); https://doi.org/10.1038/s43586-023-00278-z

214. B.S. Lalia, V. Kochkodan, R. Hashaikeh, N. Hilal. *Desalination*, **326**, 77 (2013); https://doi.org/10.1016/j.desal.2013.06.016

215. Y. Qin, H. Yang, Z. Xu, F. Li. *ACS Omega*, **3** (4), 4231 (2018); https://doi.org/10.1021/acsomega.7b02094

216. X. Xiao, M.A. Shehzad, A. Yasmin, Z. Zhang, X. Liang, L. Ge, J. Zhang, L. Wu, T. Xu. *J. Membr. Sci.*, **597**, 117776 (2020); https://doi.org/10.1016/j.memsci.2019.117776

217. E.F. Abdrashitov, D.A. Kritskaya, V.C. Bokun, A.N. Ponomarev, K.S. Novikova, E.A. Sanginov, Y.A. Dobrovolsky. *Solid State Ionics*, **286**, 135 (2016); https://doi.org/10.1016/j.ssi.2016.01.025

Accepted manuscript
This manuscript will be edited for style and proof read. The final will be replaced with Version of Record.

218. A.N. Ponomarev, D.A. Kritskaya, E.F. Abdrashitov, V.Ch. Bokun, E.A. Sanginov, K.S. Novikova, Yu.A. Dobrovol'skii. *Russ. J. Electrochem.*, **55** (8), 738 (2019) [*Электрохимия*, **55** (8), 940 (2019)]; https://doi.org/10.1134/S1023193519080123

219. Yu.A. Dobrovolsky, E.A. Sanginov, N.G. Bukun, A.N. Ponomarev, D.A. Kritskaya, E.F. Abdrashitov. *Nanotechnol. Russ.*, **15** (3–6), 319 (2020) [*Рос. нанотехнологии*, **15** (3), 329 (2020)]; https://doi.org/10.1134/S1995078020030039

220. N.A. Gvozdik, E.A. Sanginov, L.Z. Abunaeva, D.V. Konev, A.A. Usenko, K.S. Novikova, K.J. Stevenson, Y.A. Dobrovolsky. *ChemPlusChem*, **85** (12), 2580 (2020); https://doi.org/10.1002/cplu.202000618

221. K.S. Novikova, E.F. Abdrashitov, D.A. Kritskaya, A.N. Ponomarev, E.A. Sanginov, Yu.A. Dobrovol'skii. *Russ. J. Electrochem.*, **57** (11), 1047 (2021) [*Электрохимия*, **57** (11), 645 (2021)]; https://doi.org/10.1134/S1023193521100116

222. M. Lee, H. Kim, C. Kim, H. Suh, K. Nahm, Y. Choi. *ChemistrySelect*, **2** (5), 1974 (2017); https://doi.org/10.1002/slct.201700167

223. M. Lee, J.-S. Park. *Membranes*, **14** (12), 269 (2024); https://doi.org/10.3390/membranes14120269

224. Y. Ahn, D. Kim. *Energy Storage Mater.*, **31**, 105 (2020); https://doi.org/10.1016/j.ensm.2020.06.035

225. Y. Ahn, D. Kim. *J. Ind. Eng. Chem.*, **110**, 395 (2022); https://doi.org/10.1016/j.jiec.2022.03.016

226. R. Zhou, W. Liu, Y.W. Leong, J. Xu, X. Lu. *ACS Appl. Mater. Interfaces*, **7** (30), 16548 (2015); https://doi.org/10.1021/acsami.5b04034

227. D.-H. Kim, J.-S. Park, M. Choun, J. Lee, M.-S. Kang. *Electrochim. Acta*, **222**, 212 (2016); https://doi.org/10.1016/j.electacta.2016.10.041

228. H.-B. Song, D.-H. Kim, M.-S. Kang. *Membranes*, **12** (2), 196 (2022); https://doi.org/10.3390/membranes12020196

229. H. Fan, Y. Xu, F. Zhao, Q.-B. Chen, D. Wang, J. Wang. *Chem. Eng. J.*, **472**, 144856 (2023); https://doi.org/10.1016/j.cej.2023.144856

230. N. Ul Afsar, M. Holmboe, C.A. Ohlin, N.A. Khan, L. Ge, T. Xu, N. Tavajohi. *Nat. Commun.*, **16** (1), 9120 (2025); https://doi.org/10.1038/s41467-025-64196-2

231. T. Wilberforce, A.G. Olabi, E.T. Sayed, K. Elsaid, M.A. Abdelkareem. *Sci. Total Environ.*, **761**, 143203 (2021); https://doi.org/10.1016/j.scitotenv.2020.143203

Accepted manuscript
This manuscript will be edited, formatted, and proofread before it will be published with a version of record.

232. M. Beccarello, G. Di Foggia. *Energies*, **16** (3), 1345 (2023); https://doi.org/10.3390/en16031345
233. K.M. Abraham. *ACS Energy Lett.*, **5** (11), 3544 (2020); https://doi.org/10.1021/acsenergylett.0c02181
234. T.P. Nguyen, I.T. Kim. *Materials*, **16** (21), 6869 (2023); https://doi.org/10.3390/ma16216869
235. P.-A. Le, V.D. Trung, P.L. Nguyen, T.V. Bac Phung, J. Natsuki, T. Natsuki. *RSC Adv.*, **13** (40), 28262 (2023); https://doi.org/10.1039/D3RA05158G
236. C. Ding, H. Zhang, X. Li, T. Liu, F. Xing. *J. Phys. Chem. Lett.*, **4** (8), 1281 (2013); https://doi.org/10.1021/jz4001032
237. P. Alotto, M. Guarnieri, F. Moro. *Renewable Sustainable Energy Rev.*, **29**, 325 (2014); https://doi.org/10.1016/j.rser.2013.08.001
238. K. Lourenssen, J. Williams, F. Ahmadpour, R. Clemmer, S. Tasnim. *J. Energy Storage*, **25**, 100844 (2019); https://doi.org/10.1016/j.est.2019.100844
239. A. Barzigar, E. Ebadati, A.S. Mujumdar, S.M. Hosseinalipour. *Next Res.*, **2** (4), 100767 (2025); https://doi.org/10.1016/j.nexres.2025.100767
240. A.B. Yaroslavtsev, I.A. Stenina. *Mendeleev Commun.*, **31** (4), 423 (2021); https://doi.org/10.1016/j.mencom.2021.07.001
241. Y. Sugimoto, R. Ujike, M. Higa, Y. Kakihana, M. Higa. *Membranes*, **12** (11), 1141 (2022); https://doi.org/10.3390/membranes12111141
242. S. Chae, H. Kim, J. Gi Hong, J. Jang, M. Higa, M. Pishnamazi, J.-Y. Choi, R. Chandula Walgama, C. Bae, I.S. Kim, J.-S. Park. *Chem. Eng. J.*, **452**, 139482 (2023); https://doi.org/10.1016/j.cej.2022.139482
243. A.B. Yaroslavtsev, I.A. Stenina, D.V. Golubenko. *Pure Appl. Chem.*, **92** (7), 1147 (2020); https://doi.org/10.1515/pac-2019-1208
244. W. Wang, Y. Zhang, X. Yang, H. Sun, Y. Wu, L. Shao. *Engineering*, **25**, 204 (2023); https://doi.org/10.1016/j.eng.2021.09.020
245. Ö. Tekinalp, P. Zimmermann, S. Holdcroft, O.S. Burheim, L. Deng. *Membranes*, **13** (6), 566 (2023); https://doi.org/10.3390/membranes13060566
246. H. Rosentreter, C. Scope, T. Oddoy, A. Lerch, J. Meier-Haack. *Desalination*, **599**, 118412 (2025); https://doi.org/10.1016/j.desal.2024.118412

Accepted manuscript
This manuscript will be edited, formatted, and proofread. The file will be replaced with Version of Record

247. T. Kai, W. Ueno, T. Yamaguchi, S. Nakao. *J. Polym. Sci., Part A: Polym. Chem.*, **43** (10), 2068 (2005); https://doi.org/10.1002/pola.20691

248. N.A. Zhilyaeva, E.Yu. Mironova, M.M. Ermilova, N.V. Orekhova, G.N. Bondarenko, M.G. Dyakova, N.V. Shevlyakova, V.A. Tverskoy, A.B. Yaroslavtsev. *Pet. Chem.*, **56** (11), 1034 (2016) [*Мембраны и мембранные технологии*, **6** (4), 382 (2016)]; https://doi.org/10.1134/S0965544116110165

249. A.S. Yelnikova, P.A. Yurova, A.V. Parshina, Yu.A. Ippolitov, V.I. Popov, I.A. Stenina, O.V. Bobreshova, A.B. Yaroslavtsev. *Membr. Membr. Technol.*, **7** (5), 258 (2025); https://doi.org/10.1134/S2517751625600918

250. P.H. Gleick, H. Cooley. *Annu. Rev. Environ. Resour.*, **46** (1), 319 (2021); https://doi.org/10.1146/annurev-environ-012220-101319

251. G. Chen. *Sep. Purif. Technol.*, **38** (1), 11 (2004); https://doi.org/10.1016/j.seppur.2003.10.006

252. H. Strathmann. *Desalination*, **264** (3), 268 (2010); https://doi.org/10.1016/j.desal.2010.04.069

253. R. Singh, N.P. Hankins. In *Emerging Membrane Technology for Sustainable Water Treatment*. (Eds N.P. Hankins, R. Singh). (Amsterdam: Elsevier, 2016). P. 15; https://doi.org/10.1016/B978-0-444-63312-5.00002-4

254. Md.J.K. Ahmed, M. Ahmaruzzaman. *J. Water Process Eng.*, **10**, 39 (2016); https://doi.org/10.1016/j.jwpe.2016.01.014

255. C.F. Carolin, P.S. Kumar, A. Saravanan, G.J. Joshiba, Mu. Naushad. *J. Environ. Chem. Eng.*, **5** (3), 2782 (2017); https://doi.org/10.1016/j.jece.2017.05.029

256. M. Qasim, M. Badrelzaman, N.N. Darwish, N.A. Darwish, N. Hilal. *Desalination*, **459**, 59 (2019); https://doi.org/10.1016/j.desal.2019.02.008

257. Y. Yao, P. Zhang, C. Jiang, R.M. DuChanois, X. Zhang, M. Elimelech. *Nat. Sustain.*, **4** (2), 138 (2020); https://doi.org/10.1038/s41893-020-00619-w

258. Y. Pang, J. Zhang, R. Ma, Z. Qu, E. Lee, T. Luo. *ACS Energy Lett.*, **5** (2), 437 (2020); https://doi.org/10.1021/acsenergylett.9b02611

259. Y. Zhao, D. You, W. Yang, H. Yu, Q. Pan, S. Song. *Environ. Sci. Water Res. Technol.*, **8** (1), 151 (2022); https://doi.org/10.1039/D1EW00593F

260. J. Liao, J. Xu, H. Ruan, J. Mu, X. Jie, W. Li, Y. Xu, J. Shen. *Desalination*, **546**, 116202 (2023); https://doi.org/10.1016/j.desal.2022.116202

Accepted manuscript
This manuscript will be edited, formatted, and proofread; the file will be replaced with a version of record.

261. M. Sedighi, M.M. Behvand Usefi, A.F. Ismail, M. Ghasemi. *Desalination*, **549**, 116319 (2023); https://doi.org/10.1016/j.desal.2022.116319
262. K. Tado, F. Sakai, Y. Sano, A. Nakayama. *Desalination*, **378**, 60 (2016); https://doi.org/10.1016/j.desal.2015.10.001
263. A. Campione, L. Gurreri, M. Ciofalo, G. Micale, A. Tamburini, A. Cipollina. *Desalination*, **434**, 121 (2018); https://doi.org/10.1016/j.desal.2017.12.044
264. E. Jashni, S.M. Hosseini, J.N. Shen, B. Van Der Bruggen. *Ionics*, **25** (11), 5595 (2019); https://doi.org/10.1007/s11581-019-03068-4
265. S. Al-Amshawee, M.Y.B.M. Yunus, A.A.M. Azoddein, D.G. Hassell, I.H. Dakhil, H.A. Hasan. *Chem. Eng. J.*, **380**, 122231 (2020); https://doi.org/10.1016/j.cej.2019.122231
266. G.V. Talekar, S. Mutnuri. *Front. Energy Res.*, **8**, 20 (2020); https://doi.org/10.3389/fenrg.2020.00020
267. M. Aliaskari, A.I. Schäfer. *Water Res.*, **190**, 116683 (2021); https://doi.org/10.1016/j.watres.2020.116683
268. H. Fan, Y. Huang, P. Cruz-Grace, N.Y. Yip. *ACS ES&T Eng.*, **4** (9), 2294 (2024); https://doi.org/10.1021/acsestengg.4c00246
269. J. Li, J. Guo, X. Zhang, H. Su, Y. Tang, X. Li, Y. Zhao, T. Luo, Z. Liu, X. Wang. *Ind. Eng. Chem. Res.*, **64** (47), 22854 (2025); https://doi.org/10.1021/acs.iecr.5c03450
270. A.D. Manin, A.A. Lysova, I.A. Stenina, S.A. Novikova, A.B. Yaroslavtsev. *Membr. Membr. Technol.*, **7** (4), 207 (2025); https://doi.org/10.1134/S2517751625600827
271. A. Merkel, G. Rudolph-Schöpping, S. Suwal, F. Lipnizki, S.K. Lillevang, L. Ahrné. *J. Membr. Sci.*, **694**, 122429 (2024); https://doi.org/10.1016/j.memsci.2024.122429
272. A. Merkel, T. León, L. Jofre, J.L. Cortina, L. Dvořák, L. Ahrné. *J. Food Eng.*, **378**, 112106 (2024); https://doi.org/10.1016/j.jfoodeng.2024.112106
273. X. Liu, Y. Gou, J. Bi, Z. Li. *Sep. Purif. Technol.*, **373**, 133555 (2025); https://doi.org/10.1016/j.seppur.2025.133555
274. A. Lugo, M.F. Ahmed, T.L. Oddonetto, P.S. Senanayake, I. Basnayake, Z. Stoll, M. Ehsani, N.E. Moe, J. Barber, H. Wang, P. Xu. *Desalination*, **615**, 119290 (2025); https://doi.org/10.1016/j.desal.2025.119290
275. D. Yang, H. Liu, Z.H. Foo, Q. She. *Desalination*, **615**, 119306 (2025); https://doi.org/10.1016/j.desal.2025.119306

Accepted manuscript
This manuscript will be edited for style and proof read. The file will be replaced with Version of Record

276. G. Doornbusch, M. Van Der Wal, M. Tedesco, J. Post, K. Nijmeijer, Z. Borneman. *Desalination*, **505**, 114973 (2021); https://doi.org/10.1016/j.desal.2021.114973
277. P. Wang, H. Chen, Q. Ren. *Desalination*, **624**, 119904 (2026); https://doi.org/10.1016/j.desal.2026.119904
278. M.M. Kabir, G.Md. Sabur, Mst.M. Akter, S.Y. Nam, K.S. Im, L. Tijing, H.K. Shon. *Desalination*, **569**, 117041 (2024); https://doi.org/10.1016/j.desal.2023.117041
279. G. Sim, M. Pishnamazi, D. Seo, S.R. Kong, J. Lee, Y. Park, S.R. Chae. *Chem. Eng. J.*, **497**, 154640 (2024); https://doi.org/10.1016/j.cej.2024.154640
280. F.E. Bortot Coelho, V.R. Moreira, D. Majuste, V.S.T. Ciminelli, M.C.S. Amaral. *Desalination*, **612**, 118900 (2025); https://doi.org/10.1016/j.desal.2025.118900
281. J. Mustafa, A.H. Al-Marzouqi, N. Ghasem, M.H. El-Naas, B. Van Der Bruggen. *Desalination*, **548**, 116263 (2023); https://doi.org/10.1016/j.desal.2022.116263
282. J. Bi, T. Chen, Y. Xie, R. Shen, B. Li, M. Sun, X. Guo, Y. Zhao. *J. Environ. Sci.*, **142**, 21 (2024); https://doi.org/10.1016/j.jes.2023.11.014
283. Y. Tanaka. *Ion Exchange Membranes: Fundamentals and Applications*. 2nd ed. (Amsterdam: Elsevier, 2015). P. 255; https://doi.org/10.1016/B978-0-444-63319-4.00012-2
284. R.K. Nagarale, G.S. Gohil, V.K. Shahi. *Adv. Colloid Interface Sci.*, **119** (2–3), 97 (2006); https://doi.org/10.1016/j.cis.2005.09.005
285. N.-S. Kwak, W.H. Jung, H.-M. Park, T.S. Hwang. *Chem. Eng. J.*, **215–216**, 375 (2013); https://doi.org/10.1016/j.cej.2012.10.065
286. N. J., R.K. Singh. *J. Mater. Chem. A*, **13** (43), 36853 (2025); https://doi.org/10.1039/D5TA05392G
287. Y. Tanaka. *Ind. Eng. Chem. Res.*, **50** (18), 10765 (2011); https://doi.org/10.1021/ie2005498
288. Y. Ren, A. Zhang, L. Li, L. Ma, Q. Jin, M. Yuan, G. He, F. Zhang. *Sep. Purif. Technol.*, **305**, 122419 (2023); https://doi.org/10.1016/j.seppur.2022.122419
289. S. Sarkar, P. Patnaik, R. Mondal, U. Chatterjee. *ACS Appl. Polym. Mater.*, **5** (3), 1977 (2023); https://doi.org/10.1021/acsapm.2c02045
290. F. Deboli, B. Van Der Bruggen, M.L. Donten. *Desalination*, **535**, 115794 (2022); https://doi.org/10.1016/j.desal.2022.115794

Accepted manuscript
This manuscript will be edited for style and proof read. The file will be replaced with Version of Record

291. D. You, Z. Feng, J. Wu, Z. Xiao, X. Li, Y. Yu. *Desalination*, **574**, 117240 (2024); https://doi.org/10.1016/j.desal.2023.117240

292. A.S.S. Kachooei, S. Rowshanzamir. *J. Power Sources*, **656**, 238116 (2025); https://doi.org/10.1016/j.jpowsour.2025.238116

293. B. Wang, J. Yan, H. Wang, R. Li, R. Fu, C. Jiang, V. Nikonenko, N. Pismenskaya, Y. Wang, T. Xu. *J. Membr. Sci.*, **670**, 121348 (2023); https://doi.org/10.1016/j.memsci.2023.121348

294. V.A. Troitskiy, M.A. Ponomar, R.M. Salikhov, N.V. Smirnova, K.G. Sabbatovskii, S.A. Mareev, D.Yu. Butylskii, V.V. Nikonenko. *Membr. Membr. Technol.*, **7** (5), 246 (2025); https://doi.org/10.1134/S251775162560092X

295. L. Kong, G. Yan, K. Hu, Y. Yu, N. Conte, K.R. Mckenzie Jr, M.J. Wagner, S.G. Boyes, H. Chen, C. Liu, X. Liu. *Nat. Commun.*, **16** (1), 806 (2025); https://doi.org/10.1038/s41467-025-56071-x

296. Z. Ji, Q. Chen, J. Yuan, J. Liu, Y. Zhao, W. Feng. *Sep. Purif. Technol.*, **172**, 168 (2017); https://doi.org/10.1016/j.seppur.2016.08.006

297. X.-Y. Nie, S.-Y. Sun, Z. Sun, X. Song, J.-G. Yu. *Desalination*, **403**, 128 (2017); https://doi.org/10.1016/j.desal.2016.05.010

298. G. Cao, K. Zhang, X. Liu, S. Zhang, C. Jiang, T. Xu. *Chin. J. Chem. Eng.*, **86**, 45 (2025); https://doi.org/10.1016/j.cjche.2025.07.006

299. A.H.M.G. Hyder, B. Nuraeni, S.M. Gallagher, M. Wasilk, J.D. Macholz, A.L. Lipson, J. Spangenberger. *ACS Sustainable Chem. Eng.*, **13** (12), 4651 (2025); https://doi.org/10.1021/acssuschemeng.4c07708

300. M. Reig, H. Farrokhzad, B. Van Der Bruggen, O. Gibert, J.L. Cortina. *Desalination*, **375**, 1 (2015); https://doi.org/10.1016/j.desal.2015.07.023

301. M. Boucher, N. Turcotte, V. Guillemette, G. Lantagne, A. Chapotot, G. Pourcelly, R. Sandeaux, C. Gavach. *Hydrometallurgy*, **45** (1–2), 137 (1997); https://doi.org/10.1016/S0304-386X(96)00069-2

302. G. Yadav, N. Yadav, S. Kapoor, G. Singh, P. Garg, P. Attri, R.K. Sharma, G.R. Chaudhary. *J. Mater. Chem. A*, **14** (17), 9805 (2026); https://doi.org/10.1039/D5TA07013A

303. D. Wang, Q. Chen, B. He, H. Fan, H. Zhang, P. Li, J. Wang. *J. Membr. Sci.*, **744**, 125215 (2026); https://doi.org/10.1016/j.memsci.2026.125215

Accepted manuscript
This manuscript will be edited for style and proof read before it will be replaced with Version of Record.

304. J. Lambert, M. Avila-Rodriguez, G. Durand, M. Rakib. *J. Membr. Sci.*, **280** (1–2), 219 (2006); https://doi.org/10.1016/j.memsci.2006.01.021

305. S.M. Hosseini, S.S. Madaeni, A.R. Heidari, A. Amirimehr. *Desalination*, **284**, 191 (2012); https://doi.org/10.1016/j.desal.2011.08.057

306. L. Ge, B. Wu, D. Yu, A.N. Mondal, L. Hou, N.U. Afsar, Q. Li, T. Xu, J. Miao, T. Xu. *Chin. J. Chem. Eng.*, **25** (11), 1606 (2017); https://doi.org/10.1016/j.cjche.2017.06.002

307. Y. Zhang, L. Wang, W. Sun, Y. Hu, H. Tang. *J. Ind. Eng. Chem.*, **81**, 7 (2020); https://doi.org/10.1016/j.jiec.2019.09.002

308. T. Luo, S. Abdu, M. Wessling. *J. Membr. Sci.*, **555**, 429 (2018); https://doi.org/10.1016/j.memsci.2018.03.051

309. D.V. Golubenko, A.D. Manin, Y. Wang, T. Xu, A.B. Yaroslavtsev. *Desalination*, **531**, 115719 (2022); https://doi.org/10.1016/j.desal.2022.115719

310. D.V. Golubenko, A.D. Manin, L. Wu, T. Xu, A.B. Yaroslavtsev. *Desalination*, **573**, 117178 (2024); https://doi.org/10.1016/j.desal.2023.117178

311. M.-L. Liu, Y. Chen, C. Hu, C.-X. Zhang, Z.-J. Fu, Z. Xu, Y.M. Lee, S.-P. Sun. *Nat. Commun.*, **15** (1), 7271 (2024); https://doi.org/10.1038/s41467-024-51540-1

312. M. Kumar, B.P. Tripathi, V.K. Shahi. *J. Membr. Sci.*, **340** (1–2), 52 (2009); https://doi.org/10.1016/j.memsci.2009.05.010

313. A.K. Thakur, M. Manohar, V.K. Shahi. *J. Mater. Chem. A*, **3** (35), 18279 (2015); https://doi.org/10.1039/C5TA04468E

314. D.V. Golubenko, Yu.A. Karavanova, S.S. Melnikov, A.R. Achoh, G. Pourcelly, A.B. Yaroslavtsev. *J. Membr. Sci.*, **563**, 777 (2018); https://doi.org/10.1016/j.memsci.2018.06.024

315. D. Golubenko, D. Petukhov, R.A. Al-Juboori, D. Johnson, N. Hilal. *ACS Appl. Polym. Mater.*, **6** (19), 11762 (2024); https://doi.org/10.1021/acsapm.4c01782

316. A.A. Lysova, A.D. Manin, D.V. Golubenko, I.I. Ponomarev, V.A. Altynov, N. Hilal, A.B. Yaroslavtsev. *J. Membr. Sci.*, **716**, 123518 (2025); https://doi.org/10.1016/j.memsci.2024.123518

317. D.V. Golubenko, A.B. Yaroslavtsev. *J. Membr. Sci.*, **635**, 119466 (2021); https://doi.org/10.1016/j.memsci.2021.119466

Accepted manuscript
This manuscript will be edited for style and proof read. The final version will be published with Version of Record.

318. K.A. Bondarenko, A.D. Manin, P.A. Yurova, I.A. Stenina, A.B. Yaroslavtsev. *Membr. Membr. Technol.*, **7** (3), 166 (2025); https://doi.org/10.1134/S2517751625600839
319. S. Abdu, M.-C. Martí-Calatayud, J.E. Wong, M. García-Gabaldón, M. Wessling. *ACS Appl. Mater. Interfaces*, **6** (3), 1843 (2014); https://doi.org/10.1021/am4048317
320. A.A.E. Elozeiri, J.E. Dykstra, R.G.H. Lammertink, H.H.M. Rijnaarts. *ACS Appl. Mater. Interfaces*, **17** (14), 22004 (2025); https://doi.org/10.1021/acsami.5c00155
321. T. Rijnaarts, D.M. Reurink, F. Radmanesh, W.M. De Vos, K. Nijmeijer. *J. Membr. Sci.*, **570–571**, 513 (2019); https://doi.org/10.1016/j.memsci.2018.10.074
322. H. Farrokhzad, S. Darvishmanesh, G. Genduso, T. Van Gerven, B. Van Der Bruggen. *Electrochim. Acta*, **158**, 64 (2015); https://doi.org/10.1016/j.electacta.2015.01.062
323. J. Li, J. Zhu, S. Yuan, X. Li, Z. Zhao, Y. Zhao, Y. Liu, A. Volodine, J. Li, J. Shen, B. Van Der Bruggen. *Ind. Eng. Chem. Res.*, **57** (18), 6275 (2018); https://doi.org/10.1021/acs.iecr.8b00695
324. A.T. Besha, M.T. Tsehaye, D. Aili, W. Zhang, R.A. Tufa. *Membranes*, **10** (1), 7 (2019); https://doi.org/10.3390/membranes10010007
325. F. Roghmans, E. Evdochenko, M.C. Martí-Calatayud, M. Garthe, R. Tiwari, A. Walther, M. Wessling. *J. Membr. Sci.*, **600**, 117854 (2020); https://doi.org/10.1016/j.memsci.2020.117854
326. X. Pang, Y. Tao, Y. Xu, J. Pan, J. Shen, C. Gao. *J. Membr. Sci.*, **595**, 117544 (2020); https://doi.org/10.1016/j.memsci.2019.117544
327. D. Golubenko, A. Yaroslavtsev. *J. Membr. Sci.*, **612**, 118408 (2020); https://doi.org/10.1016/j.memsci.2020.118408
328. T. Sata. *J. Membr. Sci.*, **93** (2), 117 (1994); https://doi.org/10.1016/0376-7388(94)80001-4
329. Ö. Tekinalp, P. Zimmermann, O.S. Burheim, L. Deng. *J. Membr. Sci.*, **666**, 121148 (2023); https://doi.org/10.1016/j.memsci.2022.121148
330. M. Irfan, T. Xu, L. Ge, Y. Wang, T. Xu. *J. Membr. Sci.*, **588**, 117211 (2019); https://doi.org/10.1016/j.memsci.2019.117211
331. H.J. Cassady, E.C. Cimino, M. Kumar, M.A. Hickner. *J. Membr. Sci.*, **508**, 146 (2016); https://doi.org/10.1016/j.memsci.2016.02.048

Accepted manuscript
This manuscript will be edited, formatted, and proof read. The final version will be replaced with the version of record.

332. D. You, J. Zhang, S. Yuan, D. Mao, X. Li, Y. Yu. *Desalination*, **623**, 119858 (2026); https://doi.org/10.1016/j.desal.2026.119858

333. G. Zhao, J. Sun, G. Tang, G. Pan, H. Yu, Y. Li, Y. Zhang, Y. Liu. *Sep. Purif. Technol.*, **335**, 126184 (2024); https://doi.org/10.1016/j.seppur.2023.126184

334. I.S. Kim, C.W. Hwang, Y.J. Kim, A. Canlier, K.S. Jeong, T.S. Hwang. *Macromol. Res.*, **25** (11), 1063 (2017); https://doi.org/10.1007/s13233-017-5145-2

335. J.H. Chen, A. Masaharu, Y. Maekawa. *Adv. Mater. Res.*, **881–883**, 1157 (2014); https://doi.org/10.4028/www.scientific.net/AMR.881-883.1157

336. L. Hou, J. Pan, D. Yu, B. Wu, A.N. Mondal, Q. Li, L. Ge, T. Xu. *J. Membr. Sci.*, **528**, 243 (2017); https://doi.org/10.1016/j.memsci.2017.01.036

337. M. Jian, T. Ma, Z. Wang, X. Ding, H. Gao, S. Pan, B. Wang, L. Yang, L. Jiang, J. Gao. *Angew. Chem., Int. Ed.*, **64** (51), e202515502 (2025); https://doi.org/10.1002/anie.202515502

338. R. Mondal, S. Pal, D.V. Bhalani, V. Bhadja, U. Chatterjee, S.K. Jewrajka. *Desalination*, **445**, 85 (2018); https://doi.org/10.1016/j.desal.2018.07.032

339. D. You, D. Mao, X. Li, Y. Yu. *J. Appl. Polym. Sci.*, **142** (25), e57065 (2025); https://doi.org/10.1002/app.57065

340. J.G. Kim, J. Ku, J. Jung, Y.S. Park, G.H. Choi, S.S. Hwang, J.-H. Lee, A.S. Lee. *J. Cleaner Prod.*, **438**, 140779 (2024); https://doi.org/10.1016/j.jclepro.2024.140779

341. J.-H. Lee, D.-H. Kim, M.-S. Kang. *Membranes*, **13** (12), 894 (2023); https://doi.org/10.3390/membranes13120894

342. B. Seo, N. Jeong, J.-O. Kim, S. Chae, H. Kim. *Sep. Purif. Technol.*, **388**, 136728 (2026); https://doi.org/10.1016/j.seppur.2025.136728

343. M. Higa, S. Morinaga, R. Ujike, H. Kawasaki, K. Okamoto, Y. Takaoka, Y. Sugimoto, M. Higa. *J. Membr. Sci.*, **736**, 124689 (2025); https://doi.org/10.1016/j.memsci.2025.124689

344. K. Nijmeijer, S. Metz. In *Sustainable Water for the Future: Water Recycling versus Desalination*. (Eds I.C. Escobar, A.I. Schäfer). (Sustainability Science and Engineering. Vol. 2). (Amsterdam: Elsevier, 2010). P. 95; https://doi.org/10.1016/S1871-2711(09)00205-0

345. Z. Jia, B. Wang, S. Song, Y. Fan. *Renewable Sustainable Energy Rev.*, **31**, 91 (2014); https://doi.org/10.1016/j.rser.2013.11.049

Accepted manuscript
This manuscript will be edited, formatted, and proofread. The final version may be replaced with Version of Record

346. N.Y. Yip, D. Brogioli, H.V.M. Hamelers, K. Nijmeijer. *Environ. Sci. Technol.*, **50** (22), 12072 (2016); https://doi.org/10.1021/acs.est.6b03448

347. A. Siria, M.-L. Bocquet, L. Bocquet. *Nat. Rev. Chem.*, **1** (11), 0091 (2017); https://doi.org/10.1038/s41570-017-0091

348. A.H. Avci, D.A. Messana, S. Santoro, R.A. Tufa, E. Curcio, G. Di Profio, E. Fontananova. *Membranes*, **10** (8), 168 (2020); https://doi.org/10.3390/membranes10080168

349. J.G. Hong, B. Zhang, S. Glabman, N. Uzal, X. Dou, H. Zhang, X. Wei, Y. Chen. *J. Membr. Sci.*, **486**, 71 (2015); https://doi.org/10.1016/j.memsci.2015.02.039

350. R.A. Tufa, S. Pawlowski, J. Veerman, K. Bouzek, E. Fontananova, G. Di Profio, S. Velizarov, J. Goulão Crespo, K. Nijmeijer, E. Curcio. *Appl. Energy*, **225**, 290 (2018); https://doi.org/10.1016/j.apenergy.2018.04.111

351. M. Yasukawa, S. Mehdizadeh, T. Sakurada, T. Abo, M. Kuno, M. Higa. *Desalination*, **491**, 114449 (2020); https://doi.org/10.1016/j.desal.2020.114449

352. P. Dlugolecki, K. Nymeijer, S. Metz, M. Wessling. *J. Membr. Sci.*, **319** (1–2), 214 (2008); https://doi.org/10.1016/j.memsci.2008.03.037

353. R.A. Tufa, E. Curcio, W. Van Baak, J. Veerman, S. Grasman, E. Fontananova, G. Di Profio. *RSC Adv.*, **4** (80), 42617 (2014); https://doi.org/10.1039/C4RA05968A

354. E. Güler, R. Elizen, M. Saakes, K. Nijmeijer. *J. Membr. Sci.*, **458**, 136 (2014); https://doi.org/10.1016/j.memsci.2014.01.060

355. M. Vanoppen, E. Criel, G. Walpot, D.A. Vermaas, A. Verliefde. *npj Clean Water*, **1** (1), 9 (2018); https://doi.org/10.1038/s41545-018-0010-1

356. J. Moreno, S. Grasman, R. Van Engelen, K. Nijmeijer. *Environ. Sci. Technol.*, **52** (18), 10856 (2018); https://doi.org/10.1021/acs.est.8b01886

357. E. Altıok, T.Z. Kaya, E. Güler, N. Kabay, M. Bryjak. *Water*, **13** (6), 814 (2021); https://doi.org/10.3390/w13060814

358. J.-E. Cha, S. Jang, D.-J. Seo, J. Hwang, M.H. Seo, Y.-W. Choi, W.B. Kim. *Chem. Eng. J.*, **454**, 140091 (2023); https://doi.org/10.1016/j.cej.2022.140091

359. J. Choi, S. Yang, N.-J. Jeong, H. Kim, W.-S. Kim. *Langmuir*, **34** (37), 10837 (2018); https://doi.org/10.1021/acs.langmuir.8b01666

Accepted manuscript
This manuscript will be edited, formatted, and proofread before it will be replaced with Version of Record.

360. S. Yang, Y.-W. Choi, J. Choi, N. Jeong, H. Kim, J.-Y. Nam, H. Jeong. *ACS Sustainable Chem. Eng.*, **7** (14), 12200 (2019); https://doi.org/10.1021/acssuschemeng.9b01450

361. S. Yang, W.-S. Kim, J. Choi, Y.-W. Choi, N. Jeong, H. Kim, J.-Y. Nam, H. Jeong, Y.H. Kim. *J. Membr. Sci.*, **573**, 544 (2019); https://doi.org/10.1016/j.memsci.2018.12.034

362. T.R. Willson, I. Hamerton, J.R. Varcoe, R. Bance-Soualhi. *Sustainable Energy Fuels*, **3** (7), 1682 (2019); https://doi.org/10.1039/C8SE00579F

363. Y.J. Lee, M.S. Cha, S.-G. Oh, S. So, T.-H. Kim, W.S. Ryoo, Y.T. Hong, J.Y. Lee. *RSC Adv.*, **9** (47), 27500 (2019); https://doi.org/10.1039/C9RA04984C

364. H. Kim, J. Choi, N. Jeong, Y.-G. Jung, H. Kim, D. Kim, S. Yang. *Membranes*, **11** (8), 609 (2021); https://doi.org/10.3390/membranes11080609

365. X. Tong, B. Zhang, Y. Chen. *J. Membr. Sci.*, **516**, 162 (2016); https://doi.org/10.1016/j.memsci.2016.05.060

366. H. Susanto, M. Fitrianingtyas, A.M. Samsudin, A. Syakur. *Int. J. Energy Res.*, **41** (10), 1474 (2017); https://doi.org/10.1002/er.3728

367. F. Kotoka, I. Merino-Garcia, S. Velizarov. *Membranes*, **10** (8), 160 (2020); https://doi.org/10.3390/membranes10080160

368. T. Sampedro, C. Tristán, L. Gómez-Coma, M. Fallanza, I. Ortiz, R. Ibañez. *Membranes*, **13** (6), 546 (2023); https://doi.org/10.3390/membranes13060546

369. M. Vaselbehagh, H. Karkhanechi, R. Takagi, H. Matsuyama. *J. Membr. Sci.*, **530**, 232 (2017); https://doi.org/10.1016/j.memsci.2017.02.036

370. J. Moreno, V. Díez, M. Saakes, K. Nijmeijer. *J. Membr. Sci.*, **550**, 155 (2018); https://doi.org/10.1016/j.memsci.2017.12.069

371. S. Pawlowski, R.M. Huertas, C.F. Galinha, J.G. Crespo, S. Velizarov. *Desalination*, **476**, 114183 (2020); https://doi.org/10.1016/j.desal.2019.114183

372. E. Güler, W. Van Baak, M. Saakes, K. Nijmeijer. *J. Membr. Sci.*, **455**, 254 (2014); https://doi.org/10.1016/j.memsci.2013.12.054

373. A. Manin, D. Golubenko, S. Novikova, A. Yaroslavtsev. *Membranes*, **13** (7), 624 (2023); https://doi.org/10.3390/membranes13070624

Accepted manuscript
This manuscript will be edited for style and proofread before it will be replaced with Version of Record

374. H. Kim, D. Kim, H. Seo, H.-Y. Park, J. Choi, H. Kim, J. Yoo, Y.-W. Choi, H. Yang, S.-C. Jeon, Y.-G. Jung, S. Yang. *J. Membr. Sci.*, **654**, 120568 (2022); https://doi.org/10.1016/j.memsci.2022.120568

375. S.H. Kwak, S.-R. Kwon, S. Baek, S.-M. Lim, Y.-C. Joo, T.D. Chung. *Sci. Rep.*, **6** (1), 26416 (2016); https://doi.org/10.1038/srep26416

376. H.-K. Kim, M.-S. Lee, S.-Y. Lee, Y.-W. Choi, N.-J. Jeong, C.-S. Kim. *J. Mater. Chem. A*, **3** (31), 16302 (2015); https://doi.org/10.1039/C5TA03571F

377. M. Yue, H. Lambert, E. Pahon, R. Roche, S. Jemei, D. Hissel. *Renewable Sustainable Energy Rev.*, **146**, 111180 (2021); https://doi.org/10.1016/j.rser.2021.111180

378. F. Cuevas, J. Zhang, M. Latroche. *Engineering*, **7** (6), 715 (2021); https://doi.org/10.1016/j.eng.2021.04.010

379. V.M. Maestre, A. Ortiz, I. Ortiz. *Renewable Sustainable Energy Rev.*, **152**, 111628 (2021); https://doi.org/10.1016/j.rser.2021.111628

380. A. Abánades. *Energies*, **16** (1), 437 (2022); https://doi.org/10.3390/en16010437

381. Z. Abdin, N. Al Khafaf, B. McGrath, K. Catchpole, E. Gray. *Sustainable Energy Fuels*, **7** (9), 2042 (2023); https://doi.org/10.1039/D3SE00099K

382. M. Ambrosetti, D. Bonincontro, R. Balzarotti, A. Beretta, G. Groppi, E. Tronconi. *Catal. Today*, **387**, 107 (2022); https://doi.org/10.1016/j.cattod.2021.06.003

383. J.O. Ighalo, P.B. Amama. *Int. J. Hydrogen Energy*, **51**, 688 (2024); https://doi.org/10.1016/j.ijhydene.2023.10.177

384. A.Yu. Alent'ev, A.V. Volkov, I.V. Vorotyntsev, A.L. Maksimov, A.B. Yaroslavtsev. *Membr. Membr. Technol.*, **3** (5), 255 (2021) [*Мембраны и мембранные технологии*, **11** (5), 283 (2021)]; https://doi.org/10.1134/S2517751621050024

385. M. Zhang, R. Liu, H. Sun. *Sci. Rep.*, **15** (1), 13779 (2025); https://doi.org/10.1038/s41598-025-97810-w

386. K. Ham, S. Bae, J. Lee. *J. Energy Chem.*, **95**, 554 (2024); https://doi.org/10.1016/j.jechem.2024.04.003

387. M. Kayfeci, A. Keçebaş, M. Bayat. In *Solar Hydrogen Production: Processes, Systems and Technologies*. (Eds F. Calise, M. Dentice D'Accadia, M. Santarelli, A. Lanzini, D. Ferrero). (Amsterdam: Academic Press, 2019). P. 45; https://doi.org/10.1016/B978-0-12-814853-2.00003-5

Accepted manuscript
This manuscript will be edited for style and proof read. The final version of record will be replaced with version of record.

388. M. El-Shafie. *Results Eng.*, **20**, 101426 (2023); https://doi.org/10.1016/j.rineng.2023.101426
389. M. Bonanno, K. Müller, B. Bensmann, R. Hanke-Rauschenbach, D. Aili, T. Franken, A. Chromik, R. Peach, A.T.S. Freiberg, S. Thiele. *Adv. Mater. Technol.*, **9** (2), 2300281 (2024); https://doi.org/10.1002/admt.202300281
390. G. Zwaschka, L. Thiel, R. Leskau. *Int. J. Hydrogen Energy*, **138**, 58 (2025); https://doi.org/10.1016/j.ijhydene.2025.05.146
391. I. Stenina, A. Yaroslavtsev. *Processes*, **11** (1), 56 (2022); https://doi.org/10.3390/pr11010056
392. S. Shiva Kumar, H. Lim. *Energy Rep.*, **8**, 13793 (2022); https://doi.org/10.1016/j.egyr.2022.10.127
393. D. Li, E.J. Park, W. Zhu, Q. Shi, Y. Zhou, H. Tian, Y. Lin, A. Serov, B. Zulevi, E.D. Baca, C. Fujimoto, H.T. Chung, Y.S. Kim. *Nat. Energy*, **5** (5), 378 (2020); https://doi.org/10.1038/s41560-020-0577-x
394. M. Chatenet, B.G. Pollet, D.R. Dekel, F. Dionigi, J. Deseure, P. Millet, R.D. Braatz, M.Z. Bazant, M. Eikerling, I. Staffell, P. Balcombe, Y. Shao-Horn, H. Schäfer. *Chem. Soc. Rev.*, **51** (11), 4583 (2022); https://doi.org/10.1039/D0CS01079K
395. L. Wan, Z. Xu, B. Wang. *Chem. Eng. J.*, **426**, 131340 (2021); https://doi.org/10.1016/j.cej.2021.131340
396. S.M. Saba, M. Müller, M. Robinius, D. Stolten. *Int. J. Hydrogen Energy*, **43** (3), 1209 (2018); https://doi.org/10.1016/j.ijhydene.2017.11.115
397. C. Immerz, M. Paidar, G. Papakonstantinou, B. Bensmann, T. Bystron, T. Vidakovic-Koch, K. Bouzek, K. Sundmacher, R. Hanke-Rauschenbach. *J. Appl. Electrochem.*, **48** (6), 701 (2018); https://doi.org/10.1007/s10800-018-1178-2
398. S. Giancola, M. Zatoń, Á. Reyes-Carmona, M. Dupont, A. Donnadio, S. Cavaliere, J. Rozière, D.J. Jones. *J. Membr. Sci.*, **570–571**, 69 (2019); https://doi.org/10.1016/j.memsci.2018.09.063
399. C. Hu, L. Zhang, J. Gong. *Energy Environ. Sci.*, **12** (9), 2620 (2019); https://doi.org/10.1039/C9EE01202H
400. C. Li, J.-B. Baek. *Nano Energy*, **87**, 106162 (2021); https://doi.org/10.1016/j.nanoen.2021.106162

Accepted manuscript
This manuscript will be edited for style and formatted and proofread before it is published. Please note that during the production process errors may be discovered which could affect the content, and all legal disclaimers that apply to the journal pertain. This manuscript will be replaced with Version of Record.

401. N. Chen, S.Y. Paek, J.Y. Lee, J.H. Park, S.Y. Lee, Y.M. Lee. *Energy Environ. Sci.*, **14** (12), 6338 (2021); https://doi.org/10.1039/D1EE02642A
402. W. Song, Z. Sun, M. Guo, Y. Tang, M. Zhang, K. Su, J. Li, Z. Li. *Chem. Eng. J.*, **503**, 158688 (2025); https://doi.org/10.1016/j.cej.2024.158688
403. L. Liu, J. Wang, G. Yang, S. Wang, J. Wang, Z. Ren, W. Guo, P. Liu. *ACS Omega*, **10** (9), 9007 (2025); https://doi.org/10.1021/acsomega.4c07167
404. N. Du, C. Roy, R. Peach, M. Turnbull, S. Thiele, C. Bock. *Chem. Rev.*, **122** (13), 11830 (2022); https://doi.org/10.1021/acs.chemrev.1c00854
405. S. Grigoriev, V. Porembsky, V. Fateev. *Int. J. Hydrogen Energy*, **31** (2), 171 (2006); https://doi.org/10.1016/j.ijhydene.2005.04.038
406. B. Lee, J. Heo, S. Kim, C. Sung, C. Moon, S. Moon, H. Lim. *Energy Convers. Manage.*, **162**, 139 (2018); https://doi.org/10.1016/j.enconman.2018.02.041
407. S. Shiva Kumar, V. Himabindu. *Mater. Sci. Energy Technol.*, **2** (3), 442 (2019); https://doi.org/10.1016/j.mset.2019.03.002
408. A.S. Aricò, S. Siracusano, N. Briguglio, V. Baglio, A. Di Blasi, V. Antonucci. *J. Appl. Electrochem.*, **43** (2), 107 (2013); https://doi.org/10.1007/s10800-012-0490-5
409. D.-H. Kim, M.-S. Kang. *Chem. Lett.*, **47** (10), 1265 (2018); https://doi.org/10.1246/cl.180560
410. S. Siracusano, F. Pantò, S. Tonella, C. Oldani, A.S. Aricò. *Int. J. Hydrogen Energy*, **47** (35), 15557 (2022); https://doi.org/10.1016/j.ijhydene.2022.03.061
411. Ľ. Staňo, M. Stano, P. Ďurina. *Int. J. Hydrogen Energy*, **45** (1), 80 (2020); https://doi.org/10.1016/j.ijhydene.2019.10.233
412. A. Albert, A.O. Barnett, M.S. Thomassen, T.J. Schmidt, L. Gubler. *ACS Appl. Mater. Interfaces*, **7** (40), 22203 (2015); https://doi.org/10.1021/acsami.5b04618
413. A. Albert, T. Lochner, T.J. Schmidt, L. Gubler. *ACS Appl. Mater. Interfaces*, **8** (24), 15297 (2016); https://doi.org/10.1021/acsami.6b03050
414. R. Qelibari, E.C. Ortiz, N. Van Treel, F. Lombeck, C. Schare, A. Münchinger, N. Dumbadze, G. Titvinidze, C. Klose, S. Vierrath. *Adv. Energy Mater.*, **14** (5), 2303271 (2024); https://doi.org/10.1002/aenm.202303271
415. G. Gupta, K. Scott, M. Mamlouk. *J. Power Sources*, **375**, 387 (2018); https://doi.org/10.1016/j.jpowsour.2017.07.026

Accepted manuscript
This manuscript will be edited, formatted, and proof read. The final version will be published with Version of Record

416. M. Najibah, E. Tsoy, H. Khalid, Y. Chen, Q. Li, C. Bae, J. Hnát, M. Plevová, K. Bouzek, J.H. Jang, H.S. Park, D. Henkensmeier. *J. Membr. Sci.*, **640**, 119832 (2021); https://doi.org/10.1016/j.memsci.2021.119832

417. J.-H. Park, Y. Park, T.-S. Jeon, Y. Seo, J.-S. Park. *Appl. Sci.*, **15** (3), 1495 (2025); https://doi.org/10.3390/app15031495

418. J. Choi, H. Kim, S. Jeon, M. Lee, Y. Nam, Y.S. Park, S.E. An, M. Kim, C. Lee, H. Park, H. Cho, A.S. Lee, J. Lee. *Small*, **21** (41), e04491 (2025); https://doi.org/10.1002/smll.202504491

419. M. Xie, X. Jiang, Y. Lu. *Hydrogen*, **7** (1), 32 (2026); https://doi.org/10.3390/hydrogen7010032

420. H. Sethia, A. Priyam. *Next Energy*, **9**, 100460 (2025); https://doi.org/10.1016/j.nxener.2025.100460

421. Y. Li, M.-S. Yao, Y. He, S. Du. *Nano-Micro Lett.*, **17** (1), 148 (2025); https://doi.org/10.1007/s40820-025-01648-w

422. I. Sebbani, M.K. Ettouhami, M. Boulakhbar. *Cleaner Energy Syst.*, **10**, 100168 (2025); https://doi.org/10.1016/j.cles.2024.100168

423. J. Li, T. Wu, C. Cheng, J. Li, K. Zhou. *Processes*, **12** (2), 249 (2024); https://doi.org/10.3390/pr12020249

424. P. Gupta, B. Toksha, M. Rahaman. *Chem. Rec.*, **24** (1), e202300295 (2024); https://doi.org/10.1002/tcr.202300295

425. E.Yu. Safronova, I.A. Stenina, A.B. Yaroslavtsev. *Russ. J. Inorg. Chem.*, **55** (1), 13 (2010) [*Журн. неорган. химии*, **55** (1), 16 (2010)]; https://doi.org/10.1134/S0036023610010031

426. J. Lou, Y. Lu, D. Yang, X. Pan, B. Li, P. Ming. *Int. J. Hydrogen Energy*, **94**, 756 (2024); https://doi.org/10.1016/j.ijhydene.2024.11.056

427. I.V. Falina, N.A. Kononenko, S.A. Shkirskaya, O.A. Demina, Yu.M. Volfkovich, V.E. Sosenkin, M.V. Gritsay. *Membr. Membr. Technol.*, **4** (5), 281 (2022) [*Мембраны и мембранные технологии*, **12** (5), 323 (2022)]; https://doi.org/10.1134/S2517751622050043

428. E.V. Nazyrova, N.A. Kononenko, S.A. Shkirskaya, O.A. Demina. *Membr. Membr. Technol.*, **4** (3), 145 (2022) [*Мембраны и мембранные технологии*, **12** (3), 165 (2022)]; https://doi.org/10.1134/S2517751622030064

Accepted manuscript
This manuscript will be edited, formatted, and proofread. The final version of Record will be published with DOI.

429. R. Komoda, K. Yamada, M. Kubota, P. Ginet, F. Barbier, J. Furtado, L. Prost. *Int. J. Hydrogen Energy*, **44** (54), 29007 (2019); https://doi.org/10.1016/j.ijhydene.2019.09.146
430. E.Yu. Safronova, A.K. Osipov, A.B. Yaroslavtsev. *Pet. Chem.*, **58** (2), 130 (2018) [*Мембраны и мембранные технологии*, **8** (1), 34 (2018)]; https://doi.org/10.1134/S0965544118020044
431. A. Kusoglu, A.Z. Weber. *Chem. Rev.*, **117** (3), 987 (2017); https://doi.org/10.1021/acs.chemrev.6b00159
432. Y. Prykhodko, K. Fatyeyeva, L. Hespel, S. Marais. *Chem. Eng. J.*, **409**, 127329 (2021); https://doi.org/10.1016/j.cej.2020.127329
433. T. Sherazi, S. Ahmad, M. Kashmiri, M. Guiver. *J. Membr. Sci.*, **325** (2), 964 (2008); https://doi.org/10.1016/j.memsci.2008.09.028
434. K. Kim, S.-K. Kim, J.O. Park, S.-W. Choi, K.-H. Kim, T. Ko, C. Pak, J.-C. Lee. *J. Membr. Sci.*, **537**, 11 (2017); https://doi.org/10.1016/j.memsci.2017.05.014
435. S. Ryu, B. Lee, J. Kim, C. Pak, S. Moon. *Int. J. Energy Res.*, **45** (13), 19136 (2021); https://doi.org/10.1002/er.7017
436. D. Golubenko, O. Korchagin, D. Voropaeva, V. Bogdanovskaya, A. Yaroslavtsev. *Polymers*, **14** (18), 3833 (2022); https://doi.org/10.3390/polym14183833
437. Y. Oshiba, M. Kosaka, T. Yamaguchi. *Int. J. Hydrogen Energy*, **44** (54), 28996 (2019); https://doi.org/10.1016/j.ijhydene.2019.09.143
438. B.-Y. Wang, C.K. Tseng, C.-M. Shih, Y.-L. Pai, H.-P. Kuo, S.J. Lue. *J. Membr. Sci.*, **464**, 43 (2014); https://doi.org/10.1016/j.memsci.2014.03.076
439. G.-M. Liao, P.-C. Li, J.-S. Lin, W.-T. Ma, B.-C. Yu, H.-Y. Li, Y.-L. Liu, C.-C. Yang, C.-M. Shih, S.J. Lue. *J. Power Sources*, **304**, 136 (2016); https://doi.org/10.1016/j.jpowsour.2015.11.025
440. H.-B. Song, J.-H. Park, J.-S. Park, M.-S. Kang. *Energies*, **14** (15), 4433 (2021); https://doi.org/10.3390/en14154433
441. A. Moura, J. Fajín, M. Mandado, M. Cordeiro. *Catalysts*, **7** (2), 47 (2017); https://doi.org/10.3390/catal7020047
442. Y. Zuo, W. Sheng, W. Tao, Z. Li. *J. Mater. Sci. Technol.*, **114**, 29 (2022); https://doi.org/10.1016/j.jmst.2021.10.031

Accepted manuscript
This manuscript will be edited for style and proof read. The final version of Record

443. H. Lei, X. Yang, Z. Chen, D. Rawach, L. Du, Z. Liang, D. Li, G. Zhang, A.C. Tavares, S. Sun. *Adv. Mater.*, **37** (8), 2410106 (2025); https://doi.org/10.1002/adma.202410106

444. K. Yassin, I.G. Rasin, S. Brandon, D.R. Dekel. *J. Membr. Sci.*, **690**, 122164 (2024); https://doi.org/10.1016/j.memsci.2023.122164

445. J. Zhang, W. Zhu, T. Huang, C. Zheng, Y. Pei, G. Shen, Z. Nie, D. Xiao, Y. Yin, M.D. Guiver. *Adv. Sci.*, **8** (15), 2100284 (2021); https://doi.org/10.1002/advs.202100284

446. P. Teppor, R. Jäger, M. Paalo, A. Adamson, M. Härmas, O. Volobujeva, J. Aruväli, R. Palm, E. Lust. *Int. J. Hydrogen Energy*, **47** (38), 16908 (2022); https://doi.org/10.1016/j.ijhydene.2022.03.199

447. Z.F. Pan, L. An, T.S. Zhao, Z.K. Tang. *Prog. Energy Combust. Sci.*, **66**, 141 (2018); https://doi.org/10.1016/j.pecs.2018.01.001

448. L. Wang, M. Bellini, H.A. Miller, J.R. Varcoe. *J. Mater. Chem. A*, **6** (31), 15404 (2018); https://doi.org/10.1039/C8TA04783A

449. G. Huang, M. Mandal, X. Peng, A.C. Yang-Neyerlin, B.S. Pivovar, W.E. Mustain, P.A. Kohl. *J. Electrochem. Soc.*, **166** (10), F637 (2019); https://doi.org/10.1149/2.1301910jes

450. J.C. Douglin, J.R. Varcoe, D.R. Dekel. *J. Power Sources Adv.*, **5**, 100023 (2020); https://doi.org/10.1016/j.powera.2020.100023

451. J.C. Douglin, R.K. Singh, S. Haj-Bsoul, S. Li, J. Biemolt, N. Yan, J.R. Varcoe, G. Rothenberg, D.R. Dekel. *Chem. Eng. J. Adv.*, **8**, 100153 (2021); https://doi.org/10.1016/j.ceja.2021.100153

452. M.-S. Lee, T. Kim, S.-H. Park, C.-S. Kim, Y.-W. Choi. *J. Mater. Chem.*, **22** (28), 13928 (2012); https://doi.org/10.1039/c2jm32628k

453. T. Son, T.-H. Kim, S. Nam. *Polymers*, **12** (11), 2758 (2020); https://doi.org/10.3390/polym12112758

454. P. Sithambaranathan, M.M. Nasef, A. Ahmad, A. Abbasi, T.M. Ting. *Membranes*, **13** (1), 105 (2023); https://doi.org/10.3390/membranes13010105

455. C. Schmidt, G. Schmidt-Naake. *Macromol. Mater. Eng.*, **292** (10–11), 1164 (2007); https://doi.org/10.1002/mame.200700188

456. E. Güler, S. Sadeghi, S. Alkan Gürsel. *Int. J. Hydrogen Energy*, **43** (16), 8088 (2018); https://doi.org/10.1016/j.ijhydene.2018.03.087

Accepted manuscript
This manuscript will be edited, formatted and proof read. The file will be replaced with Version of Record.

457. H.B. Youcef, L. Gubler, A. Foelske-Schmitz, G.G. Scherer. *J. Membr. Sci.*, **381** (1–2), 102 (2011); https://doi.org/10.1016/j.memsci.2011.07.021

458. K. Jetsrisuparb, H. Ben Youcef, A. Wokaun, L. Gubler. *J. Membr. Sci.*, **450**, 28 (2014); https://doi.org/10.1016/j.memsci.2013.08.037

459. L. Gubler, M. Slaski, A. Wokaun, G.G. Scherer. *Electrochem. Commun.*, **8** (8), 1215 (2006); https://doi.org/10.1016/j.elecom.2006.05.029

460. X. Ke, M. Drache, U. Gohs, U. Kunz, S. Beuermann. *Membranes*, **8** (4), 102 (2018); https://doi.org/10.3390/membranes8040102

461. X. Ke, Y. Zhang, U. Gohs, M. Drache, S. Beuermann. *Polymers*, **11** (7), 1175 (2019); https://doi.org/10.3390/polym11071175

462. F. Liu, B. Yi, D. Xing, J. Yu, H. Zhang. *J. Membr. Sci.*, **212** (1–2), 213 (2003); https://doi.org/10.1016/S0376-7388(02)00503-3

463. H. Tang, X. Wang, M. Pan, F. Wang. *J. Membr. Sci.*, **306** (1–2), 298 (2007); https://doi.org/10.1016/j.memsci.2007.09.008

464. C. Lee, S.M. Jo, J. Choi, K.-Y. Baek, Y.B. Truong, I.L. Kyratzis, Y.-G. Shul. *J. Mater. Sci.*, **48** (10), 3665 (2013); https://doi.org/10.1007/s10853-013-7162-7

465. S.-H. Yun, S.-H. Oh, J.-J. Woo, J.-Y. Lee, J.-H. Lee, S.-B. Lee, C.-M. Min, J. Lee, J.-S. Lee, S.-H. Moon. *RSC Adv.*, **3** (46), 24154 (2013); https://doi.org/10.1039/c3ra44089c

466. L. Wang, J.J. Brink, J.R. Varcoe. *Chem. Commun.*, **53** (86), 11771 (2017); https://doi.org/10.1039/C7CC06392J

467. R. Espiritu, M. Mamlouk, K. Scott. *Int. J. Hydrogen Energy*, **41** (2), 1120 (2016); https://doi.org/10.1016/j.ijhydene.2015.10.108

468. S.A. Franklin, M. Mohammadpour, Y. Cui, R. Bance-Soualhi, C. Crean, W.E. Mustain, H. Lin, J.R. Varcoe. *J. Mater. Chem. A*, **14** (10), 5877 (2026); https://doi.org/10.1039/D5TA08440G

469. A.L.G. Biancolli, S. Bsoul-Haj, J.C. Douglin, A.S. Barbosa, R.R. De Sousa, O. Rodrigues, A.J.C. Lanfredi, D.R. Dekel, E.I. Santiago. *J. Membr. Sci.*, **641**, 119879 (2022); https://doi.org/10.1016/j.memsci.2021.119879

470. S. Maurya, S.-H. Shin, M.-K. Kim, S.-H. Yun, S.-H. Moon. *J. Membr. Sci.*, **443**, 28 (2013); https://doi.org/10.1016/j.memsci.2013.04.035

Accepted manuscript
This manuscript will be edited for style, and proof read. The final version will be published with Version of Record

471. D.S. Hwang, T.A. Sherazi, J.Y. Sohn, Y.C. Noh, C.H. Park, M.D. Guiver, Y.M. Lee. *J. Membr. Sci.*, **495**, 206 (2015); https://doi.org/10.1016/j.memsci.2015.07.067
472. D.-H. Kim, M.-S. Kang. *Energies*, **13** (18), 4761 (2020); https://doi.org/10.3390/en13184761
473. X. Yang, K.R. Adair, X. Gao, X. Sun. *Energy Environ. Sci.*, **14** (2), 643 (2021); https://doi.org/10.1039/D0EE02714F
474. F.M.N.U. Khan, M.G. Rasul, A.S.M. Sayem, N. Mandal. *Energy Rep.*, **9**, 11 (2023); https://doi.org/10.1016/j.egyr.2023.08.069
475. L. Elbinger, M. Enke, N. Ziegenbalg, J.C. Brendel, U.S. Schubert. *Energy Storage Mater.*, **65**, 103063 (2024); https://doi.org/10.1016/j.ensm.2023.103063
476. A. Machín, C. Morant, F. Márquez. *Batteries*, **10** (1), 29 (2024); https://doi.org/10.3390/batteries10010029
477. P.U. Nzereogu, A. Oyesanya, S.N. Ogba, S.O. Ayanwunmi, M.S. Sobajo, V.C. Chimsunum, V.O. Ayanwunmi, M.O. Amoo, O.T. Adefemi, C.C. Chukwudi. *Hybrid Adv.*, **8**, 100339 (2025); https://doi.org/10.1016/j.hybadv.2024.100339
478. F. Wu, K. Zhang, Y. Liu, H. Gao, Y. Bai, X. Wang, C. Wu. *Energy Storage Mater.*, **33**, 26 (2020); https://doi.org/10.1016/j.ensm.2020.08.002
479. H. Chen, M. Zheng, S. Qian, H.Y. Ling, Z. Wu, X. Liu, C. Yan, S. Zhang. *Carbon Energy*, **3** (6), 929 (2021); https://doi.org/10.1002/cey2.146
480. S. Mohapatra, S. Sharma, A. Sriperumbuduru, S.R. Varanasi, S. Mogurampelly. *J. Chem. Phys.*, **156** (21), 214903 (2022); https://doi.org/10.1063/5.0087824
481. L. Han, L. Wang, Z. Chen, Y. Kan, Y. Hu, H. Zhang, X. He. *Adv. Funct. Mater.*, **33** (32), 2300892 (2023); https://doi.org/10.1002/adfm.202300892
482. L. Meabe, I. Aldalur, S. Lindberg, M. Arrese-Igor, M. Armand, M. Martinez-Ibañez, H. Zhang. *Mater. Futures*, **2** (3), 033501 (2023); https://doi.org/10.1088/2752-5724/accdf3
483. T. Parmar, P.K. Patel, R. Hirani, R. Vaishnav, S. Vanshiya, N. Gamit, D. Vasava. *Russ. J. Electrochem.*, **61** (12), 868 (2025); https://doi.org/10.1134/S1023193525700223
484. M.K. Majeed, R. Iqbal, M.Z. Ashfaq, M. Akram, M.U. Majeed, A. Saleem. *Energy Storage Mater.*, **86**, 104831 (2026); https://doi.org/10.1016/j.ensm.2025.104831

Accepted manuscript
This manuscript will be published after it has been typeset, and proof read. The final version may be replaced with Version of Record.

485. D.M. Reinoso, M.A. Frechero. *Energy Storage Mater.*, **52**, 430 (2022); https://doi.org/10.1016/j.ensm.2022.08.019

486. J.C. Barbosa, D.M. Correia, A. Fidalgo-Marijuan, R. Gonçalves, S. Ferdov, V. De Zea Bermudez, S. Lanceros-Mendez, C.M. Costa. *ACS Appl. Mater. Interfaces*, **15** (27), 32301 (2023); https://doi.org/10.1021/acsami.3c03361

487. J. Mu, S. Liao, L. Shi, B. Su, F. Xu, Z. Guo, H. Li, F. Wei. *Polym. Chem.*, **15** (6), 473 (2024); https://doi.org/10.1039/D3PY01311A

488. W. Chae, B. Kim, W.S. Ryoo, T. Earmme. *Polymers*, **15** (4), 803 (2023); https://doi.org/10.3390/polym15040803

489. Y. Luo, L. Gao, W. Kang. *J. Energy Chem.*, **89**, 543 (2024); https://doi.org/10.1016/j.jechem.2023.11.005

490. D.Yu. Voropaeva, S.A. Novikova, T.L. Kulova, A.B. Yaroslavtsev. *Ionics*, **24** (6), 1685 (2018); https://doi.org/10.1007/s11581-017-2333-1

491. D. Voropaeva, S. Novikova, T. Xu, A. Yaroslavtsev. *J. Phys. Chem. B*, **123** (48), 10217 (2019); https://doi.org/10.1021/acs.jpcb.9b08555

492. O.V. Bushkova, E.A. Sanginov, S.D. Chernyuk, R.R. Kayumov, L.V. Shmygleva, Yu.A. Dobrovolsky, A.B. Yaroslavtsev. *Membr. Membr. Technol.*, **4** (6), 433 (2022); https://doi.org/10.1134/S2517751622070010

493. D. Voropaeva, E. Safronova, S. Novikova, A. Yaroslavtsev. *J. Phys. Chem. C*, **128** (10), 4143 (2024); https://doi.org/10.1021/acs.jpcc.3c07673

494. S. Thayumanasundaram, V.S. Rangasamy, J.-P. Locquet. *Solid State Ionics*, **406**, 116483 (2024); https://doi.org/10.1016/j.ssi.2024.116483

495. Y. Zhong, L. Zhong, S. Wang, J. Qin, D. Han, S. Ren, M. Xiao, L. Sun, Y. Meng. *J. Mater. Chem. A*, **7** (42), 24251 (2019); https://doi.org/10.1039/C9TA08795H

496. Z. Hajian, S.-A. Safavi-Mirmahalleh, A.R. Moghaddam, H. Roghani-Mamaqani, M. Salami-Kalajahi. *J. Power Sources*, **629**, 235971 (2025); https://doi.org/10.1016/j.jpowsour.2024.235971

497. M. Nasef. *Solid State Ionics*, **171** (3–4), 243 (2004); https://doi.org/10.1016/j.ssi.2004.05.004

498. J.M. Ko, B.G. Min, D.-W. Kim, K.S. Ryu, K.M. Kim, Y.G. Lee, S.H. Chang. *Electrochim. Acta*, **50** (2–3), 367 (2004); https://doi.org/10.1016/j.electacta.2004.01.127

Accepted manuscript
This manuscript will be edited for style and proofread before it is published with Version of Record.

499. K. Gao, X. Hu, T. Yi, C. Dai. *Electrochim. Acta*, **52** (2), 443 (2006); https://doi.org/10.1016/j.electacta.2006.05.049
500. J.-H. Choi, S.-J. Gwon, J.-Y. Shon, C.-H. Jung, Y.-E. Ihm, Y.-M. Lim, Y.-C. Nho. *J. Ind. Eng. Chem.*, **14** (1), 116 (2008); https://doi.org/10.1016/j.jiec.2007.08.005
501. M.M. Nasef, H. Saidi, K.Z.M. Dahlan. *Nucl. Instrum. Methods Phys. Res., Sect. B*, **265** (1), 168 (2007); https://doi.org/10.1016/j.nimb.2007.08.044
502. S.-J. Gwon, J.-H. Choi, J.-Y. Sohn, S.-J. An, Y.-E. Ihm, Y.-C. Nho. *Nucl. Instrum. Methods Phys. Res., Sect. B*, **266** (15), 3387 (2008); https://doi.org/10.1016/j.nimb.2008.05.017
503. S.-J. Gwon, J.-H. Choi, J.-Y. Sohn, Y.-E. Ihm, Y.-C. Nho. *Nucl. Instrum. Methods Phys. Res., Sect. B*, **267** (19), 3309 (2009); https://doi.org/10.1016/j.nimb.2009.06.117
504. S. Li, K. Gao. *Ionics*, **16** (6), 555 (2010); https://doi.org/10.1007/s11581-010-0434-1
505. X.-L. Miao, J.-H. Li, Q. Xiang, J.-Q. Xu, L.-F. Li, J.-Y. Li. *Nucl. Sci. Tech.*, **28** (6), 77 (2017); https://doi.org/10.1007/s41365-017-0226-7
506. D. Kim. *Solid State Ionics*, **144** (3–4), 329 (2001); https://doi.org/10.1016/S0167-2738(01)00977-8
507. H. Jeon, D. Kim. *J. Membr. Sci.*, **624**, 119029 (2021); https://doi.org/10.1016/j.memsci.2020.119029
508. K. Xue, Y. Zhao, P. Lee, D.Y.W. Yu. *Energy Environ. Mater.*, **6** (4), e12395 (2023); https://doi.org/10.1002/eem2.12395
509. G.-J. Hwang, S.-W. Kim, D.-M. In, D.-Y. Lee, C.-H. Ryu. *J. Ind. Eng. Chem.*, **60**, 360 (2018); https://doi.org/10.1016/j.jiec.2017.11.023
510. C.H.L. Tempelman, J.F. Jacobs, R.M. Balzer, V. Degirmenci. *J. Energy Storage*, **32**, 101754 (2020); https://doi.org/10.1016/j.est.2020.101754
511. H.-N. Moon, H.-B. Song, M.-S. Kang. *Membranes*, **11** (11), 867 (2021); https://doi.org/10.3390/membranes11110867
512. M.-S. Kang. *J. Korean Electrochem. Soc.*, **16** (4), 204 (2013); https://doi.org/10.5229/JKES.2013.16.4.204
513. S.-J. Seo, B.-C. Kim, K.-W. Sung, J. Shim, J.-D. Jeon, K.-H. Shin, S.-H. Shin, S.-H. Yun, J.-Y. Lee, S.-H. Moon. *J. Membr. Sci.*, **428**, 17 (2013); https://doi.org/10.1016/j.memsci.2012.11.027

Accepted manuscript
This manuscript will be edited for style and proof read. The file will be replaced with Version of Record.

514. M. Jung, W. Lee, N. Nambi Krishnan, S. Kim, G. Gupta, L. Komsiyska, C. Harms, Y. Kwon, D. Henkensmeier. *Appl. Surf. Sci.*, **450**, 301 (2018); https://doi.org/10.1016/j.apsusc.2018.04.198
515. Z. Wang, J. Jiang, Z. Dong, Y. Song, L. Zhao. *New J. Chem.*, **47** (17), 8013 (2023); https://doi.org/10.1039/D2NJ05386A
516. P. Kumar, S. Suhag, J.R. Mandal, V.K. Shahi. *ACS Appl. Energy Mater.*, **8** (11), 7371 (2025); https://doi.org/10.1021/acsaem.5c00729
517. Z. Wang, Y. Song, J. Jiang, W. Zhao, M. Zhang, Z. Dong, L. Zhao. *Ionics*, **30** (2), 901 (2024); https://doi.org/10.1007/s11581-023-05342-y
518. J. Qiu, J. Ni, M. Zhai, J. Peng, H. Zhou, J. Li, G. Wei. *Radiat. Phys. Chem.*, **76** (11–12), 1703 (2007); https://doi.org/10.1016/j.radphyschem.2007.01.012
519. J. Qiu, J. Zhang, J. Chen, J. Peng, L. Xu, M. Zhai, J. Li, G. Wei. *J. Membr. Sci.*, **334** (1–2), 9 (2009); https://doi.org/10.1016/j.memsci.2009.02.009
520. J. Qiu, M. Zhai, J. Chen, Y. Wang, J. Peng, L. Xu, J. Li, G. Wei. *J. Membr. Sci.*, **342** (1–2), 215 (2009); https://doi.org/10.1016/j.memsci.2009.06.043
521. X. Li, A.R. Dos Santos, M. Drache, X. Ke, U. Gohs, T. Turek, M. Becker, U. Kunz, S. Beuermann. *J. Membr. Sci.*, **524**, 419 (2017); https://doi.org/10.1016/j.memsci.2016.10.053
522. G. Hu, Y. Wang, J. Ma, J. Qiu, J. Peng, J. Li, M. Zhai. *J. Membr. Sci.*, **407–408**, 184 (2012); https://doi.org/10.1016/j.memsci.2012.03.042
523. J. Kim, Y. Lee, J.-D. Jeon, S.-Y. Kwak. *J. Power Sources*, **383**, 1 (2018); https://doi.org/10.1016/j.jpowsour.2018.02.028
524. W. Lee, M. Jung, D. Serhiichuk, C. Noh, G. Gupta, C. Harms, Y. Kwon, D. Henkensmeier. *J. Membr. Sci.*, **591**, 117333 (2019); https://doi.org/10.1016/j.memsci.2019.117333
525. D.Y. Nikumbe, C.M. Pawar, D.D. Khairnar, P. Madiyan, R.K. Nagarale. *ACS Appl. Energy Mater.*, **8** (9), 6056 (2025); https://doi.org/10.1021/acsaem.5c00465
526. J. Qiu, M. Li, J. Ni, M. Zhai, J. Peng, L. Xu, H. Zhou, J. Li, G. Wei. *J. Membr. Sci.*, **297** (1–2), 174 (2007); https://doi.org/10.1016/j.memsci.2007.03.042
527. S. Sreenath, N. P. S, C.M. Pawar, D.Y. Nikumbe, B. Bhatt, J.C. Chaudhari, R.K. Nagarale. *ACS Appl. Energy Mater.*, **5** (11), 13661 (2022); https://doi.org/10.1021/acsaem.2c02328

Accepted manuscript
This manuscript will be edited for style and proof read. The final version of record.

528. S.M. Aldoshin, V.P. Ananikov, I.P. Beletskaya, A.A. Berlin, L.B. Boinovich, V.I. Bukhtiyarov, A.A. Voshkin, Yu.G. Gorbunova, K.V. Grigorovich, U.M. Dzhemilev, M.P. Egorov, I.L. Eremenko, V.K. Ivanov, S.N. Kalmykov, V.P. Kolotov, A.L. Maximov, A.M. Muzafarov, B.F. Myasoedov, O.G. Sinyashin, K.A. Solntsev, A.R. Khokhlov, A.Yu. Tsivadze, A.A. Yaroslavov, A.B. Yaroslavtsev. *Russ. Chem. Rev.*, **95** (11), RCR5247 (2026) [*Успехи химии*, **95** (11), RCR5247 (2026)]; https://doi.org/10.59761/RCR5247

Accepted manuscript
This manuscript will be edited, formatted, and proof read. The file will be replaced with Version of Record.